# A unified model of inflation, dark matter, neutrino masses and baryogenesis

António Torres Manso
Mestrado em Física (Especialização Teórica)
Departamento de Física e Astronomia
2018

**Orientador**
João G. Rosa, Investigador Auxiliar, Departamento de Física, Universidade Aveiro

**Coorientador**
Orfeu Bertolami, Professor Catedrático, Faculdade Ciências da Universidade do Porto

MSc

U.PORTO

FACULDADE DE CIÊNCIAS
UNIVERSIDADE DO PORTO

Todas as correções determinadas pelo júri, e só essas, foram efetuadas.

O Presidente do Júri,

Porto, ______/______/________

MSc

UNIVERSIDADE DO PORTO

MASTER THESIS

# A unified model of inflation, dark matter, neutrino masses and baryogenesis


*Author:*
António Torres MANSO

*Supervisor:*
João G. Rosa

*Co-supervisor:*
Orfeu Bertolami


*A thesis submitted in fulfilment of the requirements for the degree of Mestrado em Física (Especialização Teórica)*

*at the*


Faculdade Ciências
Departamento de Física e Astronomia


December 2018

*" Don't expect to be motivated every day to get out there and make things happen. You won't be. Don't count on motivation. Count on Discipline. "*

Jocko Willink

# *Agradecimentos*

Em primeiro lugar, gostaria de agradecer ao meu orientador, Professor João Rosa, pelo acompanhamento e supervisão ao longo deste ano. Foi fantástico e muito motivante estudar todos estes tópicos sob a sua orientação. Muito obrigado pela grande disponibilidade para discutir e responder às minhas questões.

Gostaria de agradecer ao Professor Orfeu Bertolami por assegurar este projeto e pelas revisões ao trabalho. Agradeço também a todos os professores que partilharam comigo conhecimentos e que contribuíram para o crescente fascínio por esta área.

À Cristiana, a minha grande companheira, agradeço pelo o que até hoje partilhámos. O teu apoio, paciência e amor foram incansáveis e essenciais para levar este trabalho avante.

Aos meus pais, Filipa e José, que sempre estiveram a meu lado e à minha irmã Maria, cuja paciência devo ter esgotado inúmeras vezes, muito obrigado pelo amor que sempre partilharam comigo. Todos os ”puxões-de-orelha” que me puseram na ”linha”, conselhos e momentos de partilha trouxeram-me até aqui.

Não posso deixar de agradecer a uma grande família que me acolheu desde muito novo, que me viu crescer e que também faz parte daquilo que sou hoje. Um obrigado a todos que me acompanharam no Karaté.

Por último mas não menos importante, agradeço aos amigos que trilharam este caminho comigo, parceiros na universidade, na escola e nas ”minis”.

UNIVERSIDADE DO PORTO

# *Abstract*

Faculdade Ciências
Departamento de Física e Astronomia

Mestrado em Física (Especialização Teórica)

**A unified model of inflation, dark matter, neutrino masses and baryogenesis**

by António Torres MANSO

The origin of neutrino masses, the inflationary evolution, the nature of dark matter particles and the baryon asymmetry in the Universe constitute some of the most important and unanswered problems in the interface between particle physics and cosmology. In this work, we present a short review of these four topics and their connection to experimental observations, setting the stage for a unified model description.

We present a unified model in which, based on the incomplete decay of the inflaton field [1], where the same field may describe inflation as well as account for the present dark matter abundance, while still reproducing a successful reheating. This is accomplished imposing a discrete symmetry on the inflaton and its decay products, two right-handed neutrinos, that forbids the inflaton decay at late times.

We observe a successful transition to a radiation dominated Universe in which the inflaton particles may or not evaporate, i.e. join the thermal bath. In the former case, the stable inflaton particles will follow the common Weakly Interacting Massive Particle evolution, eventually decoupling and freezing out, thus yielding a thermal dark matter relic. In the latter case, after their decay is no longer allowed, the remnant inflaton particles will behave as a condensate in a Dark Radiation regime to later turn into a stable non-relativistic fluid, thus behaving as Cold Dark Matter.

The introduction of the right-handed neutrinos and their interactions with the Standard Model's particles present a mechanism to generate the observed light neutrino masses, through the seesaw mechanism. At the same time, it provides the necessary ingredients for a lepton number generation which is later converted into a baryon asymmetry through non-perturbative processes present in the Standard Model.

UNIVERSIDADE DO PORTO

# *Resumo*

Faculdade Ciências
Departamento de Física e Astronomia

Mestre de Ciência

**Um modelo de unificação de inflação, materia escura, massas de neutrinos e bariogénese**

por António Torres MANSO

As massas dos neutrinos, o período de inflação na evolução do Universo, a origem de matéria escura e a existente assimetria entre partículas e anti-partículas no Universo constituem alguns dos problemas mais importantes e ainda por resolver em física de partículas e cosmologia. Consequentemente, neste trabalho apresentamos uma introdução a estes tópicos para mais tarde descrever um modelo de unificação.

Nesta tese é desenvolvido um modelo em que, com base num mecanismo de decaimento incompleto do inflatão [1], o mesmo campo escalar possa descrever o período de inflação, bem como as abundâncias atuais de matéria escura, mantendo simultaneamente uma transição para a física do modelo padrão através de um reaquecimento eficiente. Através da imposição de uma simetria discreta no inflatão e nos seus produtos de decaimento, dois neutrinos direitos, asseguramos a estabilidade do inflatão até ao presente.

Verificamos uma transição para uma era de domínio de radiação na qual as restantes partículas do inflatão poderão ser excitadas até ao estado do banho térmico. Neste cenário, estas partículas seguirão a evolução comum de uma particula massiva com interações fracas. Caso não evaporem, quando o decaimento para os neutrinos direitos é cinematicamente proibido, o condensado do inflatão fica estável e comporta-se com radiação. Mais tarde irá mimetizar um fluido não relativista estável que identificamos como matéria escura fria.

A introdução dos neutrinos direitos e as respetivas interações com o modelo padrão dão origem às massas observadas dos neutrinos leves através do mecanismo de "seesaw". Simultaneamente, permitem a produção de uma assimetria no número leptónico que será mais tarde numa assimetria bariónica através de processos não-perturbativos existentes no modelo padrão de física da partículas.

# Contents

**Acknowledgements** **v**

**Abstract** **vii**

**Resumo** **ix**

**Contents** **xi**

**List of Figures** **xiii**

**List of Tables** **xv**

**Abbreviations** **xvii**

**1 Introduction** **1**

**2 Neutrinos** **5**
2.1 Neutrinos in the Standard Model . . . . . . . . . . . . . . . . . . . . . . . . . . 5
2.2 Massive Neutrinos . . . . . . . . . . . . . . . . . . . . . . . . . . . . . . . . . . 6
2.2.1 Right Handed Neutrinos and the Seesaw Mechanism . . . . . . . . . . 7
2.2.2 Neutrino Mass Matrix, flavours and the $U_{PMNS}$ Mixing Matrix . . . . 9
2.2.3 Neutrino Oscillations . . . . . . . . . . . . . . . . . . . . . . . . . . . . 11
2.2.4 Experimental Observations . . . . . . . . . . . . . . . . . . . . . . . . 12

**3 Standard Cosmology** **15**
3.1 Friedmann-Robertson-Walker Universe . . . . . . . . . . . . . . . . . . . . . . 15
3.2 Equilibrium Thermodynamics . . . . . . . . . . . . . . . . . . . . . . . . . . . 16

**4 Inflation** **21**
4.1 Problems of the Hot Big Bang Model . . . . . . . . . . . . . . . . . . . . . . . 21
4.2 First Approach on Inflation . . . . . . . . . . . . . . . . . . . . . . . . . . . . 23
4.3 Inflation Dynamics: Introduction of a Scalar Field . . . . . . . . . . . . . . . . 25
4.4 Slow-Roll Inflation . . . . . . . . . . . . . . . . . . . . . . . . . . . . . . . . . 27
4.5 Reheating . . . . . . . . . . . . . . . . . . . . . . . . . . . . . . . . . . . . . . 29
4.6 Quantum Fluctuations during Inflation . . . . . . . . . . . . . . . . . . . . . . 30
4.6.1 Metric and Matter Perturbations . . . . . . . . . . . . . . . . . . . . . . 31
4.6.2 Horizon Entry, Exit and Re-Entry . . . . . . . . . . . . . . . . . . . . . 32
4.6.3 Quantum Fluctuations in de Sitter Space . . . . . . . . . . . . . . . . . 33

4.6.4 Quadratic and Quartic Potentials . . . . . . . . . . . . . . . . . . . . . 36

**5 Dark Matter** **39**
5.1 Evidence for Dark matter . . . . . . . . . . . . . . . . . . . . . . . . . . . . 39
5.2 Candidates for Dark Matter . . . . . . . . . . . . . . . . . . . . . . . . . . . 41
5.3 Thermal Abundance of WIMP's . . . . . . . . . . . . . . . . . . . . . . . . . 42

**6 Baryogenesis** **45**
6.1 Observational Evidence for Baryon Asymmetry . . . . . . . . . . . . . . . . 45
6.2 Sakharov Conditions for Baryogenesis . . . . . . . . . . . . . . . . . . . . . 47
6.3 Models of Baryogenesis . . . . . . . . . . . . . . . . . . . . . . . . . . . . . 49

**7 An Inflaton Dark Matter Model [1]** **51**
7.1 Minimal Model: Symmetries and Dynamics . . . . . . . . . . . . . . . . . . 52

**8 Inflaton Dark Model with Neutrinos** **57**
8.1 Right Handed Neutrinos as the Fermions in the Inflaton Dark Matter Model 57
8.2 Inflation with a non-minimal Coupling to Gravity . . . . . . . . . . . . . . . 59
8.3 Reheating in the Quartic Potential, $\lambda\phi^4$ . . . . . . . . . . . . . . . . . . . . . . 62
8.4 Condensate Evaporation $\Omega_{CDM}$ and Right-Handed Neutrino Decay . . . . . 65
8.5 Connection with Low Energy Phenomena: Neutrino Masses . . . . . . . . . . 70
8.6 Resulting parameter space . . . . . . . . . . . . . . . . . . . . . . . . . . . 74

**9 Leptogenesis in the Inflaton Dark Matter Model** **81**
9.1 A model of Thermal Leptogenesis . . . . . . . . . . . . . . . . . . . . . . . . 82
9.2 Thermal Leptogenesis and the Inflaton Dark Matter model . . . . . . . . . . . 89

**10 Conclusions** **93**

**Bibliography** **97**

# List of Figures


4.1 Evolution of a density/curvature perturbation during and after inflation [48] 33

5.1 Rotation curve of NGC 6503 [62]. . . . . . . . . . . . . . . . . . . . . . . . . . . 40

5.2 Image of the Bullet Custer from Chandra Satellite. The green contours are reconstructions of the gravitational potential inferred by weak gravitational lensing while luminous matter was obtained through X-ray imaging. [64]. . . 41

6.1 Abundances of $^3$He, $^4$He, D, $^6$Li and $^7$Li as predicted by the Standard Model of BBN. The bands show the 95% C.L. range. Boxes indicate the observed light element abundances. The narrow vertical band indicates the CMB measurements of the cosmic baryon density, while the wider band indicates the BBN concordance range (both at 95% C.L.) [77]. . . . . . . . . . . . . . . . . . . . . 46

7.1 Examples of the inflaton's forbidden decays due to the imposed symmetry. We represent the light scalar, gauge and fermion fields in blue for a clean understanding. . . . . . . . . . . . . . . . . . . . . . . . . . . . . . . . . . . . . . . 52

7.2 Numerical integration of the inflaton-radiation dynamical system of equations for $m_\phi = 10^{-3} M_P$, $M_1 = 0.55\, m_\phi$ and $h = 1$. Time evolution (A) of the inflaton and radiation energy density. In the green dashed line the radiation constancy regime is represented. Comparison (B) between Hubble parameter and the inflaton decay width, with the dashed line representing the maximum value of the decay width. Results are given in Plank units, $M_P = 1$ [1] . . . . . . . . 54

8.1 Observational predictions for an inflaton non-minimal coupling to gravity with a quartic potential for 50-60 e-folds of inflation. The red contours correspond to the 68% and 95% C.L. results from Planck [54] . . . . . . . . . . . 61

8.2 Numerical integration of the inflaton-radiation dynamical system of equations for $M_1 = 5 \times 10^{-5}$, $h = 1$ and $\lambda = 10^{-3}$. In (A) we show the time evolution of the inflaton and radiation energy density. In the green dashed line the radiation-damped-oscillator regime is represented. In (B) we give the comparison between Hubble parameter and the inflaton decay width and in the dashed line we represent the maximum value of the decay width. Results are given in Plank units, $M_P = 1$. . . . . . . . . . . . . . . . . . . . . . . . . . . . . 63

8.3 Dominant Feynman diagrams for evaporation processes . . . . . . . . . . . . 66

8.4 Resulting parameter space for $\xi = 0.1$, 1, and 10 for $g_\star = 100$. Orange lines represent reheating temperatures and the dashed line, $M_1 = T_R$, limits evaporation conditions. Condition (8.85) defines the complete decay and no reheating regions, and conditions (8.86),(8.87) limit the no-evaporation region. . . . . . . . . . . . . . . . . . . . . . . . . . . . . . . . . . . . . . . . . . . . 77

8.5 Resulting parameter space for $\xi = 0.1$, 1, and 10 for $g_\star = 100$ with no evaporation. Orange lines represent reheating temperatures and the blue dashed line, $M_1 = T_R$, limits the evaporation conditions. The $h = 1$, $T_R < T_{BBN}$ and $T_{CDM} < T_{eq}$ limits are also represented with the dashed lines. Condition (8.96) defines the complete decay and no reheating regions and conditions (8.97) and (8.98) limit the evaporation region. . . . . . . . . . . . . . . . . . . . . . . . . . 80

9.1 Diagrams contributing to the CP asymmetry $\epsilon$. . . . . . . . . . . . . . . . . . . . 83

9.2 Washout processes: Inverse decay, 2↔2 processes $\Delta L = 2$ and $\Delta L = 1$. . . . . 87

9.3 Resulting parameter space for $\xi = 2$, 10. Thermal leptogenesis region starts to appear for $\xi = 2$ due to the high required reheating temperatures. . . . . . . 92

# List of Tables

2.1 Neutrino oscillation data [45]. . . . . . . . . . . . . . . . . . . . . . . . . . . . . . . . 14

# Abbreviations

| | |
|---|---|
| **SM** | **S**tandard **M**odel |
| **EW** | **E**lectro**w**eak |
| **SCM** | **S**tandard **C**osmological **M**odel |
| **vev** | **V**acuum **E**xpectation **V**alue |
| **CKM** | **C**abibbo-**K**obayashi-**M**askawa |
| **PMNS** | **P**ontecorvo-**M**aki-**N**akagawa-**S**akata |
| **TBM** | **T**ri-**B**imaximal **M**ixing |
| **IH (NH)** | **I**nverted (**N**ormal) **H**ierarchy |
| **MSW** | **M**ikheyev-**S**mirnov-**W**olfenstein |
| **GUT** | **G**rand **U**nified **T**heory |
| **GR** | **G**eneral **R**elativity |
| **FRW** | **F**riedmann **R**obertson-**W**alker |
| **BB** | **B**ig **B**ang |
| **NMC** | **N**on-**M**inimal **C**oupling |
| **DM** | **D**ark **M**atter |
| **WIMP** | **W**eakly **I**nteracting **M**assive **P**article |
| **CL** | **C**onfidence **L**evel |
| **CDM** | **C**old **D**ark **M**atter |
| **BBN** | **B**ing **B**ang **N**ucleosyntesis |
| **CMB** | **C**osmic **M**icrowave **B**ackground |
| **C** | **C**harge Conjugation transformation |
| **P** | **P**arity transformation |
| **T** | **T**ime Reversal transformation |
| **IDM** | **I**nflaton **D**ark **M**atter |

# Chapter 1

# Introduction

The Standard Model of particle physics (SM) presents the best description ever achieved of elementary particle interactions. It has been very successful in a wide range of particle phenomena, from the prediction of the anomalous magnetic moment of the electron to the prediction of several elementary particles before their experimental discovery. Despite all of its achievements, experiments on neutrino oscillations, which the SM predict to be massless, revealed some flaws in the theory. Due to such experiments, we now know neutrinos must be massive, but the mechanism for mass generation remains unknown. The SM only includes left-handed neutrinos, with three generation of them, as opposed to the other fermions, which have also a right-handed component. Going beyond the SM, though without violating its structural symmetries, and allowing for the existence of right-handed neutrinos, also in three generations, could explain the mass appearance through what is known as the seesaw mechanism.

Moving now to the Universe's cosmological evolution and its description, the starting point for its analysis rests on the Standard Cosmological Model (SCM).The assumption of homogeneity and isotropy of space, represented in the Friedmann-Robertson-Walker space-time metric, together with the identification of the relative abundances of the Universe components, reveal how it may evolve and expand. However, some puzzles remain unanswered, in particular the flatness, horizon and the large scale structure problems. An inflationary evolution, developed in the 1980's, with an introduction of an early phase of accelerated expansion, prior to the radiation domination epoch, would flatten the universe and also stretch the initial small inhomogeneities to the observed today's large scale structures. The causality problem would then be solved by an initial causal contact between regions that today are too far to interact, reconnecting the theory to the almost perfect isotropy of the cosmic microwave background (CMB).

A common problem to both particle physics interactions and the cosmological behavior comes in the energy budget of the Universe. Only around 25% of the Universe is made of matter, and only about 15% is accounted for by SM particles leaving the remaining part, referred to as dark matter, to be described by new physics.

Another important open question about the Universe is the observed asymmetry between particles and anti-particles. Assuming an inflationary evolution, diluting any initial asymmetry in the Universe, the observed asymmetry should have been generated dynamically after inflation. Such mechanisms must follow the conditions derived by Sakharov [2]; (1) baryon-number violation, (2) C - and CP -violation, and (3) departure from thermal equilibrium. Within the SM, no mechanisms are able to generate the required amount of asymmetry, thus requiring extensions to new physics.

In this thesis we develop an inflationary model, regulated by a non-minimal coupling of the inflaton scalar field to gravity, which with an imposition of a symmetry will decay to two fermions, later to be identified with right-handed neutrinos[1]. Despite the need for an effective reheating, the inflaton does not decay completely, leaving room for this same scalar field to account for the dark matter in the Universe. The introduction of right-handed neutrinos, as decay products of the inflaton, and their interaction with the SM particles through an Yukawa coupling, allows for the generation of the observed light neutrino masses through the seesaw mechanism. As a final application of this model, we look at how the baryon asymmetry could be generated through thermal Leptogenesis. This description is based on the analysis present in [5].

We start in chapter 2 with a brief description of neutrino physics. Beginning with the SM paradigm, we then introduce massive neutrinos and the seesaw mechanism. A simple description of neutrino oscillations and their experimental features is also given.

In chapter 3 we present the basic aspects of Standard Cosmology with equilibrium thermodynamics. Then, we proceed in chapter 4 to describe the dynamics of inflation, exploring both the slow-roll dynamics and the evolution of quantum fluctuations of the inflaton field.

We continue by reviewing the introductory topics for this project in chapters 5 and 6 where we discuss the standard points on Dark Matter and Baryogenesis. In the former, the weakly interacting massive particles (WIMP) abundance calculation is also described.

In chapter 7 we present a review on the Inflaton Dark Matter model [1], on which this work is based, by describing the inflation and reheating dynamics with an imposed interchange symmetry on the Lagrangian. Reheating is studied with a quadratic potential obtaining constraints on the fermion masses and reheating temperatures.

[1]For other examples of scenarios where neutrinos are coupled to the dark sector, see e.g. [3, 4]

To produce a more realistic model, in chapter 8, we introduce a non-minimal coupling to gravity of the inflaton and a potential including both quadratic and quartic terms. The fermions are identified with two of the right-handed neutrinos, allowing mass terms for the light neutrinos. Furthermore, we describe how the inflaton scalar field can account for the present dark matter abundance, while successfully reheating the universe.

Finally we give, in chapter 9, an embedding of the thermal Leptogenesis scenario within our model, imposing important restrictions on the model parameters. A conclusion and a discussion of future work is given in chapter 10.

# Chapter 2

# Neutrinos

## 2.1 Neutrinos in the Standard Model

The Standard Model (SM) of electroweak (EW) and strong interactions is based on the gauge group $SU(3)_c \times SU(2)_L \times U(1)_Y$. The $SU(3)_c$ sector describes the strong interactions [6–8] and $SU(2)_L \times U(1)_Y$ the electroweak interactions [9–11]. In the SM there are 3 families (generations) of fermions, and in each generation there are 15 chiral fermions: 2 charged leptons, 1 neutrino and 12 quarks (3 colors).

From experiments in the late 1950's and early 1960's with beta and other weak decays, charged current weak interactions were established to be left-handed, implying that the underlying theory follows a $SU(2)_L$ local group. This organizes the participating fermions as left-handed and transforming as doublets. Besides the fermions, the Standard Model contains a zero spin scalar particle, the Higgs boson, and 12 vector fields, responsible for the gauge interactions. The SM Lagrangian can be decomposed in 4 sections:

$$\mathcal{L}_{SM} = \mathcal{L}_{Dirac} + \mathcal{L}_{Gauge} + \mathcal{L}_{Higgs} + \mathcal{L}_{Yuk} \,. \tag{2.1}$$

The Dirac sector includes the kinetic term and the fermion-gauge boson interactions through the covariant derivative. There is a term for each fermion of the model. The Gauge section encodes the gauge bosons kinetic terms and self interaction in the field strengths of each sub group of the SM gauge group.

The third term in equation (2.1) describes the Higgs boson dynamics including the spontaneous symmetry breaking of the electroweak group, $SU(2)_L \times U(1)_Y$, into the electromagnetic group $U(1)_{EM}$. The Higgs potential is written as

$$V(H) = -\mu^2 H^\dagger H + \lambda (H^\dagger H)^2 \,, \tag{2.2}$$

with $\mu^2 > 0$ such that $H$ acquires a vacuum expectation value $\langle H \rangle = \frac{1}{\sqrt{2}} \begin{pmatrix} 0 \\ v \end{pmatrix}$. The symmetry breaking process [12, 13], attributes masses to the Goldstone bosons related to the broken generators of $SU(2)_L \times U(1)_Y$, which are "eaten" by massive weak gauge bosons [14]:

$$M_{W^\pm} = \frac{g}{2} v \simeq 80 \text{ GeV}, \qquad M_Z = \frac{M_W}{\cos\theta_W} \simeq 91 \text{ GeV}, \tag{2.3}$$

where $v = 246$ GeV and $\theta_W$ is the Weinberg mixing angle. Since the $U(1)_{EM}$ symmetry is preserved, the fourth gauge boson remains massless and corresponds to the photon.

The interactions between fermions and the scalar particles are regulated by the Yukawa terms

$$\mathcal{L}_{Yuk} = y^\ell_{ij} \bar{L}_i H \ell_{jR} + y^d_{ij} \bar{Q}_i H d_{jR} + i\, y^u_{ij} \bar{Q}_i \tau_2 H u_{jR} + h.c.\,, \tag{2.4}$$

where $i$, $j$ are generation labels, $L$ and $Q$ represent the left-handed lepton and quark doublets, $\ell$, $u$, $d$ are the right-handed leptons and quarks. The $y_{ij}$ are the Yukawa coupling $3 \times 3$ matrices. After the electroweak symmetry breaking the Yukawa terms become

$$\mathcal{L}_{Yuk} = y^\ell_{ij} \frac{v}{\sqrt{2}} \bar{\ell}_i \ell_{jR} + y^d_{ij} \frac{v}{\sqrt{2}} \bar{d}_i d_{jR} + y^u_{ij} \frac{v}{\sqrt{2}} \bar{u}_i u_{jR} + h.c.\,, \tag{2.5}$$

allowing these fermions to acquire a mass. For example $m_e = y^e_{11} \frac{v}{\sqrt{2}} = 0.511$ MeV. If we had introduced directly a mass, as in the Dirac equation, the mass term would violate the $SU(2)_L \times U(1)_Y$ gauge symmetry explicitly, since it includes both left- and right-chiral representations. The Higgs mechanism is the simplest process that overcomes these restrictions.

The Standard Model does not include a right-handed neutrino and hence $m_\nu = 0$, a result that is valid to all orders in perturbation theory.

## 2.2 Massive Neutrinos

As established in the Standard Model, left-handed neutrinos together with charged leptons form the electroweak doublets. The former are known to have zero electric charge and no color. In early experiments neutrinos seemed to be massless and since right-handed neutrinos have yet to be observed they were not included in the SM. Thus, similarly to the photons, they were considered to be massless. More recent experiments on neutrino oscillations revealed their massive nature, pointing towards new physics. Please note that in the photon case, its zero mass comes from the conserved gauge symmetry which governs the electromagnetic interactions and for the neutrinos such a symmetry principle does not exist within the SM. A solution may come with the introduction of right-handed neutrinos, singlets under the $SU(2)_L$ gauge group as apposed the right-handed charged leptons.

Since neutrinos present no color and electric charge they allow for different possibilities in the construction of their mass terms. Neutrino masses could come from Majorana mass terms, that would violate the lepton number $L$. Their mass could also arise from a mixing with singlets of the SM symmetry group, for example, singlet fermions in extra dimensions. Please note that, although the lepton number is observed to be conserved in the SM interactions, it is not a required symmetry of the theory. Its violation in different processes would not in principle be wrong. Nevertheless, it is crucial that the possible mass generation mechanisms respond to the experimental observations in the neutrino masses and mixing angles.

A powerful way to generate neutrino masses [15, 16], using only the existent particles in the SM, comes from introducing extra degrees of freedom parametrized in non-renormalizable operators. The only dimension-five operator in these conditions consistent with gauge invariance [17] is

$$\frac{\lambda_{ij}}{M}(L_i H)^T (L_j H)\,, \tag{2.6}$$

where $i, j = e, \mu, \tau$ , $H$ and $L$ are the Higgs and lepton doublets, $\lambda_{ij}$ are dimensionless couplings and $M$ is the cutoff scale, the new physics scale above EW symmetry breaking. This term is called the Weinberg operator and violates the Lepton number symmetry. A Majorana neutrino mass term is therefore created

$$m_{ij} = \frac{\lambda_{ij} \langle H \rangle^2}{M}\,. \tag{2.7}$$

A possible interpretation could be that the operator is generated by some graviton-Planck scale effect. However $M \sim M_P$ and $\lambda \sim 1$ [18, 19] would lead to $m_{ij} = 10^{-5}$ eV, in disagreement with the observations, see section 2.2.4. Some new physics beyond the SM must then be introduced to obtain the desired masses.

### 2.2.1 Right Handed Neutrinos and the Seesaw Mechanism

Let us allow for the existence of right-handed neutrinos as singlets of the SM gauge group. These extra fermions present a very benign addition to the SM Lagrangian since they do not affect SM gauge anomaly cancellations and have very little experimental restrictions. In this scenario one can introduce the Yukawa coupling

$$y_\nu N^c\, H\, L + h.c\,, \tag{2.8}$$

that after electroweak symmetry breaking would lead to

$$m_D = y_\nu \langle H \rangle\,. \tag{2.9}$$

From experimental data we have the requirement of at least two $N$ fields in order to have at least two massive neutrinos. From equation (2.9) in order to have $m_D \sim 0.1$ eV, $y_\nu \sim 10^{-12}$ is required. It is indeed a very small value for the Yukawa coupling, especially when compared to charged fermion couplings. To compare, look at the order of the electron coupling, $O(10^{-5})$. It thus seems that this model is incomplete. There is another possibility for a mass term concerning the neutrinos. As said before, there could exist Majorana mass terms since the right-handed neutrinos would be singlets under SM gauge group. A term like

$$\frac{1}{2} N\, M_R N^c + h.c. \tag{2.10}$$

would be allowed. In the case of the three neutrino species, the mass parameters $m_D$ and $M_R$ are considered as $3 \times 3$ (nondiagonal) matrices. If we combine the two mass terms we have

$$\mathcal{L}_{\nu mass} = y_\nu^{\alpha i} \bar{N}_i \, H \, L_\alpha - \frac{1}{2} M_R^{ij} N_i N_j^c + h.c\,. \tag{2.11}$$

After EW symmetry breaking, this equation describes six potentially massive Majorana fermions all of which are linear combinations of $\nu_L$ and $N$ fields. Introducing $N_L = N^c$ we have that the general mass matrix, in the basis $(\nu_L, N_L)$ [15], is written as

$$M_\nu = \begin{pmatrix} 0 & m_D^T \\ m_D & M_R \end{pmatrix} . \tag{2.12}$$

The eigenvalues of this matrix will be the new Majorana fermion's mass terms. For both $M_R$ and $m_D \neq 0$ there are 3 possible regimes. However, to us, the most important comes when $M_R \gg m_D$. In this case, neutrino masses may split into two subsets. The first composed by the heavy neutrinos with masses approximately $M_R$, and then the light neutrinos with mass given by

$$\mathcal{M}_\nu = -m_D^T M_R^{-1} m_D\,. \tag{2.13}$$

The latter neutrinos are the ones which are observed experimentally and are parametrically lighter than the EW scale by a factor $\frac{m_D}{M_R}$. We see that with this mechanism, the neutrino Yukawa coupling is allowed to be of the same order of the charged lepton ones, while having arbitrarily large masses for the right-handed neutrinos, since their mass term is not constrained by any gauge symmetry. This is known as the the "seesaw" (type 1) mechanism [20–24] and gives a natural explanation for the smallness of neutrino masses.

As said before the introduction of right-handed neutrinos is benign to the SM Lagrangian since they only couple to SM particles via the Yukawa interactions. However, the motivation behind this addition must be understood. One of the strongest arguments to the inclusion of right-handed neutrinos comes from Grand Unified Theories (GUT) [16]. The

GUT gauge group $SO(10)$ predicts the existence of chiral fermions that are singlets under $SU(5) \to SU(3)_c \times SU(2)_L \times U(1)_Y$, the SM gauge group. These singlets could be what we call right-handed neutrinos. In $SO(10)$, the right-handed neutrino exists inside the **16** representation, and there are as many right-handed neutrinos as SM fermion generations. In some models, the right-handed neutrino mass is related to the GUT spontaneous symmetry breaking scale $M_{GUT}$ giving $M_R \sim M_{GUT} \sim 10^{16}$ GeV.

### 2.2.2 Neutrino Mass Matrix, flavours and the $U_{PMNS}$ Mixing Matrix

The left-handed electron, muon and tau neutrinos ($\nu_e$, $\nu_\mu$, $\nu_\tau$) are the states that form the weak doublets together with the charged leptons $e$, $\mu$ and $\tau$. These neutrino states are defined as the flavour neutrino states. In the SM interactions, both members of the weak doublet form the weak charged current

$$J^\mu = \bar{\ell}\gamma^\mu(1-\gamma_5)\nu_\ell \qquad \ell = e,\, \mu,\, \tau\,. \tag{2.14}$$

It is important to note that these phenomenologically defined flavour eigenstates, the ones represented in the weak charged current, may not precisely coincide with the theoretical flavour states, a result that may come from mixing with other heavy leptons as realized before in the seesaw mechanism.

There is also a difference in what is called the neutrino mass eigenstates and the neutrino flavour eigenstates, due to the observed neutrino oscillations. The flavour neutrinos, $\nu_e$, $\nu_\mu$, $\nu_\tau$, have no definite mass, and turn out to be combinations of the mass eigenstates $\nu_1$, $\nu_2$, $\nu_3$. We define the $U_{PMNS}$ matrix as

$$\nu_f = U_{PMNS}\nu\,, \tag{2.15}$$

where $\nu_f$ are the flavour states and $\nu$ the mass states. $U_{PMNS}$ is then a $3\times 3$ unitary matrix termed after Pontecorvo, Maki, Nakagawa and Sakata [25–27]. From equation (2.14) we see that the weak charged current ends up mixing neutrino mass states as

$$J^\mu = \bar{\ell}\gamma^\mu(1-\gamma_5)U_{PMNS}\nu\,. \tag{2.16}$$

Let us write the mass Lagrangian terms in what is called the "symmetry" basis $(\widetilde{\nu}, \widetilde{\ell})$ [15].

$$\mathcal{L} = \frac{1}{2}\bar{\widetilde{\nu}}\mathcal{M}_\nu\widetilde{\nu}^c_L + \widetilde{\ell}_L M_L \widetilde{\ell}_R + h.c. \tag{2.17}$$

This symmetry basis is the basis in which the underlying and unknown theory of fermion masses is formulated. Here, both $\mathcal{M}_\nu$ and $M_L$ are generally non-diagonal. Writing these mass terms we have also assumed that the light neutrinos are Majorana particles. It is possible to diagonalize these mass matrices by

$$M_\nu^d = U_\nu^T \mathcal{M}_\nu U_\nu \,, \qquad M_\ell^d = U_\ell^\dagger M_\ell V_\ell \,, \tag{2.18}$$

where $M_{\nu,\ell}^d$ are diagonal matrices and the unitary transformation matrices $U_\ell$, $V_\ell$ *and* $U_\nu$ connect the symmetry basis with mass eigenstates as $\widetilde{\nu} = U_\nu \nu$, $\widetilde{\ell}_L = U_\ell \ell_L$ and $\widetilde{\ell}_R = V_\ell \ell_R$. Inserting this in the charged current we obtain,

$$J^\mu = \bar{\widetilde{\ell}} \gamma^\mu (1-\gamma_5) \widetilde{\nu} = \bar{\ell} \gamma^\mu (1-\gamma_5) U_\ell^\dagger U_\nu \nu \,, \tag{2.19}$$

and identify the mixing matrix with

$$U_{PMNS} = U_\ell^\dagger U_\nu \,. \tag{2.20}$$

This mixing matrix is by convention parametrized as

$$U_{PMNS} = U_{23}(\theta_{23}) U_{13}(\theta_{13}, \delta) U_{12}(\theta_{12}) I_\phi \,, \tag{2.21}$$

where $U_{ij}$ are matrices of rotations in the $ij$ plane by $\theta_{ij}$, $\delta$ is the Dirac CP-violating phase, and $I_\phi = diag\left(1, e^{i\phi_1}, e^{i\phi_2}\right)$ corresponds to the Majorana CP-violating phases.

Following what is called the “bottom-up” approach [15], using experimental data we can infer possible structures underlying the neutrino mixing matrix . The detected maximal 2-3 mixing, large 1-2 mixing and small 1-3 mixing point that some “textbook” mixing matrices may be able to draw us a first draft of the unknown physics. Examples like the bimaximal $U_{bm} = U_{23}^m U_{12}^m$, where we have maximal $\left(\frac{\pi}{4}\right)$ rotations in 2-3 and 1-2 subspaces, and the tribimaximal mixing matrix, $U_{TBM} = U_{23}^m U_{12}\left(\theta_{12}\right)$ with $\sin^2\theta_{12} = \frac{1}{3}$, are commonly used for this first lowest order approximation.

$$U_{TBM} = \frac{1}{\sqrt{6}} \begin{pmatrix} 2 & \sqrt{2} & 0 \\ -1 & \sqrt{2} & \sqrt{3} \\ 1 & -\sqrt{2} & \sqrt{3} \end{pmatrix} \tag{2.22}$$

Nevertheless, these matrices may reveal certain symmetries and deviations from them can explain effects from the violation of such symmetries.

In this bottom-up approach we should obtain by reconstruction the neutrino mass matrix in a flavour basis. Here, the mass matrix of the charged leptons is diagonal and therefore the neutrino mass is diagonalized by $U_{PMNS} = U_\nu$ . From equation (2.18) we have

$$\mathcal{M}_\nu = U^*_{PMNS} M^d_\nu U^\dagger_{PMNS} \, , \tag{2.23}$$

where $\mathcal{M}_\nu$ is the flavour basis and

$$M^d_\nu = diag\left(m_1, m_2 e^{-2i\phi_1}, \, m_3 e^{-2i\phi_2}\right) . \tag{2.24}$$

### 2.2.3 Neutrino Oscillations

Measurements of neutrino fluxes coming from different sources revealed a difference between the expected, with massless neutrinos, and the observed results. This anomaly was detected in both solar and atmospheric neutrino experiments and constitutes one of the first evidences of physics beyond the SM. These oscillations are caused by neutrino mixings and constitute the most precise measurement of light neutrino masses and mixing angles.

The physics behind this process is similar to strangeness oscillations in neutral kaons $K^0 - \bar{K}^0$. These particles are produced in strong interactions, with quark composition $d\bar{s}$ and $s\bar{d}$ respectively. However, none of the two is a physical particle. Instead they work as superpositions of the physical states $K_L$ and $K_S$, which do not have a defined value of strangeness.

In the SM model, neutrinos only interact through the weak force. They are generated, for example, in charged lepton decays or leptonic nuclear processes and come out in the flavour eigenstates , $\nu_e$, $\nu_\mu$ and $\nu_\tau$. The mass eigenstates, $\nu_i$ with $i = 1, 2, 3$ are related to the flavour states through an unitary transformation as described in the previous section in equation (2.15).

The propagation of each neutrino mass eigenstate in vacuum is written as

$$i \frac{\partial}{\partial t} \left|\nu_i\right\rangle = E_i \left|\nu_i\right\rangle \tag{2.25}$$

with a free particle solution of the form

$$\left|\nu_i(t)\right\rangle = e^{iE_i t} \left|\nu_i(0)\right\rangle \, , \tag{2.26}$$

where $\left|\nu_i(0)\right\rangle$is the initial state of the neutrino. Making the ultrarelativistic approximation, due to the very small neutrino masses, we have

$$E_i = \sqrt{p_i^2 + m^2} \approx p_i + \frac{m_i^2}{2p_i} . \tag{2.27}$$

Since the different mass eigenvalues are produced coherently $p_i = p \approx E = E_i$ and so applying equation (2.26) in (2.25), after a propagation over a distance L we have

$$|\nu_i(t)\rangle = e^{-iEt} e^{-i\frac{m_{\nu_i}^2 L}{2E}} |\nu_i(0)\rangle \,. \tag{2.28}$$

Using the mixing relation from equation (2.15) we have that the probability of finding a neutrino flavour $\beta$ in a flavour $\alpha$ beam is

$$\begin{aligned} P\left(\nu_\alpha \to \nu_\beta\right) &= \left|\left\langle \nu_\beta | \nu_\alpha(t) \right\rangle\right|^2 = \left| e^{-iEt} \sum_i U_{\alpha i}^* e^{-i\frac{m_i^2 L}{2E}} U_{\beta i} \right|^2 \\ &= \delta_{\alpha\beta} - 4 \sum_{i<j} Re\left(U_{\alpha i}^* U_{\beta i} U_{\alpha j} U_{\beta j}^*\right) \sin^2\left(\frac{\Delta m_{ij}^2 L}{4E}\right) + 2 \sum_{i<j} Im\left(U_{\alpha i}^* U_{\beta i} U_{\alpha j} U_{\beta j}^*\right) \cos^2\left(\frac{\Delta m_{ij}^2 L}{4E}\right), \end{aligned} \tag{2.29}$$

where $\Delta m_{ij}^2 = m_i^2 - m_j^2$ is the squared mass difference between the two neutrinos.

### 2.2.4 Experimental Observations

Having described the fundamental parameters and dynamics of massive neutrinos, we can now explore the basic aspects of the first indicator of such property, the neutrino oscillations experiments.

**Solar Neutrinos** Electron neutrinos $\nu_e$ are produced in nuclear reactions close to the core of the Sun. Their energy is estimated to be around $1 - 10$ MeV and through SM interactions we can further calculate the corresponding expected flux. In observations, started in the 1960s by Ray Davis and John Bahcall in the Homestake [28] experiment, only approximately a third of the expected flux was detected. In the experiment, the $\nu_e$ flux was measured indirectly by measuring the $^{37}Ar$ abundances in a water tank after the $\nu_e +^{37} Cl \to {}^{37}Ar + e^-$ reaction induced by the electron neutrinos. This deficit in the $\nu_e$ flux was called the Solar Neutrino Problem (SNP).

Solutions including neutrino oscillations, neutrino decays and alternatives to the Solar interactions were readily proposed. The Homestake results were confirmed later by SNO [29], Gallex [30], GNO [31] and the Super-Kamiokande [32], where the flavour neutrino fluxes can be measured. In the SNO experiment the electron neutrino flux was measured to be less than half of the total neutrino flux, indicating that, while propagating, neutrinos change their flavour.

**Atmospheric Neutrinos** In the collision of cosmic rays in upper layers of the Earth's atmosphere, another "type" of neutrinos may be produced. From high energy processes involving the cosmic rays, pions are generated in the atmosphere. Then, these may decay into muons and muon neutrinos, $\pi^- \to \mu^- + \bar{\nu}_\mu$, $\pi^+ \to \mu^+ + \nu_\mu$, with a likely subsequent decay of the former into electron neutrinos and muon neutrinos, $\mu^- \to e^- \bar{\nu}_e \nu_\mu$, $\mu^+ \to e^+ \nu_e \bar{\nu}_\mu$, with energies above the 100 MeV scale. Since the latter decay results in the same number of $\nu_e$ and $\nu_\mu$ a total ratio of 1:2 would be expected when considering all atmospheric neutrino production channels. Measurements in Super-Kamiokande [33] recorded a ratio smaller than 1:2 from $\nu_e : \nu_\mu$.

**Terrestrial Neutrinos** Accelerator experiments, K2K [34], T2K [35], NO$\nu$A [36], MIMOS [37, 38], provide a study with relatively high energy, around $1 - 10$ GeV, and a relatively short traveling distance between the source and the detector, $L \sim \mathcal{O}(100\text{ m}) - \mathcal{O}(10^3\text{ km})$. As it can be seen in equation (2.29) the transition amplitude is relevant when $\Delta m^2 L \sim E$. Generally studies are done on the $\nu_e \leftrightarrow \nu_\mu$ flavour transition, but with higher energies, e.g. MIMOS and OPERA, $\nu_\tau \leftrightarrow \nu_\mu$ is also possible.

Another terrestrial neutrino study source is at the nuclear reactors CHOOZ [39] and KamLAND [40]. In fission experiments, neutrons are produced, for instance in ${}^{235}_{92}U + n \to {}^{94}_{40}Zr +^{140}_{58} Ce + 2n$. These neutrons decay and generate anti-electron neutrinos $\bar{\nu}_e$. These experiments study the disappearance of $\bar{\nu}_e$ at energies around the 10 MeV scale and traveling distances of order $1 - 250$ km.

**Cosmic Neutrinos** A different source of neutrinos may come from Ultra High Energy Cosmic Rays [41]. Energies of $\sim 10^{11}$ GeV are expected, but very little is known about their production and oscillation length. Experiments AMANDA [42], AUGER [43] and ICE CUBE [44] were designed to study this "new" source.

Currently, the resulting parameters from neutrino oscillations are well measured, as presented in Table 2.1

| Parameter | Best Fit $\pm 1\sigma$ | |
|---|---|---|
| | Normal hierarchy | Inverted hierarchy |
| $\Delta m^2_{21}$ | $(7.56 \pm 0.19) \times 10^{-5}$ eV$^2$ | |
| $\Delta m^2_{32}$ | $(2.55 \pm 0.04) \times 10^{-3}$ eV$^2$ | $(2.47 \pm 0.04) \times 10^{-3}$ eV$^2$ |
| $\sin^2\theta_{12}$ | $0.321 \pm 0.015$ | |
| $\sin^2\theta_{23}$ | $0.430 \pm 0.019$ | $0.598 \pm 0.016$ |
| $\sin^2\theta_{13}$ | $(2.155 \pm 0.008) \times 10^{-2}$ | |

TABLE 2.1: Neutrino oscillation data [45].

From neutrino oscillations in vacuum, mass hierarchies cannot be extracted. Nevertheless matter effects on neutrino oscillations may present a viable way to solve such a question. For instance, when neutrinos propagate in matter, where almost no muons or taus exist, only the electron neutrinos will scatter through charged current interactions. This extra potential term in the electron neutrino Hamiltonian will enhance or suppress the oscillations, thus changing the transition rates. The effect is called MSW after Mikheyev, Smirnov and Wolfenstein. For a more complete description see [46, 47]. Terrestrial experiments may be a source to clarify this open question.

From the above table, a tribimaximal neutrino mixing matrix presents a very good approximation with $\theta_{23} = \frac{\pi}{4}$, $\theta_{13} = 0$ and $\sin^2\theta_{12} = \frac{1}{3}$. In our study connecting neutrino masses and the Inflaton Dark Matter model developed in chapter 8 we will proceed using the tribimaximal ansatz, equation (2.22).

# Chapter 3

# Standard Cosmology

## 3.1 Friedmann-Robertson-Walker Universe

The dynamics of the Universe is regulated by Einstein's equations

$$R_{\mu\nu} - \frac{1}{2} g_{\mu\nu} R = 8\pi G T_{\mu\nu} + \Lambda g_{\mu\nu} \tag{3.1}$$

where $R_{\mu\nu}$ is the Ricci tensor, $R$ the Ricci scalar, $g_{\mu\nu}$ the metric, $\Lambda$ is the cosmological constant, $G$ the Newton's gravitational constant and $T_{\mu\nu}$ is the stress-energy tensor. Assuming homogeneity and isotropy of space, Einstein's equations are simplified with the Friedmann-Robertson-Walker metric, with a line element of the form

$$ds^2 = dt^2 - a^2 \left( \frac{dr^2}{1 - kr^2} + r^2 d\Omega^2 \right) , \tag{3.2}$$

where $a(t)$ is the scale factor, $k$ is the spatial curvature, $d\Omega^2 = d\theta^2 + \sin^2\theta d\phi$ and $(t, r, \theta, \phi)$ are comoving coordinates. With the assumption that the energy content of the Universe is a perfect fluid we may write the stress energy tensor as

$$T_{\mu\nu} = -p g_{\mu\nu} + (p + \rho)\, u_\mu u_\nu , \tag{3.3}$$

where $p$ and $\rho$ are the pressure and energy density of the perfect fluid, $u^\mu$ denotes the four velocity of the fluid normalized such that $u^\mu u_\mu = 1$.

Working through the computations with the FRW metric in Einstein's equations [48] we obtain for the $\mu = \nu = 0$ component

$$H^2 + \frac{k}{a^2} = \frac{8\pi G}{3}\rho + \frac{\Lambda}{3} , \tag{3.4}$$

known as Friedmann equation, where $H$, the Hubble parameter, is defined as $H \equiv \frac{\dot{a}}{a}$. Due to the covariant conservation, from Bianchi identities, of the Einstein tensor $G_{\mu\nu} = R_{\mu\nu} - \frac{1}{2}g_{\mu\nu}R$ we also have covariant conservation of the stress-energy tensor. We then obtain an energy momentum conservation equation

$$\dot{\rho} + 3H(\rho + p) = 0\,. \tag{3.5}$$

The energy density of different fluids is thus diluted with expansion as:

- Radiation: $p_{rad} = \frac{1}{3}\rho_{rad} \to \rho_{rad} \propto a^{-4}$;
- Matter: $p_{mat} = 0 \to \rho_{mat} \propto a^{-3}$;
- Vacuum energy: $p_\Lambda = -\rho_\Lambda \to \rho_\Lambda = constant$ .

The Friedmann equation (3.4) describes the expansion of the Universe, with the Hubble parameter telling us how fast it is happening. It will play an important role when discussing particle interactions during the cosmological evolution.

From strong experimental evidence of a present flat Universe and justified within the inflation theory, see chapter 4, the curvature factor can be set to zero.

## 3.2 Equilibrium Thermodynamics

From CMB black body radiation analysis we have strong evidence for the existence of thermal equilibrium, in the early Universe, between particles and photons in what is called the thermal bath. Let us recall the basic features of equilibrium thermodynamics [48].

Species in kinetic equilibrium can be described by the Bose-Einstein or Fermi-Dirac statistics, whose distribution functions are given by

$$f\,(\mathbf{p}) = \frac{1}{\exp\left(\frac{E-\mu}{T}\right) \pm 1}\,, \tag{3.6}$$

where $E^2 = |\mathbf{p}|^2 + m^2$ is the energy of the particles, $\mu$ is the chemical potential and the (+) sign corresponds to fermions, while (-) applies to bosons. To achieve local thermal equilibrium, besides kinetic equilibrium particles must also be in chemical equilibrium. The later condition means than in an $AB \leftrightarrow CD$ process the equality $\mu_A + \mu_B = \mu_C + \mu_D$ must be verified.

The equilibrium density of particles of type $i$ with momentum in a range $d^3p$ centered at $\mathbf{p}$ is given by

$$g_i \frac{d^3 p_i}{(2\pi)^3} f\left(\mathbf{p}_i\right) \,, \tag{3.7}$$

where $g_i$ is the number of internal degrees of freedom. Thus to obtain the number density $n$, energy density $\rho$ and pressure $p$ of a dilute and weak- interacting gas of particles we use

$$n = g \int \frac{d^3 p}{(2\pi)^3} f\left(\mathbf{p}\right), \tag{3.8}$$

$$\rho = g \int \frac{d^3 p_i}{(2\pi)^3} E\left(\mathbf{p}\right) f\left(\mathbf{p}\right), \tag{3.9}$$

$$p = g \int \frac{d^3 p_i}{(2\pi)^3} \frac{|\mathbf{p}|^2}{3E\left(\mathbf{p}\right)} f\left(\mathbf{p}\right). \tag{3.10}$$

Let us see how these expressions work in their asymptotic limits, in the limit $|\mu| \ll T$.

In the relativistic case where $T \gg m$:

- Fermions
$$n_f = \frac{3}{4} g_i \frac{\zeta(3)}{\pi^2} T^3; \tag{3.11}$$

- Bosons
$$n_b = g_i \frac{\zeta(3)}{\pi^2} T^3; \tag{3.12}$$

where $\zeta(z)$ is the Riemann zeta-function. This results in $n_f = \frac{3}{4} n_b$.

For the energy density

$$\rho_b = \frac{\pi^2}{30} g_i T^4, \tag{3.13}$$

$$\rho_f = \frac{7}{8} \frac{\pi^2}{30} g_i T^4. \tag{3.14}$$

In this limit $E \sim |p|$ so from, equation (3.10), $p = \frac{\rho}{3}$.

In the non-relativistic case, where $T \ll m$, where we write $E \approx m + \frac{|p|^2}{2m}$

$$n \approx g \left(\frac{mT}{2\pi}\right)^{\frac{3}{2}} e^{-\frac{m}{T}} \,, \tag{3.15}$$

and we recover the Boltzmann distribution for both bosons and fermions. To leading order we obtain for the energy density

$$\rho = m\, n \,, \tag{3.16}$$

and for the pressure, using $\frac{|p|^2}{E} = \frac{|p|^2}{m}$, we then get

$$p = nT \,. \tag{3.17}$$

We have obtained the equation of state of a perfect gas $p = nk_BT$, where the Boltzmann constant $k_B = 1$ in natural units. Since $T \ll m$, we see that $p \ll \rho$, showing that non-relativistic particles behave as pressureless matter.

Because the energy density of a non-relativistic particle is exponentially suppressed when compared with the relativistic one, the total energy density of a system in equilibrium is essentially given by its relativistic component

$$\rho_{rad} = \frac{\pi^2}{30} g_*(T) T^4 \,, \tag{3.18}$$

where $g_*(T)$ corresponds to the effective number of relativistic degrees of freedom at temperature $T$:

$$g_*(T) = \sum_{bosons} g_i \left(\frac{T_i}{T}\right)^4 + \frac{7}{8} \sum_{fermions} g_i \left(\frac{T_i}{T}\right)^4 \,, \tag{3.19}$$

where $T_i$ denotes the effective temperature for any species. For particles in thermal equilibrium $T_i = T$ and for decoupled species $T_i \neq T$. In the Standard Model of particle physics for $T \geq 1$ TeV all degrees of freedom are in equilibrium, giving $g_\star \approx 106.75$.

We now introduce the entropy density defined as

$$s = \frac{p + \rho}{T} \,, \tag{3.20}$$

which can be derived from the First law of Thermodynamics. For relativistic species $p = \frac{\rho}{3}$, then

$$s = \frac{4}{3} \frac{\rho}{T} = \frac{2\pi^2}{45} g_{*S}(T) T^3 \,, \tag{3.21}$$

where $g_{*S}(T)$ is the effective number of relativistic degrees of freedom contributing to the entropy

$$g_{*S}(T) = \sum_{bosons} g_i \left(\frac{T_i}{T}\right)^3 + \frac{7}{8} \sum_{fermions} g_i \left(\frac{T_i}{T}\right)^3 \,. \tag{3.22}$$

From this we see that for particles in thermal equilibrium $g_{*S}(T) = g_*(T)$. For decoupled species, this is no longer true and differences can be seen at low temperatures, in particular as neutrinos decouple from the photon bath.

Entropy conservation implies that the entropy in a comoving volume remains equal as the Universe expands, $S = a^3 s$,

$$g_{*S} T^3 a^3 = const \,. \tag{3.23}$$

Far from mass thresholds, $g_{*S}$ stays approximately constant and $T \propto a^{-1}$. Using $s \propto a^{-3}$, we define the number of particles of a given species in a comoving volume as

$$N_i = a^3 n_i = \frac{n_i}{s}\,, \tag{3.24}$$

where the scale factor was redefined to absorb the constant factors. In the case where this number remains constant, for example with no particle creation or annihilation, we have

$$N_i = \begin{cases} \frac{45\zeta(3)}{2\pi^4}\frac{g_i}{g_{*S}} & for\ T \gg m_i \\ \frac{45\zeta(3)}{4\sqrt{2\pi}}\frac{g_i}{g_{*S}}\left(\frac{m_i}{T}\right)^{\frac{3}{2}} e^{-\frac{m_i}{T}} & for\ T \ll m_i\,. \end{cases} \tag{3.25}$$

As an important consequence, if there is no baryon number production or destruction the baryon-to-entropy ratio is conserved

$$\eta_s = \frac{n_B}{s} = \frac{n_b - n_{\bar{b}}}{s} = const\,. \tag{3.26}$$

Here $b$ and $\bar{b}$ denote baryons and anti-baryons.

In an expanding Universe, a given particle species is in equilibrium with the cosmic thermal bath if it interacts with the latter at a rate $\Gamma \gtrsim H$. With the temperature decrease of the Universe, interactions may reach a temperature $T_F$, called the freeze out temperature, for which

$$\Gamma(T) \lesssim H(T) \qquad for\ T \lesssim T_F\,. \tag{3.27}$$

At this moment species depart from thermal equilibrium, and their abundance remains constant after decoupling from the thermal bath, $n/s = const$.

# Chapter 4

# Inflation

## 4.1 Problems of the Hot Big Bang Model

Through a model built in a homogeneous and isotropic Friedmann-Robertson-Walker space time, expanding according to the relative abundances of relativistic, non-relativistic matter and vacuum energy, we are able to describe most of the Universe as it is observed. However, when trying to explain and predict its past evolution from the present conditions, the Hot Big Bang Model presents itself as insufficient. In order to be the complete theory, the Universe would have to start from very special and fined-tuned initial conditions, making our presently observed Universe something like an "improbable accident". Let us now analyze some of the shortcomings of Standard Cosmology [48–50].

### Horizon Problem

From measurements of the cosmic background of microwave radiation we have seen that the temperature across the sky is around 2.73 K, with very small deviations of the order of $10^{-5}$. From the time of last scattering, around 380000 years after the Big Bang, photons have free streamed throughout the Universe. Thus, we may conclude that all the points in the last scattering surface would have been at the same temperature as well.

The causal horizon at a conformal time $\tau$ is $\ell = c\,\tau$, with c being the speed of light constituting the maximum distance that can be traveled since the Big Bang at $\tau = 0$.

The proper distance is given by

$$d_H = a\,(t) \int_0^t \frac{dt}{a\,(t')}, \tag{4.1}$$

where for a radiation dominated Universe $a \propto t^{\frac{1}{2}}$ and so $d_H = 2t$. We then see that more and more scales may come into causal contact as the Universe evolves. This means that some regions may only be coming into causal contact at the present day. There are thus many causally disconnected regions at the last scattering surface, which cannot have thermalized. Therefore, unless we expect the present homogeneity to be created at the Big Bang, there is no known physical process capable of such thermalization.

### Flatness Problem

From the Friedmann equation

$$H^2 = \frac{\rho}{3M_p^2} - \frac{k}{a^2}\,, \tag{4.2}$$

and using $\Omega = \frac{\rho}{\rho_c}$, with $\rho_c = 3H^2 M_p^2$, we can write

$$\Omega^{-1} - 1 = -\frac{3M_P^2\,k}{\rho a^2}\,. \tag{4.3}$$

For a flat Universe, $k = 0$ hence $\Omega = 1$. Since in a matter dominated Universe $\rho \propto a^{-3}$ with $\Omega^{-1} - 1 \propto a$ and in a radiation dominated Universe $\rho \propto a^{-4}$, $\Omega^{-1} - 1 \propto a^2$, we see that any small deviations from unity at any time will grow as the Universe expands. Thus, $\Omega = 1$ is an unstable fixed point. Therefore, the near flatness observed today, $\Omega(a_0) \sim 1$, through Standard Big Bang Cosmology, would require extreme fine tuning of $\Omega$ in the early Universe. Deviations from flatness at BBN, GUT and Plank scale would have to follow very strict conditions:

$$|\Omega(T_{BBN}) - 1| \leqslant O(10^{-16})\,, \tag{4.4}$$

$$|\Omega(T_{GUT}) - 1| \leqslant O(10^{-55})\,, \tag{4.5}$$

$$|\Omega(T_P) - 1| \leqslant O(10^{-60})\,. \tag{4.6}$$

### Relic Density Problem

In Standard Cosmology the temperature of the Universe, defined as the temperature of the photon thermal bath, can reach arbitrarily learge values. Temperature can rise well above the SM scale and go up to the Plank scale, $M_P \sim 10^{18}$ GeV. In this limit, gravitational interactions as we describe with General Relativity may no longer work due to quantum effects.

We know that coupling constants in the SM vary with energy as a result of their quantum interactions. There is a strong suggestion that these couplings become comparable at energies around $10^{16}$ GeV, indicating the possibility of a Grand Unified Theory. We then expect one or more phase transitions to occur in the early Universe, where the higher GUT gauge groups are spontaneously broken into the SM gauge group, similarly th the electroweak Higgs mechanism. These phase transitions should produce superheavy stable particles, topological defects, such as magnetic monopoles, that would have survived until today. Such scenarios would have produced a too large relic density that would have dominated the Universe, $\Omega_{mon} \gg 1$. The Standard Cosmology has no mechanism to avoid overproduction of these relics or any process capable of diluting their abundance.

### The Origin of Large-Scale Structure in the Universe

Although the Universe is considered homogeneous and isotropic on large scales, we can clearly detect inhomogeneities on much smaller scales, like stars, clusters, voids and superclusters. These structures should arise from the non-linear gravitational growth of density fluctuations that were small and linear at the time of last scattering, as can be observed in the fluctuations in CMB temperature. We know that all physical wavelengths $\lambda(t)$, proportional to the scale factor $a(t)$, are stretched by expansion. Thus, the presently observed smaller scale structure corresponds to fluctuations on a much smaller scale that have evolved since the time of last scattering. However, the existence of a particle horizon in standard matter or radiation-dominated cosmology implies that they must have been outside the causally allowed region at some point in the past. Within standard Cosmology, there is no mechanism to generate these fluctuations on super-horizon scales.

## 4.2 First Approach on Inflation

From the shortcomings of the Hot Big Bang Model, we see that modifications in the early Universe are needed. They have to respond to the required flatness and smoothness, allow for the existence of the observed cosmic structure and reduce the abundance of unwanted relics. Let us start with the two most imperative, the horizon and flatness problems [48, 49].

The comoving horizon distance can be written as

$$\ell = \int_0^t \frac{dt}{a(t')} = \int_{a_i}^a \frac{da'}{a'^2 H(a')} \,. \tag{4.7}$$

In the radiation era $H \propto a^{-2}$, then the $\ell$ value converges when we make $a_i \to 0$, yielding a finite particle horizon. If $H$ decreases more slowly than $a^{-1}$, this integral will diverge when we take the limit of an initial singularity. Thus, there would not be a finite horizon and all the scales could be in causal contact. Using

$$a(t) \propto t^p \implies H = \frac{p}{t} \propto a^{-\frac{1}{p}} \,, \tag{4.8}$$

and we would not obtain a finite horizon for $p > 1$. Since $\ddot{a} \propto p(p-1)t^{p-1}$, in these conditions we would be in an accelerated expansion phase. So, if the Universe's expansion were accelerating at early times, one could have an arbitrarily large particle horizon.

From the analysis of the flatness problem, recalling equation (4.3) we see that if $\rho$ decreases more slowly than $a^{-2}$, the deviations from flatness may decrease. Since $\rho \propto a^{-3(1+w)}$ then $w < -\frac{1}{3}$, which would be the same condition obtained from the horizon problem, requiring an accelerated expansion period.

Therefore, an inflationary period, preceding the radiation era, may solve two of most screaming problems of the Standard Cosmology. Although a solution with a cosmological constant would satisfy these first requirements, it would not redshift away and there would be no period of matter or radiation domination. Nevertheless, a solution with a temporary $\Lambda$ behavior, that decays away, would, in principle, work well.

Let us find what would be the necessary conditions, on the accelerated expansion period, such that our needs are satisfied. First, from the horizon problem, we shall impose that all visible scales at the present moment where once in causal contact before the end of inflation and the beginning of the Standard Cosmology evolution. In order to satisfy this requirement, the size of the comoving horizon at the end of inflation must have been larger than the comoving distance that light can travel from that moment until today. Making the origin of conformal time at the end of inflation, then the accelerated expansion period should have started at a time $-\tau_i$ and as a result $\tau_i \geq \tau_0$. As said before, we want a fluid, that for a defined period of time behaves like a cosmological constant. In this period the Hubble parameter will remain approximately constant, thus

$$\tau_i = \int_{a_i}^{a_f} \frac{da}{a^2 H} \simeq \frac{1}{H_{inf} a_i}, \tag{4.9}$$

since $a_f \gg a_i$. For a radiation domination period $H \propto a^{-2}$, $a^2 H = a_f^2 H_{inf}$, then

$$\tau_0 = \int_{af}^{a_0} \frac{da}{a^2 H} = \frac{1}{H_{inf} a_f^2}, \tag{4.10}$$

since $a_0 = 1 \gg a_f$ . From the condition

$$\tau_i \geq \tau_0 \implies a_f^2 > a_i \implies \frac{a_f}{a_i} > \frac{a_0}{a_f} = \frac{T_R}{T_0}, \tag{4.11}$$

where the condition $a \propto T^{-1}$ was used and $T_R$ is the "reheating" temperature at the end of inflation. This result can be represented as

$$\frac{a_f}{a_i} = e^{N_e}, \tag{4.12}$$

with $N_e$ being the number of e-folds of the accelerated expansion. Using $T_0 \sim 10^{-4}$ eV and the reheating temperature around the GUT scale $M_{GUT} \sim 10^{16}$ GeV, then $N_e \sim 66$ e-folds. Since we expect the reheating temperature to be less than the GUT scale to avoid monopole production after inflation, the number of e-folds should be around $50 - 60$.

This very fast expansion that occurs during inflation, following an exponential behavior instead of the square root law in a radiation period, will also easily redshift and dilute away any particle species existent in the very early Universe.

## 4.3 Inflation Dynamics: Introduction of a Scalar Field

As seen previously, a solution like a cosmological constant cannot be applied for inflation and a different method to obtain an accelerated expansion is necessary. A fluid with negative pressure that is able to decay away after reproduction of the required expansion must be included [51–53]. The simplest solution comes with the introduction of a single scalar field, $\phi$, the inflaton. Recall from Quantum Field Theory that scalar fields describe relativistic bosons of spin zero. The classical values for the field $\phi$ represent the collective behavior of Bose-Einstein condensates of spin zero particles, which preserve Lorentz invariance, i.e., are invariant under both boosts and rotations.

This scalar field dynamics, with a minimal coupling to gravity, is described by the action

$$S = \int d^4x\sqrt{-g}\left[\frac{1}{2}R - \frac{1}{2}\partial_\mu\phi\partial^\mu\phi - V(\phi)\right] = S_{EH} + S_\phi\,, \tag{4.13}$$

with $S_{EH} = \int d^4x\sqrt{-g}\frac{1}{2}R$ being the Einstein-Hilbert action. In $S_\phi$ we have described both the kinetic and gradient energy through $\frac{1}{2}\partial_\mu\phi\partial^\mu\phi$ and the field's self interactions through the potential $V(\phi)$.

The energy-momentum tensor is then given by

$$T^{\mu\nu}_\phi = \frac{2}{\sqrt{-g}}\frac{\delta S_\phi}{\delta g_{\mu\nu}} = -\left(\frac{1}{2}\partial_\mu\phi\partial^\mu\phi + V(\phi)\right)g^{\mu\nu} + \partial^\mu\phi\partial^\nu\phi\,. \tag{4.14}$$

For a FRW geometry

$$T_{00} = \frac{1}{2}\dot{\phi}^2 + \frac{1}{2}\frac{(\nabla\phi)^2}{a^2} + V(\phi)\,, \tag{4.15}$$

$$T_{ij} = \partial_i\phi\partial_j\phi - a^2\gamma_{ij}\left(-\frac{1}{2}\dot{\phi}^2 + \frac{1}{2}\frac{(\nabla\phi)^2}{a^2} + V(\phi)\right)\,, \tag{4.16}$$

where the gradients are taken with respect to comoving coordinates and $(\nabla\phi)^2 = \delta^{ij}\partial_i\phi\partial_j\phi$, since $k = 0$.

Restricting to the case of a homogeneous field $\phi(t, \mathbf{x}) = \phi(t)$, the scalar field energy momentum tensor simplifies and becomes like a perfect fluid with

$$\rho_\phi = T_{00} = \frac{1}{2}\dot{\phi}^2 + V(\phi)\,, \tag{4.17}$$

$$p_\phi = g^{ij}\frac{T_{ij}}{3} = \frac{1}{2}\dot{\phi}^2 - V(\phi)\,. \tag{4.18}$$

The resulting field equation of state parameter is

$$w_\phi \equiv \frac{p_\phi}{\rho_\phi} = \frac{\frac{1}{2}\dot{\phi}^2 - V(\phi)}{\frac{1}{2}\dot{\phi}^2 + V(\phi)}\,, \tag{4.19}$$

showing that the field $\phi$ may have different equation of state parameters:

- $\rho_\phi = p_\phi$, if the kinetic term is dominant and $w = 1$;
- $\rho_\phi = -p_\phi$, if the potential term is dominant and $w = -1$;
- $\rho_\phi = 0$, if the kinetic term and potential terms are comparable and $w = 0$;
- $\rho_\phi = 3p_\phi$, while oscillating in a quartic potential and $w = 1/3$.

It is then desirable to have a dominant potential energy $V(\phi)$, such that the inflaton field reproduces an effective $\Lambda$ at early times. Considering that the field will adjust itself in order to minimize its energy , we will observe a decrease in the potential energy. As a first case, the potential may change considerably with $\phi$ and as a consequence the field will move down quickly in the potential curve. Another possibility comes if the potential term remains approximately constant. Here, the field will slowly roll towards the minimum of the potential. The latter case, called slow-roll regime, would be desirable for inflation allowing the required time for the accelerated expansion.

Let us now look at the equations of motion

$$\frac{\delta S_\phi}{\delta \phi} = \frac{1}{\sqrt{-g}}\partial_\nu\left(\sqrt{-g}g^{\mu\nu}\partial_\mu\phi\right) - V'(\phi) = 0\,. \tag{4.20}$$

In a flat FRW Universe with an homogeneous field, the inflaton equation of motion is given by

$$\ddot{\phi} + 3H\dot{\phi} + V'(\phi) = 0\,, \tag{4.21}$$

with

$$H^2 = \frac{8\pi G}{3}\rho_\phi = \frac{1}{3M_p^2}\left(\frac{1}{2}\dot{\phi}^2 + V(\phi)\right)\,. \tag{4.22}$$

From the equation of motion we see that the time variation of the inflaton field is determined by the slope of the potential and the Hubble expansion. On the one hand, the slope of the potential drives the field towards the minimum of the potential, and on the other hand the Hubble term works as an effective friction proportional to the field velocity, which damps the variation of the field.

## 4.4 Slow-Roll Inflation

For inflation to occur, we need the scalar field to behave like a cosmological constant, and this was obtained with a negligible kinetic energy when compared with potential $V(\phi)$, such that $\rho_\phi \simeq -p_\phi$. A second requirement is that the potential energy remains approximately constant, ensuring that the inflaton will roll slowly towards the minimum of the potential. In this way, we may sustain the first condition for a sufficiently long period.

These two conditions are called the slow-roll conditions, and are represented as

- $\frac{1}{2}\dot{\phi}^2 \ll V(\phi)$;
- $\ddot{\phi} \ll 3H\dot{\phi}$.

With these ensured the inflaton and Friedmann equations have the approximate form

$$3H\dot{\phi} \simeq -V'(\phi)\,, \tag{4.23}$$

$$H^2 \simeq \frac{V(\phi)}{3M_p^2}\,. \tag{4.24}$$

We can define the slow-roll parameters

$$\epsilon_\phi = \frac{1}{2}M_p^2\left(\frac{V'(\phi)}{V(\phi)}\right)^2\,, \tag{4.25}$$

$$\eta_\phi = M_p^2\left(\frac{V''(\phi)}{V(\phi)}\right)\,. \tag{4.26}$$

These two parameters will measure the relative slope and curvature of the potential function. It can be shown that the slow-roll conditions can be expressed in terms of these two parameters as

$$\epsilon_\phi \ll 1; \quad |\eta_\phi| \ll 1\,. \tag{4.27}$$

Inflation begins when the potential energy becomes dominant, and it will last until the slow-roll conditions are violated. In other words, it will last while the scalar field behaves like an effective cosmological constant. After this period, the inflaton field rolls towards the minimum of its potential and may decay into other degrees of freedom in a process called reheating.

We can also obtain the number of e-folds before inflation ends

$$N_\phi = \log\left(\frac{a_o}{a_i}\right) = \int_{ai}^{a_e} \frac{da}{a} = \int_{t_i}^{t_e} H\,dt = \int_{\phi_i}^{\phi_e} \frac{H}{\dot{\phi}} d\phi \simeq -\frac{1}{M_p^2}\int_{\phi_i}^{\phi_e} \frac{V(\phi)}{V'(\phi)} d\phi\,, \tag{4.28}$$

where the Friedmann and slow-roll equations were used.

**Example : Quadratic Potential**

$$V(\phi) = \frac{1}{2}m^2\phi^2 \tag{4.29}$$

Recalling the equation of motion, for this potential we have

$$\ddot{\phi} + 3H\dot{\phi} + m^2\phi = 0\,, \tag{4.30}$$

where $m$ represents the mass of the field, and we can see that this corresponds to a damped harmonic oscillator with two different regimes:

- $m^2 \ll H^2$. Here the field is overdamped and the mass term is negligible, such that, the field varies slowly, corresponding to the slow-roll regime;
- $m^2 \gg H^2$. Now the field is underdamped, the Hubble friction term is sub-dominant and the field will oscillate about the origin. This regime will be important for the reheating phase.

The slow-roll parameters for this potential are

$$\epsilon_\phi = \eta_\phi = \frac{2M_p^2}{\phi^2}\,. \tag{4.31}$$

The inflaton slow-roll conditions require

$$\epsilon_\phi \ll 1 \implies \phi \gg M_p \tag{4.32}$$

$$\epsilon_{\phi\,e} = 1 \implies \phi_e = \sqrt{2}M_p \ll \phi_i\,. \tag{4.33}$$

And so the number of e-folds for this potential is

$$N_e \simeq -\frac{1}{2M_p^2}\int_{\phi_i}^{\phi_e} \phi d\phi \simeq \frac{\phi_i^2}{4M_p^2}\,, \tag{4.34}$$

and for $N_e \simeq 50 - 60 \implies \frac{\phi_i}{M_p} \simeq 14 - 15$.

## 4.5 Reheating

When the slow-roll conditions are violated, the kinetic term increases and might dominate over the potential. During slow-roll we had $w = -1$, and in this phase $w$ may go up to 1. In the latter regime, called kination, the field evolves towards the minimum of the potential and executes damped oscillations about the minimum, with $w = 0$ on average for a quadratic potential. With the increase of field velocity, interactions with other degrees of freedom become important. These interactions are the mechanism that allows for the transition from inflation to the Standard Cosmology, with first a radiation and then a matter dominance epoch.

The leading effect of the interactions with other fields is the decay of the inflaton, which induces an additional friction term in the equations of motion.

$$\ddot{\phi} + 3H\dot{\phi} + V'(\phi) = -\Gamma_\phi \dot{\phi} \,. \tag{4.35}$$

This new dissipation term can be negligible during the slow-roll regime if $\Gamma_\phi \ll H$, but at later times with the decrease in $H$ it becomes crucial. We can write the last equation in terms of the energy density and pressure term, obtaining the standard energy-momentum conservation law with an extra decay term

$$\dot{\rho}_\phi + 3H\left(\rho_\phi + p_\phi\right) = -\Gamma_\phi \dot{\phi}^2 \,. \tag{4.36}$$

In general, the inflaton field is assumed to decay either directly or indirectly to Standard Model particles such that its decay products scatter of each other fast enough, $\Gamma_{scatt} > H$, to reach a state of thermal equilibrium. Since the dominant contribution to entropy in a thermal bath corresponds to its relativistic degrees of freedom, the energy from inflation will allow the formation of a thermal radiation bath. The radiation energy density will behave as

$$\dot{\rho}_r + 3H\left(\rho_r + p_r\right) = \Gamma_\phi \dot{\phi}^2 \,, \tag{4.37}$$

which using $p_r = \frac{\rho_r}{3}$ simplifies to

$$\dot{\rho}_r + 4H\rho_r = \Gamma_\phi \dot{\phi}^2 \,, \tag{4.38}$$

where $\rho_r = \frac{\pi^2}{30} g_\star T^4$.

Close to the minimum of the potential, at $\phi = \phi_m$, $V'(\phi_m) = 0$. It is possible to expand $V(\phi)$ as

$$V(\phi) = V(\phi_m) + \frac{1}{2}V''(\phi)(\phi - \phi_m)^2 + ... \tag{4.39}$$

such that to leading order, the field behaves as a damped harmonic oscillator, whatever the form of the potential. The Virial theorem for a harmonic oscillator gives, $\langle V \rangle = \left\langle \frac{\dot{\phi}^2}{2} \right\rangle = \frac{\rho_\phi}{2}$ and $p_\phi \simeq 0$, such that the inflaton behaves as non-relativistic matter. To describe the inflaton and radiation interactions we have the following system of equations

$$\dot{\rho}_\phi + 3H\rho_\phi = -\Gamma_\phi \rho_\phi \tag{4.40}$$

$$\dot{\rho}_r + 4H\rho_r = \Gamma_\phi \rho_\phi \tag{4.41}$$

$$H^2 = \frac{\rho_\phi + \rho_r}{3M_p^2} \,. \tag{4.42}$$

We can further calculate the reheating temperature, at which the inflaton decays and radiation dominates, by equating the Hubble parameter, that for a radiation epoch is given by $H = \frac{\pi}{\sqrt{90}} g_\star^{\frac{1}{2}} \frac{T^2}{M_p}$, with the inflaton decay width, to obtain

$$T_R \sim \left(M_p \Gamma_\phi\right)^{\frac{1}{2}} g_\star^{-\frac{1}{2}} \,. \tag{4.43}$$

We see here the dependence on the decay width or on the duration of reheating period $\tau_\phi = \Gamma_\phi^{-1}$, leading to a relation where a large decay width, short period, leads to a large reheating temperature. It is desirable that the reheating process is concluded before Big Bang Nucleosynthesis (BBN), $T \sim 100$ MeV, to ensure the successful generation of the light elements cosmic abundance.

## 4.6 Quantum Fluctuations during Inflation

Having introduced the dynamics of a homogeneous scalar field and how it may solve the flatness and horizon problems in the Hot Big Bang model, we now introduce an extra feat of the inflationary theory. Inflation also gives an explanation for the origin of the cosmological structure, from CMB anisotropies to the large scale structures, see [48, 49]. This provides a very useful link between inflationary evolution in the early Universe and current observations. This connection yields important constraints on current inflation models reflected in the measured quantities $n_S$, the scalar spectral index, and $r$, the tensor to scalar ratio [54]. We present a simple introduction to these quantities.

### 4.6.1 Metric and Matter Perturbations

During inflation fluctuations about the homogeneous background solution the inflaton field $\bar{\phi}(t)$ and the metric $\bar{g}_{\mu\nu}(t)$ are defined as

$$\phi(t, \mathbf{x}) = \bar{\phi}(t) + \delta\phi(t, \mathbf{x}) \tag{4.44}$$

$$g_{\mu\nu}(t, \mathbf{x}) = \bar{g}_{\mu\nu}(t) + \delta g_{\mu\nu}(t, \mathbf{x}) \,, \tag{4.45}$$

where

$$\begin{aligned} ds^2 &= g_{\mu\nu} dx^\mu dx^\nu \\ &= -(1+2\Phi)dt^2 + 2aB_i dx^i dt + a^2[(1-2\Psi)\delta_{ij} + E_{ij}]dx^i dx^j \,. \end{aligned} \tag{4.46}$$

In real space, in a Scalar-Vector-Tensor (SVT) decomposition of the metric perturbations we have

$$\begin{aligned} B_i &= \partial_i B - S \qquad \partial^i S_i = 0 \\ E_{ij} &= 2\partial_{ij}E + 2\partial_{(i}F_{j)} + h_{ij} \qquad \partial^i F_i = 0 \qquad h^i_i = \partial^i h_{ij} = 0 \,. \end{aligned} \tag{4.47}$$

Vector perturbations are not generated by inflation, thus they are ignored here.

The SVT decomposition can be easily described in Fourier space

$$X_{\mathbf{k}} = \int d^3x\, X(t, \mathbf{x}) e^{i\mathbf{k}.\mathbf{x}} \,, \; X = \delta\phi, \delta g_{\mu\nu} ... \tag{4.48}$$

It can be demonstrated that translation invariance of the linear equations of motion for the perturbations means that the different Fourier modes are decoupled from each other [49].

During inflation, the correspondent potential energy was the dominant contribution to the stress-energy tensor of the Universe. Thus, fluctuations in the inflaton field $\delta\phi$ back react on the space time geometry, as described by Einstein's equations. We can further decompose, using SVT decomposition, the stress-energy tensor, and by combining with the metric perturbations we will obtain both gauge invariant quantities, corresponding to tensor fluctuations, and gauge dependent quantities, the scalar fluctuations.

It is useful to work just with gauge invariant quantities [49], and this can be achieved with the combination of metric and energy-momentum tensor perturbations:

1. Curvature perturbations on uniform density surfaces

$$-\zeta \equiv \Psi + \frac{H}{\dot{\bar{\rho}}}\delta\rho \,, \tag{4.49}$$

where $\bar{\rho}$ and $\delta\rho$ are the energy density background and fluctuations, respectively. Geometrically $\zeta$ measures the spatial curve of constant density hypersurfaces $R^{(3)} = 4\frac{\nabla^2\Psi}{a^2}$.

2. Comoving curvature perturbations

$$\mathcal{R} \equiv \Psi - \frac{H}{\bar{p}+\bar{\rho}}\delta q\,, \tag{4.50}$$

where $\delta q$ is the scalar part of the 3-momentum density $T^0_i = \partial_i \delta q$ and $\bar{p}$ is the background pressure.

These quantities can be shown to be equal and remain constant on super horizon scales [49]. During slow-roll inflation $T^0_i = -\partial_i(\delta\phi)\dot{\bar{\phi}}$ making $\delta q = -\dot{\bar{\phi}}\delta\phi$ and hence

$$\mathcal{R} \simeq -\zeta \simeq \Psi + \frac{H}{\dot{\bar{\phi}}}\delta\phi\,. \tag{4.51}$$

An important statistical measure for the primordial scalar fluctuations is the power spectrum of $\mathcal{R}$

$$\langle \mathcal{R}_{\mathbf{k}} \mathcal{R}_{\mathbf{k}'} \rangle = (2\pi)^3 \delta(\mathbf{k}+\mathbf{k}') P_{\mathcal{R}}(k)\,, \qquad \Delta_s^2 \equiv \Delta_{\mathcal{R}}^2 = \frac{k^3}{2\pi^2} P_{\mathcal{R}}(k)\,. \tag{4.52}$$

The scale dependence of the power spectrum is defined by the scalar spectral index

$$n_s - 1 = \frac{d\ln \Delta_s^2}{d\ln k}\,, \qquad \Delta_s^2 = A_s(k_\star)\left(\frac{k}{k_\star}\right)^{n_s-1} \tag{4.53}$$

where scale invariance corresponds to $n_s = 1$.

Similarly for tensor perturbations, we have the power spectrum for the two polarization modes of $h_{ij}$, $h \equiv h_+$, $h_\times$:

$$\langle h_{\mathbf{k}} h_{\mathbf{k}'} \rangle = (2\pi)^3 \delta(\mathbf{k}+\mathbf{k}') P_h(k)\,, \qquad \Delta_h^2 = \frac{k^3}{2\pi^2} P_h(k) \tag{4.54}$$

and $\Delta_t^2 = 2\Delta_h^2$. The scale dependence here is defined as

$$n_t = \frac{d\ln \Delta_t^2}{d\ln k} \qquad \Delta_t^2 = A_t(k_\star)\left(\frac{k}{k_\star}\right)^{n_t}. \tag{4.55}$$

### 4.6.2 Horizon Entry, Exit and Re-Entry

As we will see shortly, quantum fluctuations during inflation induce a non zero variance for fluctuations in the inflaton and metric fields. The amplitude of fluctuations scales with the expansion parameter $H$ during inflation, thus it can be related with the de Sitter horizon $H^{-1}$, and quantum fluctuations can be interpreted as thermal fluctuations in de Sitter space.

These fluctuations are created on all length scales, and wavenumbers $k$. The cosmologically relevant ones start inside the horizon, within the Hubble radius, on subhorizon scales

$$k \gg aH\,. \tag{4.56}$$

However, during inflation, the comoving Hubble radius shrinks and so there is an exit of the horizon to superhorizon scales

$$k \ll aH\,. \tag{4.57}$$

As discussed above, cosmological homogeneity is characterized by the quantities $\mathcal{R}$ or $\zeta$. These quantities have the handy property of remaining constant on superhorizon scales. Hence, without knowing exactly how the end of inflation occurred, how exactly reheating occurred, we can predict some cosmological observables.

After inflation, in the standard cosmological evolution period, the comoving horizon grows, so eventually all fluctuations will re-enter the horizon and their amplitudes will unfreeze. Figure 4.1 illustrates this idea.

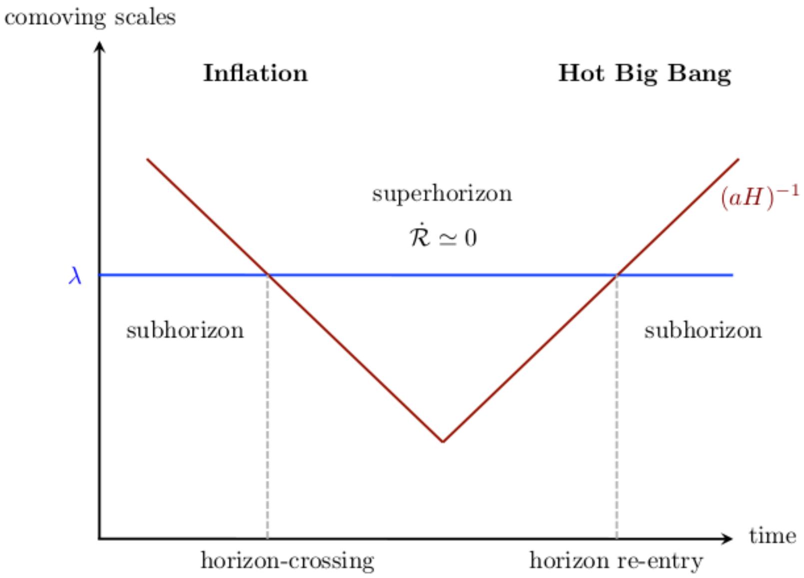


FIGURE 4.1: Evolution of a density/curvature perturbation during and after inflation [48]

.

### 4.6.3 Quantum Fluctuations in de Sitter Space

#### (a) Scalar Perturbations

Either by working through the equations of motion [48]

$$\Box\phi = -V'(\phi) \tag{4.58}$$

or the inflation action [49]

$$S = \int d^4x\sqrt{-g}\left[\frac{R}{2} - \frac{1}{2}(\nabla\phi)^2 - V(\phi)\right] \tag{4.59}$$

with $\phi = \bar{\phi} + \delta\phi$, we can study the perturbations evolution. After a Fourier transformation, we obtain the mode equation

$$\chi_k'' + \left(k^2 - \frac{2}{\tau^2}\right)\chi_k = 0 \tag{4.60}$$

where $\delta\phi_k = \chi_k(t)/a(t)$ , $\frac{a''}{a} = \frac{2}{\tau^2}$ and $a(\tau) = -\frac{1}{H\tau}$ with $H$ being constant. This corresponds to a harmonic oscillator with a time dependent frequency. We now see that the physical wavelength of the modes is exponentially stretched by expansion during inflation, $\lambda_{phys} = \frac{2\pi}{k}a$, such that at some point

$$\lambda_{phys} \gg H^{-1} \Leftrightarrow k \ll aH \tag{4.61}$$

as described previously.

After quantizing the field fluctuations in the Bunch Davies vacuum state, we can obtain the power spectrum of the scalar fluctuations $\delta\phi_k = a^{-1}\chi_k$ for superhorizon scales ($k\tau \ll 1$)

$$\langle\delta\phi_{\mathbf{k}}(t)\delta\phi_{\mathbf{k}'}(t)\rangle = (2\pi)^3\delta(\mathbf{k}+\mathbf{k}')\frac{H^2}{2k^3} \tag{4.62}$$

or

$$\Delta_\phi^2 = \frac{k^3}{2\pi^2}P_\phi(k) = \left(\frac{H}{2\pi}\right)^2 . \tag{4.63}$$

Since $\mathcal{R} \simeq \frac{H}{\dot{\phi}}\delta\phi$ and at horizon crossing $a_\star(t)H_\star(t) = k_\star$

$$P_{\mathcal{R}}(k) = \left(\frac{H}{\dot{\phi}}\right)^2 P_\phi(k) = \frac{H_\star^2}{2k^3}\left(\frac{H_\star}{\dot{\phi}_\star}\right)^2 \tag{4.64}$$

and

$$\Delta_{\mathcal{R}}^2 = \frac{H_\star^2}{(2\pi)^2}\left(\frac{H_\star}{\dot{\phi}_\star}\right)^2 . \tag{4.65}$$

Since $\mathcal{R}$ is approximately constant on super-horizon scales the spectrum at horizon crossing will determine the future spectrum until a given fluctuation re-enters the horizon.

**(b) Tensor Perturbations**

If we expand the Einstein Hilbert action with the metric perturbations we may obtain the second-order action for tensor fluctuations

$$S_{(2)}^t = \frac{M_P^2}{8}\int d\tau dx^3 a^2\left[\left(h_{ij}'\right)^2 - \left(\partial_\ell h_{ij}\right)^2\right] . \tag{4.66}$$

After defining the Fourier expansion for $h_{ij}$, considering the two polarizations of the gravitational waves we may obtain a very similar equation of motion to the scalar case, for each polarization. Each polarization of these waves is therefore just a renormalized massless field in de Sitter space

$$h^s_{\mathbf{k}} = \frac{2}{M_P}\phi^s_{\mathbf{k}} \tag{4.67}$$

Thus the power spectrum for each polarization is

$$\Delta^2_{h_s} = \frac{4}{M_P^2}\Delta^2_{\phi_k} = \frac{4}{M_P^2}\left(\frac{H}{2\pi}\right)^2 . \tag{4.68}$$

For the complete tensor perturbations:

$$\Delta^2_t = \frac{2}{\pi^2}\left(\frac{H}{M_P}\right)^2 . \tag{4.69}$$

These tensor fluctuations are often normalized relative to the measured amplitude of scalar fluctuations $\Delta^2_s \equiv \Delta^2_{\mathcal{R}} \sim 10^{-10}$, giving the tensor-to-scalar ratio

$$r \equiv \frac{\Delta^2_t(k)}{\Delta^2_s(k)}. \tag{4.70}$$

Since $\Delta^2_s$ is fixed by observations and $\Delta^2_t \propto H^2 \simeq V(\phi)$, the tensor-to-scalar ratio is a direct measure of the energy scale of inflation

$$V^{\frac{1}{4}} \sim \left(\frac{r}{0.01}\right)^{\frac{1}{4}} 10^{16}\,\mathrm{GeV}\,, \tag{4.71}$$

meaning that for $r \gtrsim 0.01$ inflation may occur around GUT scale.

Using the slow-roll equations

$$\Delta^2_s = \Delta^2_{\mathcal{R}} = \frac{1}{24\pi^2}\frac{V}{M_P^4}\frac{1}{\epsilon_\phi}\bigg|_{k=aH} \tag{4.72}$$

$$\Delta^2_t = \frac{2}{3\pi^2}\frac{V}{M_P^4}\bigg|_{k=aH} . \tag{4.73}$$

Thus, the tensor-to-scalar ratio is given by

$$r = 16\epsilon_\phi\,, \tag{4.74}$$

the scalar spectral index is

$$n_s - 1 = 2\eta_\phi - 6\epsilon_\phi \tag{4.75}$$

and the tensor spectral index is

$$n_t = -2\epsilon_\phi \,. \tag{4.76}$$

Notice that we have obtained a simple consistency relation between the tensor-to-scalar ratio and the tensor spectral index

$$r = -8n_t \,. \tag{4.77}$$

Measurements of the scalar and tensor spectra, amplitudes and scale dependence encodes information about the potential driving the inflation and can be used as a first test that inflaton models must pass.

### 4.6.4 Quadratic and Quartic Potentials

Let us now analyze how the quadratic and the quartic potentials fit in this description. In the previous sub-chapter we have calculated both the scalar spectral index and the tensor-to-scalar ratio.

Starting with the simplest of these potentials, the quadratic, using the slow-roll description and equations (4.25),(4.26) and (4.28), $\epsilon_\phi = \eta_\phi = \frac{2M_p^2}{\phi^2}$ and the number of e-folds of inflation after horizon-crossing at $\phi = \phi_\star$ is $N_e \simeq \phi_\star^2/4M_P^2$ , then

$$n_s = 1 - \frac{2}{N_e} \tag{4.78}$$

$$r = \frac{8}{N_e} \,. \tag{4.79}$$

With the expected $N_e = 50 - 60$ we obtain $n_s \simeq 0.96 - 0.967$ and $r \simeq 0.13 - 0.16$. Although the Plank data agrees with with $n_s \simeq 0.9603 \pm 0.0073$ [54], the measured tensor-to-scalar ratio excludes the simplest potential with a bound $r < 0.12$ at 95% C.L [54].

As we have just seen, the quadratic potential cannot fit experimental data. Let us now see how the quartic potential, $\lambda\phi^4$, stands.

Using again the slow-roll regime to obtain $r$ and $n_s$, with $\epsilon_\phi = \frac{8M_p^2}{\phi^2}$ , $\eta_\phi = \frac{12M_p^2}{\phi^2}$ and $N_e \simeq \phi_\star^2/8M_P^2$

$$n_s = 1 - \frac{3}{N_e} \tag{4.80}$$

$$r = \frac{16}{N_e} \,. \tag{4.81}$$

This gives for $N_e = 50 - 60$, $n_s \simeq 0.94 - 0.95$ and $r \simeq 0.27 - 0.32$. Clearly the quartic potential is also excluded with Planck data. A different kind of potential must be used to have a viable model, since these simple power law potentials do now work. As we will see, the inclusion of a non-minimal coupling of the inflation scalar field to gravity allows keeping these potentials while agreeing with experimental bounds.

# Chapter 5

# Dark Matter

There is a large body of evidence supporting the existence of dark matter from sub-galactic scales up to cosmological scales. In the former, evidence comes from galaxy rotation curves [55], weak lensing [56] and strong gravitational lensing [57, 58].

Velocity dispersions of stars, in some dwarf galaxies, imply a mass-to-light ratio of the order $10^3$. From observations at the scale of galaxies clusters, we have indication of a total cosmological matter density of order $\Omega_M \approx 0.2 - 0.3$ [59, 60], way higher than the correspondent baryon density $\Omega_B \approx 0.022$ [61].

On cosmological scales, observations of the CMB anisotropies lead to more precise measurements of the total matter and baryon content of the Universe. Since other SM particles interact either through electromagnetic or strong force, neutrinos would be the only SM candidate. However with their mass lying bellow 1 eV they cannot account for the current DM abundance.

All these methods that point towards the existence of dark matter only work through gravitational interactions, leaving no concluding information on other non-gravitational processes. Thus, instead of the existence of dark matter particles, as widely proposed in the literature, it is possible that these discrepancies could arise from deviations from General Relativity, leading to modified theories of gravity that may potentially account for the experimental observations.

## 5.1 Evidence for Dark matter

### Galactic scales

Spiral galaxies are expected to rotate around their centers with radial velocity $v(r)$. This can be measured by Doppler shift in the 21cm Hydrogen emission line of stars and intergalactic gas. From Kepler's $3^{rd}$ law we have that

$$v(r) = \sqrt{\frac{G\,M(r)}{r}}\,, \tag{5.1}$$

where $G$ is Newton's constant and $M(r)$ the mass inside a sphere of radius $r$. In a simplified picture the bulge of the galaxy is characterized by a constant density, such that $M(r) \sim r^3$. In the outer regions of the spiral arms, the density decreases quickly, such that $M(r)$ is approximately constant. We would then expect $v(r) \sim 1/\sqrt{r}$ in the spiral arms. However, from observations we see that the rotation curve becomes flat $v(r) \sim const$ for large $r$, indicating $M(r) \sim r$ , as seen in figure 5.1. This may be explained if at these large radii we have dark matter with $\rho_{DM} \propto r^{-2}$.

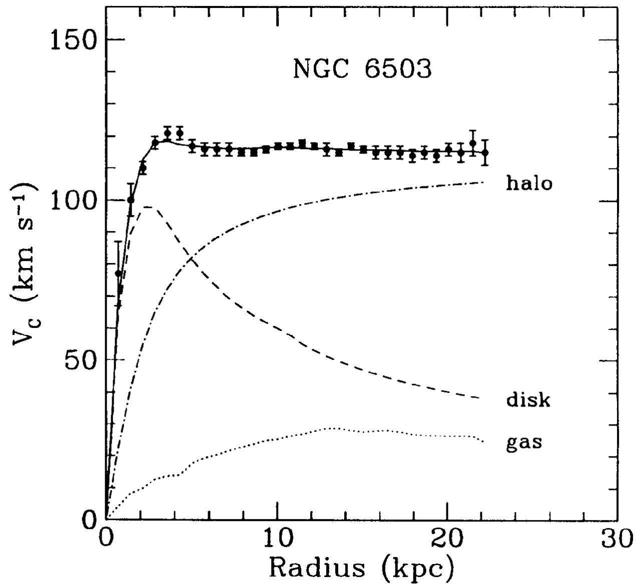


FIGURE 5.1: Rotation curve of NGC 6503 [62].

### Galaxy Clusters scales

Galaxies are not equally distributed in the Universe. Generally, they concentrate in clusters. Considering that these gravitationally bounded systems have had time to relax, we can therefore apply the Virial theorem

$$GM = 2\frac{\langle v^2 \rangle}{\langle r^{-1} \rangle} \tag{5.2}$$

to relate the observed velocity and distances to the gravitational mass, as first done by Fritz Zwicky [63].

As another example, at the Clusters scales, figure 5.2 is the X-ray image of the Bullet Cluster, where we can see clearly the separation between gravitational, in blue and reconstructed through gravitational lensing, and luminous mass obtained with X-rays .

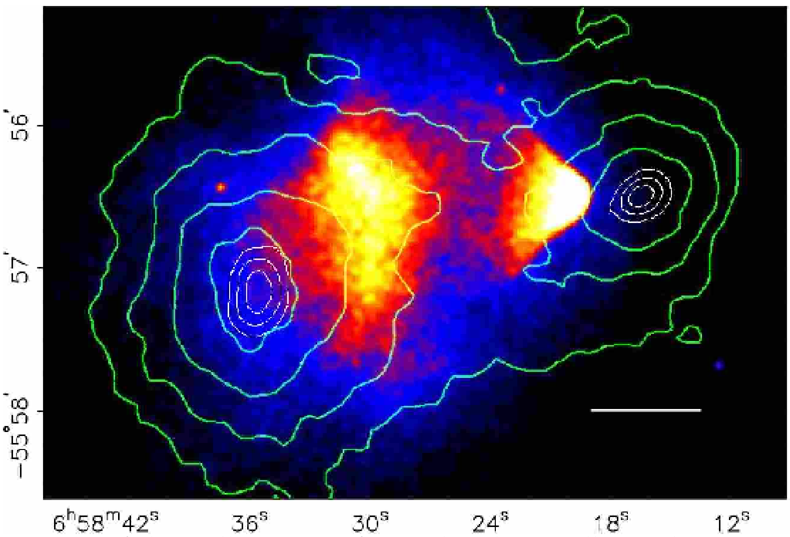


FIGURE 5.2: Image of the Bullet Custer from Chandra Satellite. The green contours are reconstructions of the gravitational potential inferred by weak gravitational lensing while luminous matter was obtained through X-ray imaging. [64].

### Cosmological scales (CMB anisotropies)

Recalling the Friedmann equation, (3.4),

$$H^2 = \frac{8\pi G}{3}\rho - \frac{k}{a^2} + \frac{\Lambda}{3} \tag{5.3}$$

and defining the critical density as

$$\rho_c = \frac{3H_0^2}{8\pi G}, \tag{5.4}$$

where $H_0^2$ is today's Hubble expansion rate, we can normalize all components in the Universe, with $\Omega_i = \rho_i/\rho_c$, such that

$$\Omega_M + \Omega_{rad} + \Omega_\Lambda + \Omega_{curv} = 1\,. \tag{5.5}$$

Observations of the anisotropies on CMB leads to the determination of the total dark matter density $\Omega_M = 0.02647 \pm 0.0033$ [54]. In contrast, measurements of the baryonic densities give $\Omega_B = 0.04910 \pm 0.00051$ [54], giving around $80 - 85\%$ of the total matter in the Universe to be non-luminous and non-baryonic material, i.e, particles that do not couple with photons.

## 5.2 Candidates for Dark Matter

There have been many proposals for what constitutes dark matter. From analyses of structure formation in the Universe we know that most dark matter should be "cold". This means that at the time of galaxy formation these dark matter particles should already be non-relativistic. In order to be considered a possible DM solution these candidates must be stable at late times, interact very weakly, or do not interact at all, with electromagnetic radiation and, finally, account for the measured relic density. The most representative candidates are axions, gravitinos and Weakly Interacting Massive Particles (WIMPs).

**Axions** Firstly proposed to solve the strong CP problem of QCD [65–68], axions are pseudo Goldstone bosons associated with the spontaneous breaking of the global "Peccei-Quinn" (PQ) $U(1)$ symmetry. In many proposals axions are produced through non-thermal coherent oscillations of the axion field near the QCD phase transition [69]. Since this axion is also presented as a solution to an independent SM problem it becomes a very attractive DM candidate. Currently, experiments like the ADMX and CAST are searching for them.

**Gravitinos** Gravitinos are the supersymmetric partner of the graviton in supersymmetric theories [70, 71]. Its couplings to ordinary particles are suppressed by a factor $O(M_W/M_P)$ which makes its interactions extremely weak. The gravitino can be produced through both thermal and non-thermal processes.

**Weakly Interacting Massive Particles (WIMPs)** This class of candidates is characterized, as in its name, by being massive particles with interactions around the weak scale. Within Standard Cosmology, their relic density can be calculated if these WIMPs were once in thermal equilibrium after the inflation. Their density would now be Boltzmann suppressed, since these WIMPs have typically frozen out when they became non-relativistic particles. These WIMP solutions are testable in laboratory and in satellite experiments [72].

## 5.3 Thermal Abundance of WIMP's

As mentioned above these dark matter particles, which have only have been inferred through gravitational processes, cannot be accounted for by SM particles. Although electroweak and strong interactions cannot occur, these DM particles may interact through weak processes.

The conventional dark matter candidates are heavy massive particles that can only have interactions of the order or lower than SM weak interactions. These candidates, the so called WIMPs, are expected to be produced in the early Universe by several mechanisms. The simplest and perhaps the most representative is the creation of a thermal abundance via decoupling and freeze out mechanisms [48].

Consider a single WIMP, $\chi$, with mass $m_\chi$ and $g_\chi$ internal degrees of freedom. In the early Universe, during the radiation dominated era, $\chi$ is kept in thermal equilibrium with SM particles. This happens through weak processes with a cross section $\sigma$. Once the interaction rate, $\Gamma_\chi$, becomes smaller than the Hubble rate, the thermalizing interactions freeze out

$$\Gamma_\chi = n_\chi \langle \sigma v \rangle \lesssim H \,. \tag{5.6}$$

Since we expect $\chi$ to be a heavy particle, we can assume that $\chi$ is non-relativistic at the time of freeze out, such that its number density is given by

$$n_\chi(T_F) = g_\chi \left( \frac{m_\chi T_F}{2\pi} \right)^{\frac{3}{2}} e^{-\frac{m_\chi}{T_F}} \,, \tag{5.7}$$

where $T_F$ is the thermal bath freeze out temperature. Since this happens in the radiation era, $H \approx \frac{\pi}{\sqrt{90}} \sqrt{g_\star} \frac{T^2}{M_p}$, we have that the equality $\Gamma_\chi = H$ gives us

$$x_F^{\frac{1}{2}} e^{-x_F} = \frac{\pi}{\sqrt{90}} \frac{(2\pi)^{\frac{2}{3}}}{g_\chi} \frac{\sqrt{g_{\star F}}}{m_\chi M_p \langle \sigma v \rangle} \,, \tag{5.8}$$

where $x_F = \frac{m_\chi}{T_F}$ and $g_{\star F}$ is the number of relativistic degrees of freedom at the time of freeze out.

After the freeze out of interactions, the number of WIMPs in a comoving volume, $N_\chi = n_\chi / s$, should be conserved. Using present data from Plank [54] and particle number conservation we infer the properties after the moment of freeze out. We then have

$$\Omega_{\chi 0} = \frac{\rho_{\chi 0}}{\rho_{c0}} = \frac{m_\chi n_\chi(T_F) s_0}{3 H_0^2 M_p^2 s_F} \tag{5.9}$$

where $\rho_{C0}$ was defined in equation (5.4). From $\Gamma_\chi = n_\chi \langle \sigma v \rangle = H(T_F)$

$$\Omega_{\chi 0} = \frac{\pi g_{\star 0}}{3\sqrt{90}} \frac{T_0^3}{M_p^3} \frac{H_0^{-2}}{\langle \sigma v \rangle} g_{\star F}^{-1/2} x_F \,. \tag{5.10}$$

If we now solve the last equation for $\langle \sigma v \rangle$, apply it in equation (5.8) and introduce the present values for $T_0$, $H_0$, and $g_{\star 0}$ we then get

$$x_F^{3/2} e^{-x_F} \approx (\Omega_{\chi 0} h^2) g_{\star F} \frac{6 \times 10^9 \text{ GeV}^2}{m_\chi M_P} \,, \tag{5.11}$$

where we took $g_\chi = 2$ for concreteness. This equation can now be solved numerically for different values of the WIMP mass. Through some work with expected values of $g_\star \sim 10$, $\Omega_{\chi 0} h^2 \sim 0.1$ [54] one obtains $x_F \sim 20 - 30$ for $m_\chi = 0.1 - 10^3$ GeV.

Writing now, using dimensional analysis, $\langle \sigma v \rangle = \frac{\alpha^2}{M^2}$, where $\alpha$ is an effective coupling and $M$ is the mass scale of the processes, we then have

$$\Omega_{\chi^0} h^2 \approx 0.1 \left( \frac{10}{g_{\star F}} \right)^{1/2} \left( \frac{x_F}{25} \right) \left( \frac{0.2}{\alpha} \right)^2 \left( \frac{M}{1 \text{ TeV}} \right)^2 . \tag{5.12}$$

Other particle physics processes are expected at the TeV scale, for example in supersymmetry, in extra-dimensions or in right handed neutrino theories. Therefore this coincidence, coming from a prediction of TeV scale interactions to explain the WIMPs relic density, presents a pleasant surprise. This is the so-called "WIMP miracle". With the LHC now colliding protons at TeV scale energies, there is thus an expectation to find WIMP dark matter particles.

# Chapter 6

# Baryogenesis

## 6.1 Observational Evidence for Baryon Asymmetry

Observations indicate that the number of baryons in the Universe is not the same as the number of anti-baryons. Until now, all the structures observed in the Universe, from stars to clusters, consist of matter and we can only detect anti-matter in cosmic rays. In the latter case, the flux of anti-protons $\bar{p}$ in comparison to the the flux of protons is

$$\frac{\bar{p}}{p} \sim 10^{-4}. \tag{6.1}$$

Nevertheless, this overabundance of matter over anti-matter could just be local, allowing other regions of the Universe to have an opposite overabundance, providing then an overall symmetric Universe. In this scenario, the boundaries between regions with opposite overabundances would lead to a huge flux of radiation which has not been detected.

From various considerations, it is then widely accepted that, at least, the observable part of our Universe must have developed a baryon asymmetry dynamically in a process that is called Baryogenesis. To justify the dynamical evolution instead of an initial condition solution two simple reasons can be provided. First, in a initial state scenario, its conditions would have to be highly fine-tuned. For example, for every 6,000,000 anti-quarks there should exist 6,000,001 quarks [73] quite implausible. Second, based in observable features of CMB radiation, there are strong arguments in favor of inflation, such that any initial baryon asymmetry would have been exponentially diluted by the accelerated expansion.

We can characterize this asymmetry with the baryon-to-entropy ratio defined in equation (3.26)

$$\eta_S = \frac{n_b - n_{\bar{b}}}{s} \sim 10^{-10}, \tag{6.2}$$

or with the baryon-to-photon ratio

$$\eta = \frac{n_b - n_{\bar{b}}}{n_\gamma} \sim 10^{-9}\,, \tag{6.3}$$

where $n_\gamma$ is the photon number density $n_\gamma = 2\frac{\zeta(3)}{\pi^2}T^3$. These two ratios are related through

$$\eta_S = \frac{1}{7.04}\eta\,, \tag{6.4}$$

where this conversion factor is valid from the present time to the epoch where neutrinos went out of equilibrium.

These values for the baryon asymmetry are inferred from two independent observations. The first comes from Big Bang Nucleosynthesis (BBN) [74–76]. Abundances of $^3$He, $^4$He, D, $^6$Li and $^7$Li are sensitive to the $\eta$ value. Theoretical predictions and experimental measurements can be seen in figure 6.1 .

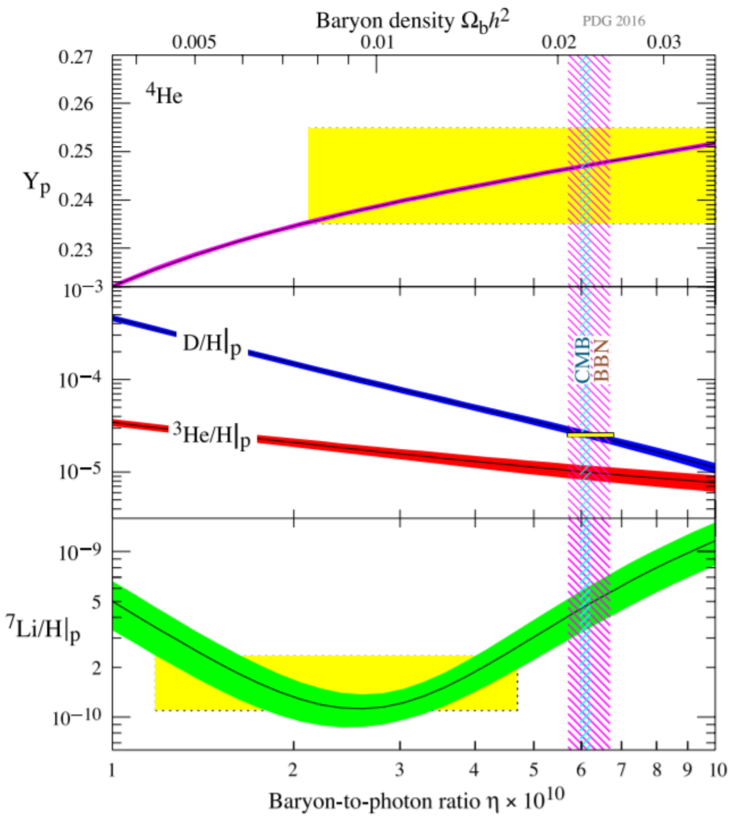


FIGURE 6.1: Abundances of $^3$He, $^4$He, D, $^6$Li and $^7$Li as predicted by the Standard Model of BBN. The bands show the 95% C.L. range. Boxes indicate the observed light element abundances. The narrow vertical band indicates the CMB measurements of the cosmic baryon density, while the wider band indicates the BBN concordance range (both at 95% C.L.) [77].

Agreement amongst abundances requires (at 95% $CL$)

$$5.8 \times 10^{-10} \leq \eta \leq 6.6 \times 10^{-10}. \tag{6.5}$$

A second way to determine the baryon asymmetry comes from the Cosmic Microwave Background anisotropies [73]. The CMB spectrum corresponds, to a very good approximation, to that of black body radiation with a nearly constant temperature $T \approx 2.73$ K. However, there are tiny fluctuations that are sensible to the matter density fluctuations at the time of last scattering. This constrains $\eta$. From WMAP results we have a constraint [78, 79]

$$\eta = (6.19 \pm 0.14) \times 10^{-10}. \tag{6.6}$$

Through figure 6.1 we observe an impressive consistency between nucleosynthesis and CMB. These two tests that come from two independent analyses, coming from two different epochs in the Universe's history, present a big triumph of the Hot Big Bang Cosmology.

Baryon number is actually an apparent accidental global symmetry of the Standard Model of particle physics. As for the Lepton number, all perturbative processes conserve this quantity, although the symmetry is not needed for the theory. In a homogeneous, baryon-symmetric Universe, since annihilations of baryons and anti-baryons are not completely efficient, we would still find small freeze-out abundances, $\frac{n_b}{s} \sim \frac{n_{\bar{b}}}{s} \sim 10^{-21}$. This is too small for what is needed for BBN and CMB. We then need a baryogenesis mechanism to explain $\eta_s \sim 10^{-10}$. A strict requirement is that it must happen before BBN and after inflation to allow the right production of light nuclear elements and to avoid a dilution of this asymmetry.

## 6.2 Sakharov Conditions for Baryogenesis

Several distinct models have been proposed to explain this asymmetry. However, they all must satisfy what are called the Sakharov conditions [2]:

### Baryon number violation

It is obvious that B number must be violated to generate the asymmetry. The standard example of a B-violating process is the decay of a heavy gauge or Higgs boson that arise in extensions of the SM . As an example [48], in Grand Unified Theories (GUT), a spontaneous symmetry breaking process is expected to occur at energies around $M_{GUT} \sim 10^{16}$ GeV, which leads to the generation of the gauge $X$ and Higgs $Y$ boson mass, allowing B-violating interactions, such as

$$X \to qq\,, \qquad X \to \bar{q}\bar{\ell}\,. \tag{6.7}$$

where $q$ and $\ell$ denote SM quarks and leptons respectively. The simultaneous existence of these two interactions implies no consistent assignment of baryon number to $X$.

In the SM, B number is violated due to the triangle anomaly, which violates conservations of the left handed baryons/ lepton current [73, 80],

$$\partial_\mu J^\mu_{B_L+L_L} = \frac{3g^2}{32\pi^2}\epsilon_{\alpha\beta\gamma\delta}W_a^{\alpha\beta}W_a^{\gamma\delta}\,, \tag{6.8}$$

where $W_a^{\alpha\beta}$ is the $SU(2)_L$ field strength. This leads to non-perturbative sphaleron processes. From its construction it involves nine left handed ($SU(2)_L$ doublets) quarks, 3 of each generation, and the left handed leptons, one from each generation. This process violates B and L by 3 units each. At zero temperature, the amplitude of the baryon number violating processes is proportional to $e^{-\frac{8\pi^2}{g^2}}$ [81], being to small too be observed. However, at high temperatures these transitions become unsuppressed [82].

### Departure from thermal equilibrium

This second condition is also clear to understand in a cosmological context. Consider a generic decay $X \to Y + B$, where $X$ represents some initial state with vanishing baryon number, $Y$ denotes all particles in the final state also with vanishing baryonic charge and $B$ corresponds to the excess of baryons produced.

If the process is in thermal equilibrium, by definition, the rates for the decay and inverse decay must be equal

$$\Gamma[X \to Y + B] = \Gamma[Y + B \to X]\,. \tag{6.9}$$

Thus, no net baryon number can be produced, since the inverse process destroys B as fast as it is produced.

In the GUT example, departure from thermal equilibrium occurs when the $X$ boson is non-relativistic, $m_X \gtrsim T$ at the time of decay $t \sim 1/\Gamma$. In this case, the energy of the final state is of order T, thus there will not be enough energy for the inverse decay to occur. The rate for $qq \to X$ or $\bar{q}\bar{\ell} \to X$ is Boltzmann suppressed $\Gamma[qq \to X] \sim e^{-\frac{m_X}{T}}$.

In the SM, departure from thermal equilibrium occurs at the electroweak phase transition [83, 84]. With the known Higgs mass, this transition is not as strong as required for a successful baryogenesis.

### C and CP violation

The last Sakharov condition is the most technical. Lets consider again the process $X \to Y + B$. If charge conjugation C is a symmetry of the interactions, then we expect the rate of the direct process to be the same as of the charge conjugated process

$$\Gamma[X \to Y + B] = \Gamma[\bar{X} \to \bar{Y} + \bar{B}]\,. \tag{6.10}$$

This means that a baryon excess B is produced at the same rate as -B, canceling as baryon number changes. Although C number violation is a necessary condition, it is not sufficient. CP symmetry must also be violated. For instance, take the X boson decay to left handed or right handed quarks

$$X \to q_L q_L\,, \qquad X \to q_R q_R\,.$$

Under C $q_L \to \bar{q}_L$, while under CP $q_L \to \bar{q}_R$ is the antiparticle of $q_R$, which is left handed. In a C violation case

$$\Gamma[X \to q_L q_L] \neq \Gamma[\bar{X} \to \bar{q_L}\bar{q_L}]\,, \tag{6.11}$$

but if CP is conserved

$$\Gamma[X \to q_L q_L] = \Gamma[\bar{X} \to \bar{q_R}\bar{q_R}] \tag{6.12}$$

$$\Gamma[X \to q_R q_R] = \Gamma[\bar{X} \to \bar{q_L}\bar{q_L}]\,. \tag{6.13}$$

This would lead to

$$\Gamma[X \to q_L q_L] + \Gamma[X \to q_R q_R] = \Gamma[\bar{X} \to \bar{q_R}\bar{q_R}] + \Gamma[\bar{X} \to \bar{q_L}\bar{q_L}]\,. \tag{6.14}$$

Thus, as long as we start with equal number of $X$ particles and $\bar{X}$ anti-particles, no asymmetry in baryon number will arise, even though a chiral symmetry may be created. Therefore CP violation must occur.

The weak interactions in the SM violate C maximally and CP via the Kobayashi-Maskawa mechanism [85]. This can be parametrized via the Jarlskog invariant [86]. Nevertheless, it is impossible to generate $\eta_s \sim 10^{-10}$ with just these mechanisms.

## 6.3 Models of Baryogenesis

As we have seen all these ingredients are present in the SM. However, there are no mechanisms that could generate a large enough baryon asymmetry. Therefore, baryogenesis imposes new physics that extends the SM. It must introduce new sources of CP violation and either provide a departure from thermal equilibrium in addition to the electroweak phase transition or modify the existing one. Here we present some ideas of possible mechanisms for baryogenesis.

**GUT Baryogenesis [48, 80]** The baryon asymmetry is generated in the out-of-equilibrium decays of the heavy bosons. The scenario is actually disfavored due to non-observation of proton decay, imposing a high lower bound in the mass of the decaying boson and, as a consequence, on the reheating temperature.

**Leptogenesis [73]** Proposed by Fukugita and Yanagida [87]. Singlets under the SM gauge group, identified as right handed neutrinos, are introduced justifying the observed neutrino masses through the seesaw mechanism. Their coupling to the SM model particles, with Yukawa interactions, gives a new source for CP violation. If the rate of these Yukawa interactions is slower than $H$, the Hubble parameter, at the time the asymmetry is generated, the out of equilibrium condition is verified. Since no consistent assignment of lepton number is possible with the Majorana mass terms, a lepton asymmetry will be generated and the SM sphaleron processes may convert it to a baryon asymmetry. To produce these right handed neutrinos several mechanism are possible. A case with thermal production will be discussed later in this work.

**Electroweak Baryogenesis [80, 83]** In these models the out-of-equilibrium condition is provided in the electroweak phase transition. Some changes to the SM proposal must occur. For example, modifications of the scalar potential such that the phase transition changes, and extra sources of CP violation. Models like the two Higgs doublet model (2HDM), where the Higgs potential violates CP, or the minimal supersymmetric standard model (MSSM), where new flavour-diagonal CP violating phase appear, may generate a successful and verifiable baryogenesis.

**The Affleck-Dine mechanism [88]** The asymmetry is generated in a classical scalar field which will later decay to baryonic particles. This field starts with a large expectation value and will roll towards the origin of its potential. When this field is far from the origin, there can be contributions to the potential from baryon and lepton number violating interactions. The rolling field will then acquire the asymmetry.

**CPT violation [89]** Baryogenesis may be generated from spontaneous CPT breaking arising in a string-based framework. Under the right circumstances, certain CPT-violating terms can produce a large baryon asymmetry at the GUT scale. If the interactions preserve $B - L$ number, the subsequent sphaleron dilution reproduces the observed value of the baryon asymmetry.

# Chapter 7

# An Inflaton Dark Matter Model [1]

As already mentioned, dark matter particles behave like a non-relativistic, non-luminous fluid and we are only sure that they have gravitational interactions. They must account for the observed galaxy rotation curves and for the large scale structure seen in the Universe. The inflaton presents itself also as a neutral and weakly interacting field. Another common feature comes from the Standard Model (SM) of particle physics being unable to solve both these problems. A possible solution might come from the hypothesis that the same scalar field accounts for both inflation and dark matter at different epochs.

As seen in the inflation section, a scalar field can reproduce different equation of state. We saw that during the slow-roll dynamics $w = -1$ and in kination $w = 1$. On the other hand, while oscillating close to the minimum the inflaton field has a potential term of the form $V(\phi) \approx \frac{1}{2}m^2\phi^2$, that makes $\langle V(\phi) \rangle \approx \left\langle \frac{\dot{\phi}^2}{2} \right\rangle$, i.e., $\rho_\phi \gg p_\phi$, as a nonrelativistic fluid.

After understanding that the scalar field can describe both inflation and dark matter we must worry about the transition. After the inflation period, by the Standard Big Bang Cosmology, we must have a radiation dominated epoch, in which production of light nuclei occurs in what is called Big Bang Nucleosynthesis, and then the matter domination phase.

Therefore, the reheating process assumes a crucial role in the theory. There is also the possibility of a transition due to non perturbative effects, mostly in the so called preheating phase. Nevertheless, such processes are not sufficient to reheat the Universe and we will leave them out of this discussion [1]. An efficient reheating must be required, obtaining the needed temperatures for Standard Cosmology evolution. However, this does not imply a complete decay of the inflaton field, leaving an open door to a unification theory. The remnant inflaton field could account for dark matter under certain conditions.

A possible solution for the reheating transition could come from an incomplete decay, through an Yukawa interaction with fermion pairs, while the field oscillates about the minimum, but only for a sufficiently large amplitude. With the imposition of the appropriate discrete symmetry the decay is blocked at late times ensuring the full stability of the remaining scalar particles. To ensure the needed reheating, the fermions produced in the decay scatter off the inflaton particles in the oscillating scalar field and lead to its evaporation. These thermalized scalar particles may eventually decouple from the thermal bath and, similarly to other WIMPs, freeze out their abundance.

## 7.1 Minimal Model: Symmetries and Dynamics

Consider a single real scalar field, the inflaton field $\phi$, with a potential energy $V(\phi)$ that originates the slow-roll dynamics. Add two new Yukawa interaction terms between the inflaton and two fermion fields, $N_1$ and $N_2$, with an imposed discrete symmetry $C_2 \subset \mathbb{Z}_2 \times S_2$ on this restricted Lagrangian. Under this interchange symmetry both the scalar field and the fermion fields transform as

$$\begin{aligned} \phi &\leftrightarrow -\phi \\ N_1 &\leftrightarrow N_2 \,. \end{aligned} \tag{7.1}$$

This will impose restrictions on the Lagrangian, which may be written as:

$$\mathcal{L}_{\text{IDM}} = \frac{1}{2}\partial_\mu\phi\partial^\mu\phi - V(\phi) + \bar{N}_1(i\gamma^\mu\partial_\mu - M_1)N_1 + \bar{N}_2(i\gamma^\mu\partial_\mu - M_2)N_2 - h\phi\bar{N}_1N_1 + h\phi\bar{N}_2N_2\,, \tag{7.2}$$

namely, both fermions have equal tree-level mass, $M_1 = M_2$, but opposite sign coupling to $\phi$. Following the assumption that the minimum of the potential lies at $\phi = 0$, such that the $\mathbb{Z}_2$ symmetry remains unbroken, and that these, besides self-interaction terms, are the only inflaton couplings to other particles, we see that when $M_1 > m_\phi/2$ the inflaton decay is not kinematically allowed. Note the importance of the imposed symmetry for blocking off-shell fermion decay modes allowing a stable inflaton bellow the kinematic threshold. For example, no other linear terms in $\phi$ besides those involving $N_1$ and $N_2$ are allowed and, as represented in figure 7.1, the decays into lighter fields cancel out when we consider both $N_1$ and $N_2$ contributions. Thus, this mechanism allows us to consider the late times inflaton as part of the present dark matter abundance.

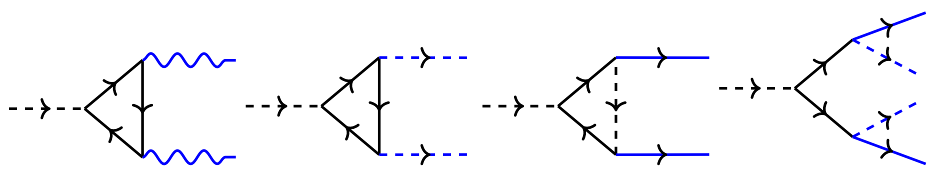

FIGURE 7.1: Examples of the inflaton's forbidden decays due to the imposed symmetry. We represent the light scalar, gauge and fermion fields in blue for a clean understanding.

Far from the origin of the potential the discrete symmetry is broken leading to a mass splitting of the fermions

$$M_{\pm} = |M_1 \pm h\phi| \ . \tag{7.3}$$

Thus, for large values of $\phi$ the inflaton may decay to the two fermions while it oscillates about the minimum after the slow-roll period, namely for field values

$$|M_1 \pm h\phi| < \frac{m_\phi}{2} \implies |\phi| \gtrsim \frac{M_1}{h} \, . \tag{7.4}$$

For Dirac fermions the decay width is given by

$$\Gamma_{\pm} = \frac{h^2}{8\pi} m_\phi \left(1 - \frac{4M_{\pm}^2}{m_\phi^2}\right)^{\frac{3}{2}} , \tag{7.5}$$

with $\Gamma_\phi = \Gamma_+ + \Gamma_-$. Due to the opposite sign of the couplings, the inflaton field will decay alternately into the two fermion particles. Assuming, for now, that the scalar field follows a purely quadratic potential, allowed by the imposed symmetry, its equation of motion is

$$\ddot{\phi} + 3H\dot{\phi} + m_\phi^2 \phi = -\Gamma_\phi \dot{\phi} \, , \tag{7.6}$$

that in terms of the energy density becomes equation (4.36).

If the fermions thermalize quickly, as seen in the reheating discussion,they will form a radiation bath at temperature $T$, and with energy density $\rho_r = \frac{\pi^2}{30} g_\star(T) T^4$, where $g_\star$ are the relativistic degrees of freedom. Having a $\phi$ dependence on the fermions mass, these particles may oscillate between relativistic and non-relativistic states. As a side effect, the $g_\star$ function may also vary with $\phi$. For simplicity we proceed considering $g_\star$ as a constant and, as we will see, it works as a good approximation.

The radiation bath will follow the relation (4.38). The complete set of differential equations is given by equations (4.36) and (4.38), which can be solved for the given parameters $(M \, , m_\phi \, , h\,)$ and initial conditions, with

$$H^2 = \frac{\frac{1}{2}\dot{\phi}^2 + \frac{1}{2} m_\phi^2 \phi^2 + \rho_r}{3M_p^2} \, . \tag{7.7}$$

A numerical solution is presented in the following figures.

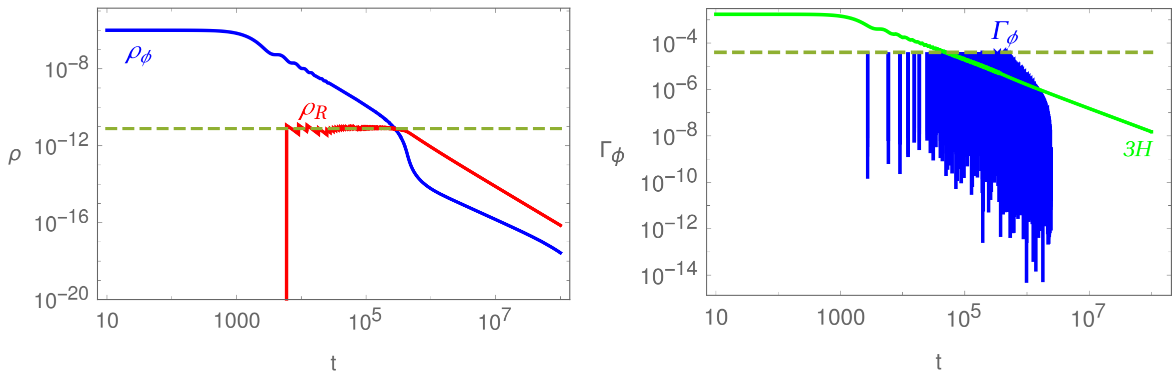


(A) (B)

FIGURE 7.2: Numerical integration of the inflaton-radiation dynamical system of equations for $m_\phi = 10^{-3} M_P$, $M_1 = 0.55\, m_\phi$ and $h = 1$. Time evolution (A) of the inflaton and radiation energy density. In the green dashed line the radiation constancy regime is represented. Comparison (B) between Hubble parameter and the inflaton decay width, with the dashed line representing the maximum value of the decay width. Results are given in Plank units, $M_P = 1$ [1]

From figure 7.2 we see that the inflaton field begins to oscillate about the origin with frequency $m_\phi$ and behaves, after the slow-roll, as cold dark matter, $\rho_\phi \propto a^{-3}$, dominating the energy density of the Universe, such that $a \propto t^{2/3}$ and $H = \frac{2}{3t}$.

Before the start of the oscillations, the decay is forbidden since $M_\pm \sim h\,|\phi| \gg m_\phi$, but it becomes allowed after the field goes through the origin. Since the fermion mass, at this phase with high $\phi$ largely exceeds the tree-level masses, the decay only occurs in short bursts on both sides of the origin. The decay width, in the beginning, corresponds to the narrow peaks represented in figure 7.2 with $\Gamma_{max} = \frac{h^2 m_\phi}{8\pi}$. Although initially $\Gamma_\phi \ll 3H$, these will become comparable and the inflaton energy density will change from a regime where it is only being redshifted, being the dominant component in the Universe's energy density, to a phase where the inflaton effectively decays reducing drastically its energy density. Meanwhile, the radiation energy density will jump and after remaining approximately constant, in a period where it redshifts and increases through the decays, it will equalize and surpass the inflaton energy density. In this latter regime, the maximum decay width will progressively decrease until the decay gets blocked. This leads to a radiation dominated Universe and a stable residual component of the scalar field that can account for dark matter.

Although this analysis was done with numerical simulation support, a semi-analytical take can be made on the constancy regime of the radiation energy density. Let us reproduce the results in [1] with a slightly different approach that will be useful in the next chapter.

In this regime, $\rho_r$ is oscillating due to the Hubble redshift and the increase from the decay processes. Before the effect of the decay becomes significant, changing drastically $\rho_\phi$, the inflaton behaves as a damped harmonic oscillator with

$$\phi(t) \approx \Phi(t)\sin(m_\phi t + \alpha), \qquad \Phi(t) = \sqrt{\frac{8}{3}}\frac{M_p}{m_\phi t}, \tag{7.8}$$

where $\alpha$ is a phase depending on the initial conditions. Let us now reconsider the radiation density equation

$$\dot{\rho}_r + 4H\rho_r = \Gamma_\phi \dot{\phi}^2 . \tag{7.9}$$

For each oscillation period $\tau_\phi$, the condition for the decay $|M_1 \pm h\phi| = \frac{m_\phi}{2}$ is valid in two occasions for each fermion during a time $\Delta t$ and the decay amplitude on average is given by $\frac{\Gamma_{max}}{2}$. The right-hand side of the equation, can be written as

$$\Gamma_\phi \dot{\phi}^2 \simeq 2\,\frac{\Gamma_{max}}{2}\,2\,\Delta t\,\tau_\phi^{-1}\,\dot{\phi}^2 , \tag{7.10}$$

For $h\phi \gg M_1$, the decay into each fermion is allowed during a short period $\Delta t \simeq (h\Phi)^{-1}$, the total oscillation period $\tau_\phi = \frac{2\pi}{m_\phi}$ and the field velocity $\dot{\phi} \simeq m_\phi \Phi$. We then have

$$\Gamma_\phi \dot{\phi}^2 \simeq \frac{h}{8\pi^2} m_\phi^4 \Phi . \tag{7.11}$$

On the other hand, the damping term can be written as

$$4H\,\rho_r = \frac{8}{3t}\rho_r , \tag{7.12}$$

and we can now solve the differential equation for $\rho_r$:

$$\dot{\rho}_r + \frac{8}{3t}\rho_r = \frac{h}{\sqrt{24}\pi^2} m_\phi^3 \frac{M_P}{t} \tag{7.13}$$

$$\rho_r = \frac{\sqrt{6}h}{32\pi^2} M_p m_\phi^3 . \tag{7.14}$$

This yields, in fact, a constant value for the radiation energy density, as already estimated with the numerical simulations. Using this result and the necessity of a reheating period, with $\rho_r > \rho_\phi = \frac{1}{2} m_\phi^2 \Phi^2$ we get that

$$\frac{\sqrt{6}}{16\pi^2} M_p h\, m_\phi \gtrsim \Phi^2 . \tag{7.15}$$

combining with the condition that the decay is only kinematically allowed for field amplitudes $|\Phi| > \frac{M_1}{h}$, a new bound on the fermion mass is obtained:

$$M_1 \lesssim \frac{6^{\frac{1}{4}} h^{\frac{3}{2}} \sqrt{m_\phi M_p}}{4\pi} . \tag{7.16}$$

As a final result, we obtain an estimate for the reheating temperature from equation (7.14):

$$T_R \simeq \left(\frac{15\sqrt{6}}{16\pi^4}\right)^{\frac{1}{4}} g_\star^{-\frac{1}{4}} h^{\frac{1}{4}} \left(\frac{m_\phi}{M_p}\right)^{\frac{3}{4}} M_p\,. \tag{7.17}$$

We have mentioned before that the inflaton could account for the DM abundance. We will develop this calculation after introducing a more complete model in the next chapter.

# Chapter 8

# Inflaton Dark Model with Neutrinos

## 8.1 Right Handed Neutrinos as the Fermions in the Inflaton Dark Matter Model

The previous analysis, with a quadratic potential, gave us a very good insight on how the oscillations around a minimum could launch the inflaton decay into the fermions and how, after the incomplete decay, the scalar field could mimic non-relativistic matter. In order to further develop the Inflaton Dark Matter (IDM) model we must, since the quadratic potential does not agree with experimental bounds, present a realistic inflation description and also ensure the transition to the Standard Model degrees of freedom from our symmetric fermions.

The former point can be solved with the introduction of a non-minimal coupling between gravity and the inflaton field, and a potential with both quartic and quadratic terms. As we will see, the quartic term will be dominant during inflation and reheating, and the quadratic potential will take control for low values of $\phi$, mimicking the dark matter fluid.

A possible solution to the second question may come from the identification of $N_1$ and $N_2$ with two right-handed neutrinos and the introduction of interactions between these fermions and the SM particles. This new interaction term, a Yukawa coupling with the Higgs boson, has the property, together with the right-handed neutrino mass term, to generate a light neutrino mass through the seesaw mechanism. This feature may account for the detected neutrino masses, instead of the massless case in the SM, as we have seen in chapter 2.

The IDM model was introduced considering that the fermions were Dirac fermions. With right-handed neutrinos we adapt the model to Weyl fermions, changing from the four-component spinor fermions to two-component ones. This only modifies the already described dynamics in the inflaton decay into these fermions, the right-handed neutrinos. In particular, the decay value presented in Eq. (7.5) must be divided by a factor of 2. This will induce some changes in the results of equations (7.14) to (7.17). In the following sections, we will change the form of the inflaton potential in the reheating phase to a quartic potential, which will modify the dynamics of reheating.

The Lagrangian for our model of IDM coupled with right-handed neutrinos is the following:

$$\mathcal{L} = \mathcal{L}_{Inf} + \mathcal{L}_{N\,Kin} + \mathcal{L}_{SM} + \mathcal{L}_{N\,Mass} + \mathcal{L}_{SM \leftrightarrow N} \,. \tag{8.1}$$

The inflation sector, as mentioned before, describes the scalar field evolution. As we have seen at the end of the inflation chapter, both quadratic and quartic potentials are in disagreement with Planck bounds [54] for $r$ and $n_s$. With the non-minimal coupling, that will impose a relation between $\xi$, the gravity coupling term, and $\lambda$, the quartic self interaction term, this problem may be solved. The inflation sector is then described by

$$\mathcal{L}_{Inf} = \frac{M^2 + \xi\phi^2}{2} R - \frac{1}{2}\partial_\mu\phi\partial^\mu\phi - V(\phi) \,, \tag{8.2}$$

where $M$ is a mass parameter, $R$ is the Ricci scalar and $\xi$ is an dimensionless coupling. Notice that if $\xi = 0$ we have the common minimal coupling to gravity and $M = M_P$. The parameter $\xi$ turns the effective Planck mass into a dynamical quantity.

The potential is given by

$$V(\phi) = \frac{1}{2} m_\phi^2 \phi^2 + \lambda\phi^4 \,. \tag{8.3}$$

The quartic term is expected to be dominant during inflation since $\lambda \gtrsim 10^{-10}$ and $m_\phi^2 \lesssim 1$ TeV, as will see with the development of the model, and $\phi$ at the end of inflation is of the order of the Planck mass, such that

$$\lambda\phi^4 \gg \frac{1}{2} m_\phi^2 \phi^2 \,. \tag{8.4}$$

However, with just a quartic term the model would be incomplete, in particular the field would be massless at the minimum and could not behave as cold dark matter. Notice that all these new terms in the Lagrangian are allowed by the $\mathbb{Z}_2$ symmetry of the IDM model, making (8.3) the most general renormalizable potential compatible with the symmetry.

The second term on the right-hand side of the Lagrangian includes the kinetic terms of the three right-handed neutrinos. Only two of the right-handed neutrinos are coupled to the inflaton as in the IDM model (7.2) and the third one is introduced for consistency with the number of left-handed neutrinos in the Standard Model. Later on, this third right-handed neutrino will be crucial in a thermal Leptogenesis construction. In the third term we include the entire SM Lagrangian.

The fourth term describes the Majorana mass terms for the right-handed neutrinos

$$\mathcal{L}_{N\,Mass} = -\frac{1}{2}(M_1 + h\phi)N_1N_1^c - \frac{1}{2}(M_2 - h\phi)N_2N_2^c - \frac{1}{2}M_3N_3N_3^c \tag{8.5}$$

with $M_1 = M_2$ imposed by the model's symmetry. In the light neutrino mass generation with the seesaw mechanism, which occurs after the spontaneous symmetry breaking of the electroweak gauge group, the inflaton field value will lie close to the minimum at the origin leaving only the bare masses for the Majorana mass matrix, $\mathbf{M}_R$.

Finally, there are the Yukawa interactions

$$\mathcal{L}_{SM\leftrightarrow N} = y_{\mathtt{i}\ell}N_i^c H\, L + h.c.\,, \tag{8.6}$$

involving the three $N_i$'s, the Higgs boson and the SM left-handed fermions. In the Higgs mechanism, a vacuum expectation value, $\langle H\rangle = \frac{v}{\sqrt{2}}\begin{pmatrix} 0 \\ 1 \end{pmatrix}$, will be attributed to the Higgs boson, producing a Dirac mass term, $\mathbf{m}_D$, for the neutrinos.

Restrictions coming from experiments in neutrino masses will then constrain our model and limit its range of parameters. A more complete analysis of the neutrino masses will be given in the following sections. For now we will focus first on the cosmological evolution of the inflaton field and the neutrinos.

## 8.2 Inflation with a non-minimal Coupling to Gravity

As mentioned earlier, the simple quadratic and quartic potentials cannot give a realistic description of the inflation period. The solution might come with the introduction of a non-minimal coupling to gravity. Let us now explore how this non-minimal coupling affects the scalar field evolution.

Writing the action with the already presented inflation Lagrangian, Eq. (8.2)

$$S_J = \int d^4x\sqrt{-g}\left[\frac{M^2 + \xi\phi^2}{2}R - \frac{1}{2}\partial_\mu\phi\partial^\mu\phi - V(\phi)\right], \tag{8.7}$$

we see that $\xi$ turns the effective Planck mass into a dynamical quantity. The present Planck mass is equal to the mass parameter $M$, since $\langle\phi\rangle = 0$ at late times.

It becomes very difficult to analyze inflation with this type of action, though by performing a conformal transformation we may get rid of the non-minimal coupling terms. Here, we will work in two different frames and this might result in differences between our observables. However, at least to leading order these observables do not change [90].

We may then change from the Jordan frame to the Einstein frame with

$$\hat{g}_{\mu\nu} = \Omega^2 g_{\mu\nu}, \qquad \Omega^2 = 1 + \frac{\xi\phi^2}{M_P^2}. \tag{8.8}$$

The transformation of the Ricci scalar can be calculated and is given by

$$R = \Omega^2 \left[\hat{R} - 6\left(\nabla^2 \ln\Omega + (\nabla \ln\Omega)^2\right)\right]. \tag{8.9}$$

This transformation leads to a non-minimal kinetic term for the inflaton field. To obtain the canonical form it is convenient to perform a field redefinition $\phi \to \chi$ by

$$\frac{d\chi}{d\phi} = \sqrt{\frac{\Omega^2 + 6\xi^2\phi^2/M_P^2}{\Omega^4}}. \tag{8.10}$$

After all these redefinitions, the action in the Einstein frame becomes

$$S_E = \int d^4x\sqrt{-\hat{g}}\left[\frac{M_P^2}{2}\hat{R} - \frac{1}{2}\partial_\mu\chi\partial^\mu\chi - U(\chi)\right], \tag{8.11}$$

where $U(\chi)$ is just a rescaling of the Jordan frame potential

$$U(\chi) = \Omega^{-4}V(\phi). \tag{8.12}$$

Having written the action in the canonical Einstein-Hilbert form allows to study inflation with the standard slow-roll approach. In analogy to what we presented in the inflation section, chapter 4, the slow-roll parameters are given by

$$\epsilon_\chi = \frac{1}{2}M_p^2\left(\frac{U'(\chi)}{U(\chi)}\right)^2, \qquad \eta_\chi = M_p^2\left(\frac{U''(\chi)}{U(\chi)}\right), \qquad N = \frac{1}{M_P^2}\int_{\chi_e}^{\chi_i}\frac{U(\chi)}{U'(\chi)}d\chi. \tag{8.13}$$

We know that during inflation the quartic term will be dominant in the potential, therefore we can neglect the quadratic term in the inflation discussion.

Using the results in Eq. (8.13) we then find

$$\epsilon_\phi = \frac{8M_P^4}{\phi^2\left[M_P^2 + \xi(1+6\xi)\phi^2\right]} \tag{8.14}$$

$$\eta_\phi = \frac{12M_P^6 + 4M_P^4\xi(1+12\xi)\phi^2 - 8M_P^2\xi^2(1+6\xi)\phi^4}{\left[M_P^2\phi + \xi(1+6\xi)\phi^3\right]^2} \tag{8.15}$$

$$N = \frac{1}{8}\left[\frac{(1+6\xi)\phi^2}{M_P^2} - 6\ln\left[M_P^2 + \xi\phi^2\right]\right]\Bigg|_{\phi_e}^{\phi_i} \simeq \frac{(1+6\xi)\phi_i^2}{8M_P^2} \tag{8.16}$$

To generate the correct value of scalar perturbations $\Delta_\mathcal{R}^2 = 2.2\times10^{-9}$, using Eq. (4.72), we obtain the condition $U/\epsilon_\chi = (0.0269 M_P)^4$. This yields a relation between the non-minimal coupling and the inflation self interaction coupling term;

$$\xi \simeq 48000\sqrt{\lambda}\,. \tag{8.17}$$

The scalar to tensor ratio, $r$, and the scalar spectral index $n_s$ can be calculated, with equations (4.74) and (4.75) giving

$$r = \frac{16(1+6\xi)}{N_e + 8N_e^2\xi} \simeq \frac{12}{N_e^2} \tag{8.18}$$

$$n_s = \frac{-3 + N_e - 18\xi - 40N_e\xi + 16N_e^2\xi - 192N_e\xi^2 - 128N_e^2\xi^2 + 64N_e^3\xi^2}{N_e + 16N_e^2\xi + 64N_e^3\xi^2} \simeq 1 - \frac{2}{N_e}, \tag{8.19}$$

where in the last expressions we present the leading results for large $\xi$ . From figure 8.1 we can see how these parameters evolve in terms of the parameter $\xi$ for $N_e = 50 - 60$.

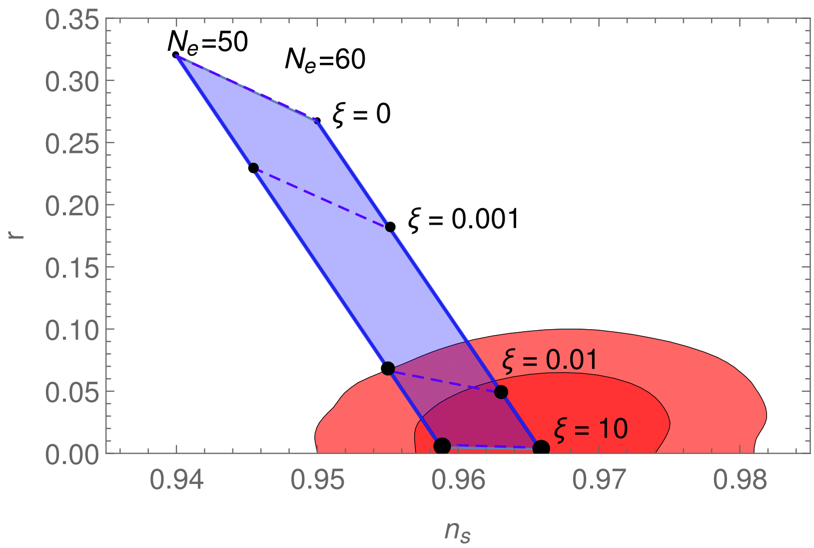


FIGURE 8.1: Observational predictions for an inflaton non-minimal coupling to gravity with a quartic potential for 50-60 e-folds of inflation. The red contours correspond to the 68% and 95% C.L. results from Planck [54]

The Planck data imposes restrictions on the gravity coupling with the inflaton, and from Eq. (8.17) we get a lower bound on $\lambda$. The 1-$\sigma$ bound, for $N_e = 60$, gives $\xi \gtrsim 0.008$ and $\lambda \simeq 2.8 \times 10^{-14}$. For $\xi = 10$, a value that will be considered in the following chapters, we have $\lambda \simeq 4.3 \times 10^{-8}$.

We can ask whether the non-minimal coupling will have any effect for low $\phi$ values, i.e. in the quadratic potential regime. However, if we take a look at the non-minimal coupling term, $M_P^2(1 + \frac{\xi\phi^2}{M_P^2})$, for a small $\phi$, an effect very close to the minimal coupling is observed, having no impact on the dynamics. Indeed solving the system of equations $\epsilon_\phi = 1$ and $\eta_\phi = 1$ we find $\phi_{end} \simeq M_P/\sqrt{\xi}$ at the end of inflation, such that the effects of the non-minimal coupling become negligible shortly after inflation has ended.

## 8.3 Reheating in the Quartic Potential, $\lambda\phi^4$

The previous analysis, in the quadratic potential, gave us a very good insight on how the oscillations around a minimum could trigger the decay into the fermions and how, after the incomplete decay, the scalar field could mimic non-relativistic matter. However, during the slow-roll period field values are expected to be high, turning relevant the inflaton self-interactions. The discrete symmetry of the model allows a quartic self-interaction term such that

$$V(\phi) = \frac{1}{2}m_\phi^2\phi^2 + \lambda\phi^4\,. \tag{8.20}$$

Thus, while field values are high, for example during the slow roll regime and the beginning of the reheating period, the quartic potential will be dominant, producing some changes to the previous analysis. The introduction of the right-handed neutrinos as the symmetry fermions of the model also imposes some changes in the results as discussed in the previous section.

After having discussed how inflation proceeds with the non-minimal coupling description, we turn to the transition to Standard Cosmology, i.e. the reheating period. As we have seen the quartic term regulates this period and some changes to the IDM model [1] with just a quadratic potential have to be introduced .

We may start from the inflaton mass. While the quartic potential is dominant, there is no longer a constant mass term, an effective mass dictates how the oscillations evolve. From the second derivative of the potential we now have

$$m_{eff} = \sqrt{12\lambda\phi^2}, \tag{8.21}$$

which depends on the field value. The inflaton equation of motion is now given by

$$\ddot{\phi} + 3H\dot{\phi} + \Gamma_\phi\dot{\phi} + 4\lambda\phi^3 = 0\,, \tag{8.22}$$

and the complete system is described by equations (4.36) and (4.38), with

$$H^2 = \frac{\frac{1}{2}\dot{\phi}^2 + \lambda\phi^4 + \rho_r}{3M_P^2}. \tag{8.23}$$

The decay width now depends on the effective mass

$$\Gamma_{\pm} = \frac{h^2}{16\pi}\sqrt{12\lambda\phi^2}\left(1 - \frac{4\,(M_1 \pm h\phi)^{\,2}}{12\lambda\phi^2}\right)^{\frac{3}{2}}\,, \tag{8.24}$$

where the extra $1/2$ factor comes from the introduction of Weyl rather than Dirac fermions.

In a similar way we can solve the system of equations numerically. The following figures illustrate an example of the numerical solution:

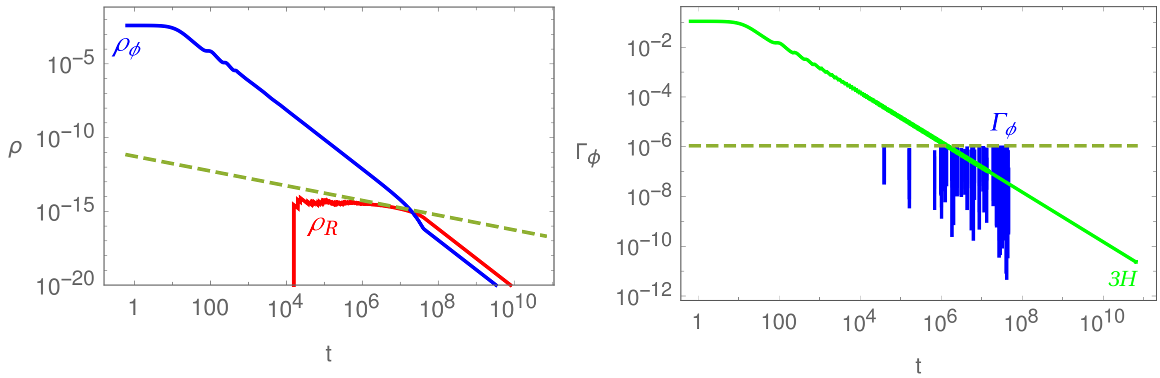


(A) (B)

FIGURE 8.2: Numerical integration of the inflaton-radiation dynamical system of equations for $M_1 = 5\times10^{-5}$, $h = 1$ and $\lambda = 10^{-3}$. In (A) we show the time evolution of the inflaton and radiation energy density. In the green dashed line the radiation-damped-oscillator regime is represented. In (B) we give the comparison between Hubble parameter and the inflaton decay width and in the dashed line we represent the maximum value of the decay width. Results are given in Plank units, $M_P = 1$.

The dynamics is very similar to the quadratic case, but as can be observed in figure 8.2, after the first oscillations, the radiation energy density decreases following a $t^{-\frac{1}{2}}$ curve instead of being constant. This is a consequence of the fact that when the inflaton field begins to oscillate, due to the quartic potential, it will behave as radiation, with $H = (2t)^{-1}$. Indeed in a radiation dominated Universe the Ricci scalar is zero, thus eliminating the mass term in equation (8.7) due to the non-minimal coupling to gravity. In this region the inflaton decays in short bursts in each oscillation and redshifts with the Hubble expansion.

Taking an analogy with the quadratic potential, where the system was described by a damped harmonic oscillator, we write the equation of motion as

$$\ddot{\phi} + 3H\dot{\phi} + \omega^2\phi = 0\,, \tag{8.25}$$

where $\omega^2 = 4\mathrm{A}\lambda\left\langle\phi^2\right\rangle$ and A is a $O(1)$ factor. From numerical simulations, in a system without the damping term, leaving a constant amplitude, a solution of the form $\phi \simeq \Phi\sin(\omega t)$ with $\omega \simeq \sqrt{3\lambda\Phi^2}$ provides a very good approximation.

Thus, we obtain for equation (8.25):

$$\phi(t) \simeq \Phi(t)\sin(\omega t + \alpha), \qquad \Phi(t) = \left(\frac{3}{\lambda}\right)^{\frac{1}{4}} \sqrt{\frac{M_p}{2t}}\,, \tag{8.26}$$

where $\alpha$ is a phase depending on the initial conditions and $\omega$ varies in time as the field's amplitude decreases with expansion.

We now consider the radiation energy density equation

$$\dot{\rho}_r + 4H\rho_r = \Gamma_\phi \dot{\phi}^2\,. \tag{8.27}$$

Similarly to what we have done for the quadratic potential,

$$\Gamma_\phi \dot{\phi}^2 = 2\,\frac{\Gamma_{max}}{2}\,2\,\Delta t\,\frac{\omega}{2\pi}\,\dot{\phi}^2\,, \tag{8.28}$$

where $2\pi/\omega$ is the oscillation period. Now $\Gamma_{max}$ is obtained for field values $\phi = M_1/h$, giving

$$\Gamma_{max} = \frac{M_1\sqrt{12\lambda}h^2}{16\pi}\,. \tag{8.29}$$

The field velocity is $\dot{\phi} \simeq \omega\Phi$ and $\Delta t$ is obtained by working with the condition

$$|M_1 \pm \phi h| = \frac{\sqrt{12\lambda\phi^2}}{2}\,, \tag{8.30}$$

applying Eq. (8.26), expanding the $\sin(\omega t)$ function and then using $\Delta t = |t_+ - t_-|$. Then, we get

$$\Delta t = \frac{M_1}{\omega h^2 \Phi}\sqrt{12\lambda}\,. \tag{8.31}$$

Thus, we have

$$\Gamma_\phi \dot{\phi}^2 \simeq \frac{9}{4\pi^2 h}\lambda^2 M^2 \Phi^3 \simeq \frac{3^{\frac{11}{4}}}{2^{\frac{7}{2}}\pi^2 h}\lambda^{\frac{5}{4}} M_1^2 M_p^{\frac{3}{2}} t^{-\frac{3}{2}}\,. \tag{8.32}$$

The damping term in (8.27) can be written as

$$4H\,\rho_r = \frac{2}{t}\rho_r\,. \tag{8.33}$$

Now we can solve (8.27) and obtain

$$\rho_r = \frac{3^{\frac{7}{4}}}{2^{\frac{5}{2}}\pi^2 h}\lambda^{\frac{5}{4}} M_1^2 M_p^{\frac{3}{2}} t^{-\frac{1}{2}} = \frac{3\sqrt{3}\lambda^{\frac{3}{2}} M_1^2 M_p}{4\pi^2 h}\Phi\,, \tag{8.34}$$

which provides a good approximation to the numerical solution as can be seen in the plots.

In this calculation we assumed the decay products, i.e. $N_1$ and $N_2$, to redshift as radiation, but this is no trivial assumption. When produced, the right-handed neutrinos are approximately massless, but their mass quickly increases with the oscillations of $\phi$, $M_{\pm} = M_1 \pm h\phi$, becoming non-relativistic particles. In this picture, the radiation bath may be composed of the relativistic right-handed neutrinos or their decay products coming from the interactions with the SM, thus leading to a transition to these degrees of freedom even before the right-handed neutrino's freeze-out temperature. It is also possible to have non-relativistic right-handed neutrinos, if their decay is not yet allowed. Nevertheless, an analysis with $H = \frac{3}{8}(1+w)$, with $w$ being the equation state parameter, would just result in a $\frac{6}{4+6w}$ factor in the energy density which would not change very much this analysis. Besides being the result that better reproduces the simulation data, the path followed presents a more conservative bound for the reheating temperature as we will see below.

Using the last result and the need for a reheating period, achieving $\rho_r > \rho_\phi = \lambda\Phi^4$ we get that

$$\frac{3\sqrt{3}\lambda^{\frac{1}{2}}M_1^2 M_p}{4\pi^2 h} > \Phi^3\,, \tag{8.35}$$

combining with the condition that the decay is only kinematically allowed for field amplitudes $|\Phi| > \frac{M}{h}$, we obtain an upper bound on the right-handed neutrino mass

$$M_1 < \frac{3\sqrt{3}\lambda^{\frac{1}{2}}h^2 M_p}{4\pi^2}\,. \tag{8.36}$$

We can also obtain the reheating temperature for this potential. However, first we must estimate $\rho_r$ at the point of equality with $\rho_\phi$. Using equations (8.34) and (8.35) at equality we obtain

$$\rho_{r\,R} = \left(\frac{3\sqrt{3}M_1^2 M_p}{4\pi^2 h}\right)^{4/3}\lambda^{5/3}\,, \tag{8.37}$$

equating to $\rho_r = \frac{\pi^2}{30}g_\star T^4$, we finally get

$$T_R \simeq 284\left(\frac{100}{g_{\star R}}\right)^{-1/4}\left(\frac{M_1}{\mathrm{GeV}}\right)^{2/3}\left(\frac{\lambda}{10^{-8}}\right)^{5/12}\left(\frac{0.1}{h}\right)^{1/3}\mathrm{GeV}\,. \tag{8.38}$$

## 8.4 Condensate Evaporation $\Omega_{CDM}$ and Right-Handed Neutrino Decay

We have seen that the inflaton scalar field becomes stable at late times, since the decays are blocked kinematically and off-shell decay modes are forbidden through the $\mathbb{Z}_2$ symmetry. Since the scalar field exhibits a non-relativistic behavior while oscillating around the minimum, the inflaton becomes a stable dark matter candidate. However, this first analysis is still incomplete, since we have not yet taken into account the scattering interactions between the produced fermions and these scalar particles .

The classical idea of the homogeneous inflaton field, a scalar field, is essentially a collection of zero-momentum bosons, a Bose-Einstein condensate. However, once the condensate starts decaying these bosons can interact with their decay products through scattering processes. In these processes the bosons can be excited and promoted to higher-momentum states, eventually thermalizing with the cosmic radiation bath, for example $N_{1,2} \langle \phi \rangle \leftrightarrow N_{1,2}\, \phi$ and $H \langle \phi \rangle \leftrightarrow H\phi$, where $\langle \phi \rangle$ denotes the condensate state and $H$ the Higgs boson. These scatterings are allowed right after the fermions are produced, and lead to a potential evaporation of the inflaton particle number, transferring it to the thermal bath. The second and third examples arise after the right-handed fermion decay, as we will see in this section.

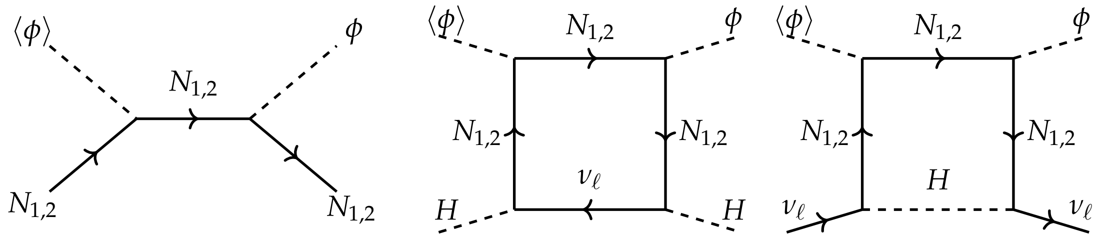

FIGURE 8.3: Dominant Feynman diagrams for evaporation processes

There is a possibility that the evaporation process occurs while the inflaton field is still the dominant component in the energy density of the the Universe. In this scenario, the scatterings would, nevertheless, excite the condensate and turn its degrees into the radiation bath. As a consequence, reheating would happen earlier and at higher temperatures. However, no apparent problems appear in this scenario, making us study the low energy limit of the evaporation dynamics.

First, we will discuss the right-handed neutrinos decays and the transition to the Standard Cosmology evolution. In order to ensure the correct generation of light elements at Nucleosynthesis, quarks, leptons and gauge bosons must be produced before the temperature drops bellow 100 MeV. The connection between the inflation description and the SM particles lies in the right-handed neutrinos interactions.

Through the interaction term in Eq. (8.6), that after spontaneous symmetry breaking generates the Dirac neutrino mass, the right handed neutrinos may decay into the Higgs and lepton doublets. All the possible decays and their respective rates are given by

$$\Gamma\left(N_{1,2} \to h\,\nu\right) = \Gamma\left(N_{1,2} \to h\,\bar{\nu}\right) = y_{eff}^2 \frac{M_1}{64\pi}\left(1 - \frac{m_h^2}{M_1^2}\right)^2 \tag{8.39}$$

$$\Gamma\left(N_{1,2} \to \ell^- W^+\right) = \Gamma\left(N_{1,2} \to \ell^+ W^-\right) = y_{eff}^2 \frac{M_1}{32\pi}\left(1 - \frac{m_W^2}{M_1^2}\right)^2 \left(1 + 2\frac{m_W^2}{M_1^2}\right) \tag{8.40}$$

$$\Gamma\left(N_{1,2} \to Z\,\nu\right) = \Gamma\left(N_{1,2} \to Z\,\bar{\nu}\right) = y_{eff}^2 \frac{M_1}{64\pi}\left(1 - \frac{m_Z^2}{M_1^2}\right)^2 \left(1 + 2\frac{m_Z^2}{M_1^2}\right). \tag{8.41}$$

where $W^\pm$, $Z$ are the weak interactions gauge bosons and $h$ is the Higgs boson with masses much higher that the correspondent leptons. The effective coupling, $y_{eff}^2$, represents the sum of the squares of the individual lepton Yukawa couplings, i.e. $y_{eff}^2 = y_{1e}^2 + y_{1\mu}^2 + y_{1\tau}^2$, with $y_{1\ell} = y_{2\ell}$ due to the $N_1 \leftrightarrow N_2$ symmetry.

Before electroweak symmetry breaking, $m_Z = m_h = m_W = 0$ , leaving the total decay rate as

$$\Gamma_D = \Gamma\left(N_{1,2} \to H\,L\right) + \Gamma\left(N_{1,2} \to \bar{H}\,\bar{L}\right) = y_{eff}^2 \frac{M_1}{8\pi}. \tag{8.42}$$

It is important to note that the physical right-handed neutrino, meaning the heavy neutrino, as referred in the introduction, is a Majorana fermion, therefore being its own antiparticle, $N_1 = \bar{N}_1$. This will be an important detail when we study CP violation in Leptogenesis.

For a significant part of the right-handed neutrino's energy density to be transfered into the SM degrees of freedom we must ensure that

$$\frac{\Gamma_D}{H} = \frac{\sqrt{90}}{8\pi^2} g_\star^{-1/2} y_{eff}^2 \frac{M_1 M_P}{T^2} > 1\,. \tag{8.43}$$

Using the relation between the effective Yukawa coupling and the light neutrino masses that we will discuss in the next section:

$$y_{eff}^2 = k\frac{m_\nu}{v^2} M_1 = \frac{k}{1.2 \times 10^{15}} \frac{M_1}{\mathrm{GeV}}, \tag{8.44}$$

where $k \sim 1 - 10$, the ratio becomes

$$\frac{\Gamma_D}{H} = \frac{\sqrt{90}}{8\pi^2} g_\star^{-1/2} k \frac{M_P m_\nu}{v^2} \left(\frac{M_1}{T}\right)^2 \sim 10^2 g_\star^{-1/2} \left(\frac{M_1}{T}\right)^2. \tag{8.45}$$

Since we expect $M_1$ above the TeV scale, the condition for a successful synthesis of light elements $\frac{\Gamma_D}{H}\Big|_{T=1\text{ MeV}} > 1$ is easily verified.

Nonetheless, the moment when these decays into the SM degrees of freedom occur is of great importance to our evaporation discussion. Let us check this ratio at the reheating temperature

$$\frac{\Gamma_D}{H}\Big|_{T=T_R} \sim 10^2 g_\star^{-1/2}\left(\frac{M_1}{T_R}\right)^2 . \quad (8.46)$$

If $T_R > M_1$, an effective decay will only happen after reheating. Here, the right-handed neutrinos belong to the thermal bath and will play an important role on the evaporation dynamics. On the other hand, if $M_1 > T_R$, the decay already happened before the inflaton-radiation equality, during the inflaton oscillations around the minimum. In the latter scenario, only the SM particles participate in the evaporation process.

Now we may turn again to the evaporation discussion. As discussed when we introduced the IDM model [1], as soon as the fermions start being produced, the temperature of the radiation bath will quickly increase, flattening out when it reaches the value for the radiation-inflaton energy density equality, corresponding to the reheating temperature that was estimated for both quadratic and quartic potentials.

Let us now compute the evaporation rate. Starting with the case where the reheating temperature is larger than $m_\phi$ and $M_1$, all the particles in the thermal bath are in thermal equilibrium and we may consider the relativistic Bose-Einstein, for the inflaton and SM bosons, and the Fermi-Dirac distributions, for right-handed neutrinos and SM fermions, respectively. The net condensate evaporation rate, where we include also the inverse processes, is given by

$$\Gamma_{evap} = \frac{1}{n_\phi}\int\prod_{i=1}^{4}\frac{d^3\mathbf{p}_i}{(2\pi)^3\,2E_i}(2\pi)^4\,\delta^4\left(p_1+p_2-p_3-p_4\right)|\mathcal{M}|^2$$
$$\times\left[f_1f_2\left(1+f_3\right)\left(1-f_4\right)-f_3f_4\left(1+f_1\right)\left(1-f_2\right)\right] , \quad (8.47)$$

where $\mathcal{M}$ is the scattering amplitude for the processes and $f_i$ are the phase space distribution factors. Considering first the right-handed neutrino scattering, figure 8.3, with large abundance of the inflaton in the condensate we expect $f_i \gg 1$, thus, to leading order for $T \gg m_\phi, M_\pm$

$$\Gamma_{evap} \simeq \frac{h^4}{12\pi^3}\left(1+\log\left(\frac{T}{m_\phi}\right)\right)T. \quad (8.48)$$

In the radiation era the evaporation rate is thus expected to catch the Hubble expansion rate, thus leading to an efficient evaporation. However, if the fermions become non-relativistic the interaction rate becomes Boltzmann suppressed. Thus, the evaporation must happen for $T \gtrsim M_1$ since

$$\frac{\Gamma_{evap}}{H}\Bigg|_{T=M_1} \simeq 10^{13}h^4 g_\star^{-1/2}\left(\frac{1\ \mathrm{TeV}}{M_1}\right) \gtrsim 1. \quad (8.49)$$

This evaporation rate is similar to the rate of other four body interactions, as inflaton and fermion annihilation. We therefore expect that, for a sufficiently large Yukawa coupling $h$, the condensate degrees of freedom are converted into the thermal bath, therefore destroying the boson condensate. This conversion will increase the radiation energy density and its temperature leading to a maximum value of the order

$$T_R^{max} = \left(\frac{90}{\pi^2}\right)^{1/4} g_\star^{-1/4}\sqrt{M_P M_1} = 8.5\times 10^{10} g_\star^{-1/4}\left(\frac{M_1}{1\ \text{TeV}}\right)^{1/2} \text{GeV}. \qquad (8.50)$$

This corresponds to the limiting case where the evaporation occurs right after the beginning of the inflaton oscillations as discussed previously.

Having the inflaton particles in the thermal bath, following the procedure described in the WIMP abundance calculation section, the inflaton is now a suitable dark matter candidate. After the annihilation and elastic scattering processes become inefficient, the inflaton will decouple from the thermal bath and its abundance will freeze out. We expect, at this moment, both the right-handed neutrinos and the scalar particle to be non-relativistic, giving an annihilation cross section, for the fermion t-channel, given by

$$\sigma_{\phi\phi} \simeq \frac{h^4}{8\pi m_\phi^2}\,. \qquad (8.51)$$

If we follow the calculation for the thermal relic abundance for a decoupled species, described before, we obtain

$$m_\phi \simeq 1.4 h^2 \left(\frac{\Omega_{\phi 0} h_0^2}{0.1}\right)^{1/2} \left(\frac{g_{\star F}}{10}\right)^{1/4} \left(\frac{\mathrm{x_F}}{25}\right)^{-3/4} \text{TeV}\,. \qquad (8.52)$$

where $g_{\star F}$ corresponds to the number of relativistic degrees of freedom at freeze-out and $x_F = m_\phi/T_F$, with $T_F$ being the freeze out temperature.

We can now relate equations (8.49) and (8.52) to obtain a restriction on the right-handed neutrino mass in order no obtain the correct dark matter relic abundance

$$m_\phi \gtrsim 4.9\times 10^{-5} \left(\frac{\Omega_{\phi 0} h_0^2}{0.1}\right)^{1/2} \left(\frac{g_{\star F}}{10}\right)^{1/2} \left(\frac{x_F}{25}\right)^{-3/4} \left(\frac{M_1}{1\ \text{GeV}}\right)^{1/2} \text{GeV}\,. \qquad (8.53)$$

Let us now consider the evaporation through the SM degrees of freedom, having as a representative the scattering with the Higgs boson, represented in figure 8.3. The corresponding loop diagram can be roughly estimated as yielding an effective four point interaction with coupling $g' \sim \frac{h y_{eff}}{\sqrt{16\pi^2}}$ up to $O(1)$ factors. The resulting cross section, with a thermal center of mass energy, corresponds to

$$\sigma_{\phi H} \simeq \frac{h^2 y_{eff}^2}{256\pi^3 T^2} \qquad (8.54)$$

Using the number density of relativistic Higgs bosons, $n_H = \frac{2}{\pi^2}\zeta(3)T^3$, and that $\Gamma_{evap} \simeq n_H \langle \sigma v \rangle$, the scattering rate can be estimated as

$$\Gamma_{evap} \simeq \frac{\zeta(3)}{128\pi^5} h^2 y_{eff}^2 T \,. \tag{8.55}$$

At one-loop order, scattering with the left-handed neutrinos, present in the thermal bath, could also be contribute as an evaporation process, see figure 8.3. However, the effective interaction term, $\phi^2 \nu_\ell^2$, is a dimension-5 operator, meaning that the effective coupling must have a $M_1^{-1}$ suppression factor. In comparison to the Higgs scattering cross section, equation (8.54), a factor $(T/M_1)^2$ appears, coming from the effective coupling and the fermion lines, leading to $\Gamma_{evap} \propto T^3/M_1^2$. As a result, the evaporation rate drops faster than the Hubble rate having no impact on the evaporation process.

In order to have an effective evaporation before electroweak symmetry breaking we then find

$$\left.\frac{\Gamma_{evap}}{H}\right|_{T=0.1\text{ TeV}} = \frac{\zeta(3)}{128\sqrt{90}\pi^6} g_\star^{-1/2} \frac{M_P}{T} h^2 y_{eff}^2 \simeq 10^{11} g_\star^{-1/2} h^2 y_{eff}^2 > 1 \,. \tag{8.56}$$

In the case $T_R > M_1$, evaporation of the inflaton condensate may proceed through scatterings with both the right-handed neutrinos and the Higgs boson, such that eqs (8.49) and (8.56) must be taken into account.

As already said, if $M_1 > T_R$, at reheating right-handed neutrinos are no longer relativistic. The interactions with these particles become Boltzmann suppressed and are no longer relevant. Since the SM particles have already been produced, the evaporation dynamics follows only through the scattering rate given in eq. (8.55) and the condition in (8.56) binds our parameters.

A still missing piece in this model dynamics is related to what was introduced in the second chapter of this thesis. Low energy neutrino phenomenology yields important constrains on the right-handed neutrino masses and Yukawa couplings. We then turn to this discussion in the next section.

## 8.5 Connection with Low Energy Phenomena: Neutrino Masses

We start from the IDM model with the decay into right-handed neutrinos, $N_1$ and $N_2$, with an imposed symmetry $\phi \leftrightarrow -\phi$, $N_1 \leftrightarrow N_2$. Assuming the existence of an extra right-handed neutrino, $N_3$, and if we then add an interaction between the right-handed neutrinos with the SM neutrinos and the Higgs boson, through Yukawa couplings, we obtain the following

Lagrangian density :

$$\mathcal{L}_{mass} = -\frac{1}{2}(M_1 + h\phi)N_1 N_1^c - \frac{1}{2}(M_2 - h\phi)N_2 N_2^c - \frac{1}{2}M_3 N_3 N_3^c \\ + y_{i\ell} N_i^c H \nu_\ell + h.c. \tag{8.57}$$

with $\ell = e, \mu, \tau$ and $i = 1, 2, 3$. We see that when $\phi \simeq 0$ the fermions masses become equal.

Let us look at the resulting mass matrices. Since we have the freedom to consider a diagonal Majorana mass matrix, then

$$M_R = \begin{pmatrix} M_1 & 0 & 0 \\ 0 & M_1 & 0 \\ 0 & 0 & M_3 \end{pmatrix}. \tag{8.58}$$

As a result of the $N_1 \leftrightarrow N_2$ symmetry we get some restrictions on the Dirac mass matrix. We write the Dirac mass elements with as:

$$a = \frac{v}{\sqrt{2}} y_{1e} = \frac{v}{\sqrt{2}} y_{2e}; \quad b = \frac{v}{\sqrt{2}} y_{1\mu} = \frac{v}{\sqrt{2}} y_{2\mu}; \quad c = \frac{v}{\sqrt{2}} y_{1\tau} = \frac{v}{\sqrt{2}} y_{2\tau}; \\ d = \frac{v}{\sqrt{2}} y_{3e}; \quad e = \frac{v}{\sqrt{2}} y_{3\mu}; \quad f = \frac{v}{\sqrt{2}} y_{3\tau}; \tag{8.59}$$

The Dirac mass matrix can be written as

$$m_D = \begin{pmatrix} m_{1e} & m_{1\mu} & m_{1\tau} \\ m_{2e} & m_{2\mu} & m_{2\tau} \\ m_{3e} & m_{3\mu} & m_{3\tau} \end{pmatrix} = \begin{pmatrix} a & b & c \\ a & b & c \\ d & e & f \end{pmatrix} \tag{8.60}$$

Applying the Seesaw mechanism (type I) result for the light neutrinos, Eq. (2.13), we get

$$\mathcal{M}_\nu = -m_D^T M_R^{-1} m_D = -\begin{pmatrix} \frac{d^2}{M_3} + \frac{2a^2}{M_1} & \frac{de}{M_3} + \frac{2ab}{M_1} & \frac{df}{M_3} + \frac{2ac}{M_1} \\ \frac{de}{M_3} + \frac{2ab}{M_1} & \frac{e^2}{M_3} + \frac{2b^2}{M_1} & \frac{ef}{M_3} + \frac{2bc}{M_1} \\ \frac{df}{M_3} + \frac{2ac}{M_1} & \frac{ef}{M_3} + \frac{2bc}{M_1} & \frac{f^2}{M_3} + \frac{2c^2}{M_1} \end{pmatrix}. \tag{8.61}$$

As a result of this symmetry, $det\, \mathcal{M}_\nu = 0$. Thus, at least one eigenvalue is zero, i.e. one of the light neutrinos must be massless.

On the other hand, since the flavour basis charged lepton mass matrix is diagonal, the mass matrix of the light neutrinos, in the same basis, is diagonalized by $U_{PMNS}$ through

$$M_\nu^d = U_{PMNS}^T \mathcal{M}_\nu U_{PMNS}. \tag{8.62}$$

Thus we obtain

$$\mathcal{M}_\nu = U^*_{PMNS} M^d_\nu U^\dagger_{PMNS} \tag{8.63}$$

where

$$M^d_\nu = \begin{pmatrix} m_1 & 0 & 0 \\ 0 & m_2 e^{-2i\phi_1} & 0 \\ 0 & 0 & m_3 e^{-2i\phi_2} \end{pmatrix}. \tag{8.64}$$

As a first approximation we will not consider the Majorana phases and using the experimental data on $\Delta m^2_{12} = \left|m_1^2 - m_2^2\right| \sim 10^{-5}$ eV$^2 \ll \Delta m^2_{23}$, it is possible to assume $m_1 \simeq m_2$ to leading order. As we have seen, the tribimaximal mixing matrix yields a very good approximation to the experimental data on mixing angles:

$$U_{PMNS} \simeq U_{TBM} = \frac{1}{\sqrt{6}} \begin{pmatrix} 2 & \sqrt{2} & 0 \\ -1 & \sqrt{2} & \sqrt{3} \\ 1 & -\sqrt{2} & \sqrt{3} \end{pmatrix} \tag{8.65}$$

Thus, we have

$$\mathcal{M}_\nu = \begin{pmatrix} m_2 & 0 & 0 \\ 0 & \frac{m_2+m_3}{2} & -\frac{m_2-m_3}{2} \\ 0 & -\frac{m_2-m_3}{2} & \frac{m_2+m_3}{2} \end{pmatrix} \tag{8.66}$$

By matching the two light neutrino mass matrices we may then obtain conditions on the parameters of the model.

Using equations (8.61) and (8.66) we obtain a system with two distinct solutions.

The first gives

$$\begin{gathered} m_2 = -\frac{v^2}{M_3}\left(\frac{y_{3e}^2}{2} + y_{3\mu}^2\right); \quad m_3 = 0; \quad y_{1e} = \pm y_{3\mu}\gamma^{\frac{1}{2}}; \quad y_{1\mu} = \mp \frac{y_{3e}}{2}\gamma^{\frac{1}{2}}; \\ y_{1\tau} = \pm \frac{y_{3e}}{2}\gamma^{\frac{1}{2}}; \quad y_{i\tau} = -y_{i\mu} \end{gathered} \tag{8.67}$$

with $i = 1, 2, 3$ and where $\gamma = \frac{M_1}{M_3}$. The resulting Dirac mass matrix is

$$m_D = \frac{v}{\sqrt{2}} \begin{pmatrix} y_{1e}(y_{3\mu}, \gamma) & y_{1\mu}(y_{3e}, \gamma) & -y_{1\mu}(y_{3e}, \gamma) \\ y_{1e}(y_{3\mu}, \gamma) & y_{1\mu}(y_{3e}, \gamma) & -y_{1\mu}(y_{3e}, \gamma) \\ y_{3e} & y_{3\mu} & -y_{3\mu} \end{pmatrix} \tag{8.68}$$

Through these results we clearly see a $\mu \leftrightarrow \tau$ symmetry. Interactions with $\nu_\mu$ have an opposite sign to $\nu_\tau$'s and with $m_3 = 0$ we have a resulting inverted neutrino mass hierarchy.

The $N_3$ right-handed neutrino does not have a connection with the inflation model, thus it would be interesting to write the mass relation in terms of the $N_{1,2}$ parameters. Through the relations specified in (8.67) we can write the $m_2$ expression in terms of $M_1$ and $y_{eff}$ as defined in the previous section. Recall that $y_{eff}^2 = y_{1e}^2 + y_{1\mu}^2 + y_{1\tau}^2$, together with the condition $y_{1\mu}^2 = y_{1\tau}^2$ we then have

$$m_2 = \frac{2v^2 y_{1\mu}^2 + v^2 y_{1e}^2}{M_1} = \frac{v^2 y_{eff}^2}{M_1}.$$

If we now apply the experimental values for $m_2$, coming from $\Delta m_{23}^2 = (2.44 \pm 0.06) \times 10^{-3}\mathrm{eV}^2$ and $m_3 = 0$ we then have

$$M_1 = 1.21 \times 10^{15}\, y_{eff}^2\ \mathrm{GeV}, \tag{8.69}$$

witch gives an important relation between the parameters of our problem.

We now turn to the second case, where the solution is

$$m_3 = -v^2 \left( \frac{2y_{1\mu}^2}{M_1} + \frac{y_{3\mu}^2}{M_3} \right); \quad m_2 = 0; \quad y_{1e} = 0; \quad y_{3e} = 0; \quad y_{i\tau} = y_{i\mu}; \tag{8.70}$$

with $i = 1, 2, 3$. The resulting Dirac mass matrix is

$$m_D = \frac{v}{\sqrt{2}} \begin{pmatrix} 0 & y_{1\mu} & y_{1\mu} \\ 0 & y_{1\mu} & y_{1\mu} \\ 0 & y_{3\mu} & y_{3\mu} \end{pmatrix}. \tag{8.71}$$

We again have a $\mu \leftrightarrow \tau$ symmetry, that is in fact a feature of the tribimaximal mixing. Due to $U_{PMNS} = U_{TBM}$ and since $m_1 \simeq m_2 = 0$ there is no interaction with $\nu_e$ resulting in null Yukawa couplings. In this case we have a normal neutrino mass hierarchy.

In the second scenario we cannot fully convert the mass relation to just $N_{1,2}$ parameters. Since $y_{1e} = 0$, we write

$$m_3 = \frac{v^2}{M_1} \left( y_{eff}^2 + y_{3\mu}^2 \gamma \right). \tag{8.72}$$

Here, after using the experimental value for $\Delta m_{23}^2$ we still have three unknown parameters, since $N_3$ interactions and masses are unknown. In order to simplify this study, we look at the possibility of $y_{eff}^2$ and $y_{3\mu}^2\gamma$ being of the same order. Then

$$M_1 = 1.21 \times 10^{15} k\, y_{eff}^2\, \mathrm{GeV}, \tag{8.73}$$

where $k \sim 1 - 10$. We will see in the next chapter that the properties of the third right-handed neutrinos becoming important for embedding a thermal leptogenesis scenario within our model.

Since the determinant of the light neutrino mass matrix, obtained through the seesaw mechanism, is zero, at least one of the neutrinos is massless. Through the imposition of tribimaximal mixing, $N_1 \leftrightarrow N_2$ symmetry and experimental values of the neutrino mass squared differences we have reduced our problem's independent parameters, obtaining relations between the right-handed neutrino masses and the Yukawa couplings.

Finally, the combination of all bounds, coming from inflation, evaporation, reheating and measured neutrino masses, will be analyzed in the next section.

## 8.6 Resulting parameter space

While describing, chronologically, the dynamics of our Inflaton Dark Matter model with right-handed neutrinos, we have determined several relations and restrictions on the model parameters. In this section we will put together all these bounds and study the allowed parameter space. Later on, we will test this model while trying to generate the observed baryon asymmetry in the Universe through thermal Leptogenesis.

First we have described inflation and the slow-roll evolution with the help of a non-minimal coupling to gravity, equation (8.2). As we have seen, Planck data on scalar perturbations $\Delta^2_{\mathcal{R}}$ resulted in a relation between $\xi$ and $\lambda$

$$\xi \simeq 48000\sqrt{\lambda}\,. \tag{8.74}$$

In this description we saw why no relation between $m_\phi$, the inflaton mass, and $\xi$ appeared. Experimental data on $r$ and $n_s$, figure 8.1, bounded $\xi$ around $\xi \gtrsim 0.008$. As described, this results in bounds on the 4-point self interaction of the inflaton.

Following the arrow of time, the next step is the reheating period. Developed within a quartic potential dominance, an estimate of the reheating temperature was obtained:

$$T_R \simeq 284 \left(\frac{100}{g_{\star R}}\right)^{-1/4} \left(\frac{M_1}{\text{GeV}}\right)^{2/3} \left(\frac{\lambda}{10^{-8}}\right)^{5/12} \left(\frac{0.1}{h}\right)^{1/3} \text{GeV}\,. \tag{8.75}$$

Also, coming from the decay blocking condition and the need of a radiation dominance period together with the incomplete decay condition, we have obtained a lower and an upper bound, respectively, on the two right-handed neutrino masses

$$\frac{m_\phi}{2} < M_1 < \frac{3\sqrt{3}\lambda^{\frac{1}{2}} h^2 M_p}{4\pi^2}\,. \tag{8.76}$$

Stepping into the right-handed neutrino decays into SM particles, we saw that the necessary conditions for a successful reheating, leading to the Standard Cosmology, are ensured. However, two different scenarios might have happened. It was possible to have the right-handed neutrino masses both heavier or lighter than the reheating temperature. As a consequence, two different evaporation mechanisms may have occurred.

If $T_R > M_1$, the right-handed neutrinos would still be on the thermal bath, playing an important role on the evaporation process. In this picture a bound on the neutrino coupling to the inflaton arises

$$h^4 \gtrsim 1.25 \times 10^{-13} g_\star^{1/2} \left(\frac{M_1}{\text{TeV}}\right) . \tag{8.77}$$

On the other hand, if $M_1 > T_R$, the right-handed neutrinos are no longer in the thermal bath having already decayed into SM degrees of freedom. In this situation, only the SM particles participate in the evaporation. One representative interaction could be the Higgs boson scattering with the condensate inflaton particles. Imposing an efficient evaporation before the electroweak scale results in

$$h^2 y_{eff}^2 \gtrsim g_\star^{1/2} 10^{-11} . \tag{8.78}$$

After evaporation occurs, the inflaton follows the common WIMP description. Using the standard calculation for the thermal relic abundance of a decoupled relativistic species, a relation between the inflaton mass and its coupling to the right-handed neutrinos was obtained

$$m_\phi = 1.4 h^2 \left(\frac{\Omega_{\phi 0} h_0^2}{0.1}\right)^2 \left(\frac{g_{\star F}}{10}\right)^{\frac{1}{4}} \left(\frac{x_F}{25}\right)^{-\frac{3}{5}} \text{TeV}. \tag{8.79}$$

Finally, in the last section, the neutrino masses and mixings resulted in two independent solutions. In the first case a simple relation between $y_{eff}^2$ and $M_1$ was obtained

$$M_1 = 1.21 \times 10^{15} y_{eff}^2 \,\text{GeV}. \tag{8.80}$$

The second case provides a more complex relation since it also includes the third right-handed neutrino mass and Yukawa couplings. However, in order to simplify the analysis we assumed $y_{3\mu}^2 \gamma$ to be of the same order of $y_{eff}^2$:

$$M_1 = 1.21 \times 10^{15} \left(y_{eff}^2 + y_{3\mu}^2 \gamma\right) \text{GeV} \simeq 1.21 \times 10^{15} k\, y_{eff}^2 \,\text{GeV} , \tag{8.81}$$

with $k \sim 1 - 10$.

To summarize we have six parameters (seven in the second case) that describe our model dynamics. Namely $\xi$, $\lambda$, $m_\phi$, $h$, $M_1$ and $y_{eff}$ (plus $y_{3\mu}^2 \gamma$ for the second case). However, three relations,

$$\xi \simeq 48000\sqrt{\lambda}\,, \tag{8.82}$$

$$m_\phi \simeq 1.4h^2\ \text{TeV}\,, \tag{8.83}$$

$$M_1 \simeq 1.21\times 10^{15}\, y_{eff}^2\ \text{GeV} \tag{8.84}$$

reduce the number of independent parameters to three (four in the second light neutrino mass scenario). These relations simplify equations (8.76), (8.77) and (8.78) in terms of $M_1$, $m_\phi$ and $\lambda$, the chosen parameters to represent the model.

$$\frac{m_\phi}{2} < M_1 < \frac{3\sqrt{3}\,\lambda^{\frac{1}{2}} M_p m_\phi}{4\pi^2\ \text{TeV}}\,, \tag{8.85}$$

$$m_\phi \gtrsim 4.9\times 10^{-5}\left(\frac{M_1}{\text{GeV}}\right)^{1/2}\text{GeV}\,, \tag{8.86}$$

$$m_\phi \gtrsim 1.7\times 10^{8}\left(\frac{\text{GeV}}{M_1}\right)\text{GeV}\,. \tag{8.87}$$

Taking into account that both $h$ and $y_{eff}$ follow from perturbative effects we represent our analysis in figure 8.4 for fixed values of $\lambda$ ($\xi$).

In the orange lines different reheating temperatures were introduced using Eq. (8.38). Since the model's natural range of values is at much higher scales, conditions like $T_R > 0.1$ GeV, the minimum allowed reheating temperature to generate the proper synthesis of light elements, are not relevant when studying this parameter space.

While satisfying all the bounds, a broad parameter space was obtained, having room for both small neutrino and inflaton masses, and large mass scenarios. The upper limits on our parameters come from the need to keep small couplings $y_{eff}$, $h < 1$ since the theory is based on a perturbative analysis. Large mass, $M_1 \gtrsim 10^{10}$ GeV, $m_\phi \gtrsim 10^3$ GeV, or high couplings, $y_{eff} \gtrsim 0.01$, $h \gtrsim 1$ and small mass solutions, $M_1 \lesssim 1$ GeV, $m_\phi \lesssim 10^{-3}$ GeV, or equivalently $y_{eff} \lesssim 10^{-7}$, $h \lesssim 10^{-3}$ are available within our unified model description.

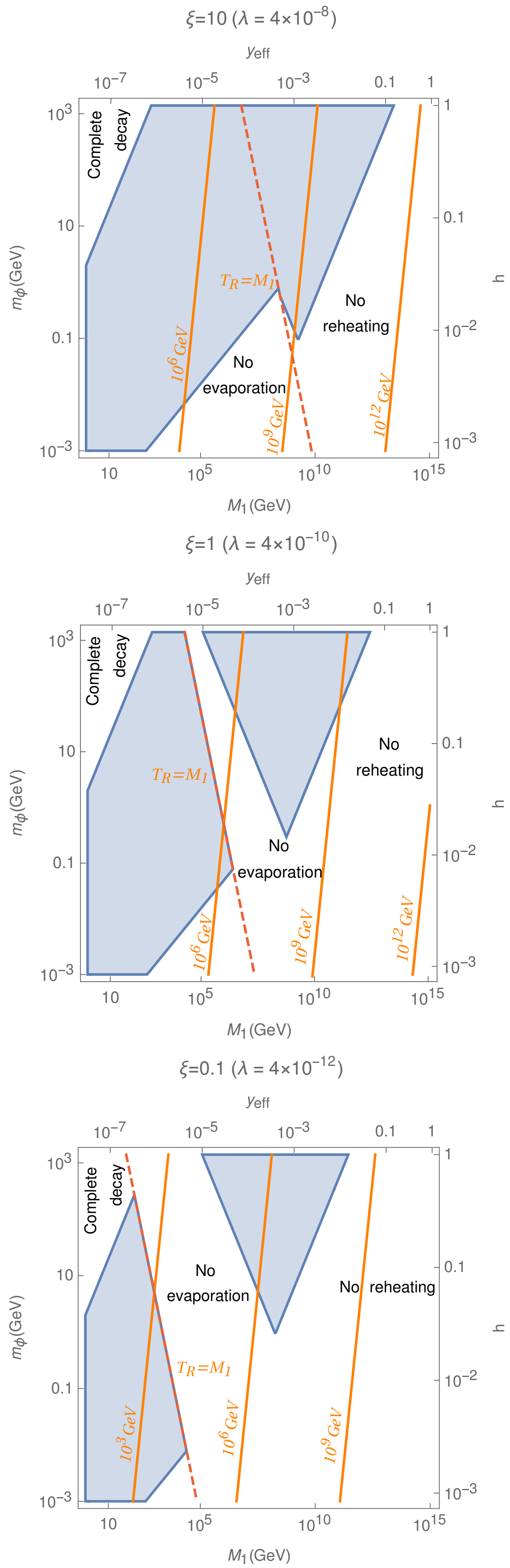


FIGURE 8.4: Resulting parameter space for $\xi = 0.1$, 1, and 10 for $g_\star = 100$. Orange lines represent reheating temperatures and the dashed line, $M_1 = T_R$, limits evaporation conditions. Condition (8.85) defines the complete decay and no reheating regions, and conditions (8.86),(8.87) limit the no-evaporation region.

The evaporation conditions and the $M_1 = T_R$ equality, in the dashed line, play an important role in this analysis. For $\xi < 10$, regions without an efficient evaporation appear in the center of the parameter space. As already mentioned, scattering with neutrinos is suppressed when compared with the Higgs interactions, being negligible for these processes. In this scenario, the inflaton particles may survive as a Bose condensate.

As we have discussed and is numerically verified in figure 8.2, the inflaton decays until it becomes kinematically blocked at

$$\phi_{DR} = \frac{M_1}{h}\,. \tag{8.88}$$

If the evaporation processes are not sufficient to excite the condensate into the thermal bath, while the quartic term dominates the inflaton potential, the condensate will stay in a Dark Radiation (DR) regime, since the scalar field is stable and behaves as a radiation fluid. Once the quadratic term becomes dominant at

$$\phi_{CDM} = \sqrt{\frac{1}{2}\frac{m_\phi^2}{\lambda}}, \tag{8.89}$$

the inflaton field will behave as Cold Dark Matter (CDM). Since the $\frac{n}{s}$ ratio becomes constant until today, we can relate it to the current data on the dark matter relic density.

$$\Omega_{\phi 0} = \frac{\rho_{\phi 0}}{\rho_{c0}} = \frac{m_\phi n_{\phi 0}}{3H_0^2 M_P^2} = \frac{m_\phi s_0}{3H_0^2 M_P^2}\left(\frac{n_\phi}{s}\right)_{CDM}. \tag{8.90}$$

Using that between $\phi_{DR}$ and $\phi_{CDM}$ the inflaton field behaves as a radiation fluid and $T_{DR} \simeq T_R$

$$\frac{\phi_{DR}}{\phi_{CDM}} \simeq \frac{T_R}{T_{CDM}}. \tag{8.91}$$

Now, the inflaton number density entropy ratio is given by

$$\left(\frac{n_\phi}{s}\right)_{CDM} = \left(\frac{\rho_\phi}{m_\phi s}\right)_{CDM} = \frac{\frac{1}{2} m_\phi \phi_{CDM}^2}{\frac{2\pi^2}{45} g_{\star CDM} T_{CDM}^3} \tag{8.92}$$

Using equations (8.38), (8.91), (8.92), and $s_0 = \frac{2\pi^2}{45} g_{\star 0} T_0^3$ in equation (8.90) we obtain

$$\Omega_{\phi 0} = \frac{\left(\frac{2}{5}\right)^{3/4} \pi^{7/2}}{27 \times 3^{1/4}} \left(\frac{g_{\star R}^{3/4} g_{\star 0}}{g_{\star CDM}}\right) \frac{T_0^3 m_\phi M_1}{\lambda^{3/4} h^2 H_0^2 M_P^3}. \tag{8.93}$$

With $H_0 = 10^{-42} h_0$ GeV, $g_{\star 0} = 3.91$, $T_0 = 2.4 \times 10^{-13}$ GeV and $M_P \simeq 2.4 \times 10^{18}$ GeV

$$\Omega_{\phi 0} h_0^2 = 2.9 \times 10^{-9} \left(\frac{g_{\star R}^{3/4}}{g_{\star CDM}}\right) \frac{1}{\lambda^{3/4} h^2} \left(\frac{m_\phi M_1}{\text{GeV}^2}\right) \tag{8.94}$$

which finally results in

$$m_\phi = 0.343 \left(\frac{g_{\star CDM}}{g_{\star R}^{3/4}}\right)\left(\frac{h}{0.1}\right)^2\left(\frac{\lambda}{10^{-8}}\right)^{3/4}\left(\frac{\Omega_{\phi 0}h_0^2}{0.1}\right)\left(\frac{\mathrm{GeV}}{M_1}\right)\mathrm{GeV}. \tag{8.95}$$

Similarly to the evaporation analysis we can study the allowed parameter space using the relations (8.82), (8.84) and (8.95) with the bounds (8.76), (8.77) and (8.78), having on the last two the inverse relation. We then find

$$\frac{m_\phi}{2} < M_1 < \frac{7.7\times 10^{10}\, M_1 m_\phi}{\lambda^{1/4}\,\mathrm{GeV}}, \tag{8.96}$$

$$m_\phi \lesssim 0.14\left(\frac{\mathrm{GeV}}{M_1}\right)^{1/2}\lambda^{3/4}\,\mathrm{GeV}, \tag{8.97}$$

$$m_\phi \lesssim 4.9\times 10^{11}\left(\frac{\mathrm{GeV}}{M_1}\right)^{2}\lambda^{3/4}\,\mathrm{GeV}. \tag{8.98}$$

Since the theory was developed from an perturbative analysis, the parameter $h$ has to be kept small, $h < 1$. As additional bounds we must impose $T_{CDM} > T_{eq}$ and $T_R > T_{BBN}$, where $T_{eq} = 0.79$ eV is the temperature at the matter-radiation energy density equality and $T_{BBN} \simeq 10$ MeV. We represent such analysis in figure 8.5.

Although the figures in the evaporation scenario and in the condensate evolution are represented with different scales due to the different $m_\phi/h$ relation, the allowed regimes seem to be complementary, having no overlap between regions. In the regime with larger masses we have the WIMP solution whereas the condensate hypothesis rests at the regime with smaller masses, very close to the BBN and the matter-radiation equality temperature bounds.

As we can see in figure 8.4, solutions with $h \simeq 1$ are possible. Having the inflation-right-handed neutrino's coupling at this order may result high radiative corrections to the inflaton potential. Allowing the introduction of superpartners, in a supersymmetry context, to the inflaton and to the right-handed neutrinos with the same coupling $h$ in the equivalent interactions we may cancel out these radiative corrections. This cancellation is only exact in a case of an exact supersymmetry, due to the opposite sign in the loops for fermions and bosons. However, since supersymmetry is broken, during inflation, the cancellation is only partial though being sufficient in this scenario. Nevertheless, such an analysis is beyond the scope of this thesis.

As a final step on this work, we will try to reproduce the generation of the observed baryon asymmetry in the Universe through Leptogenesis.

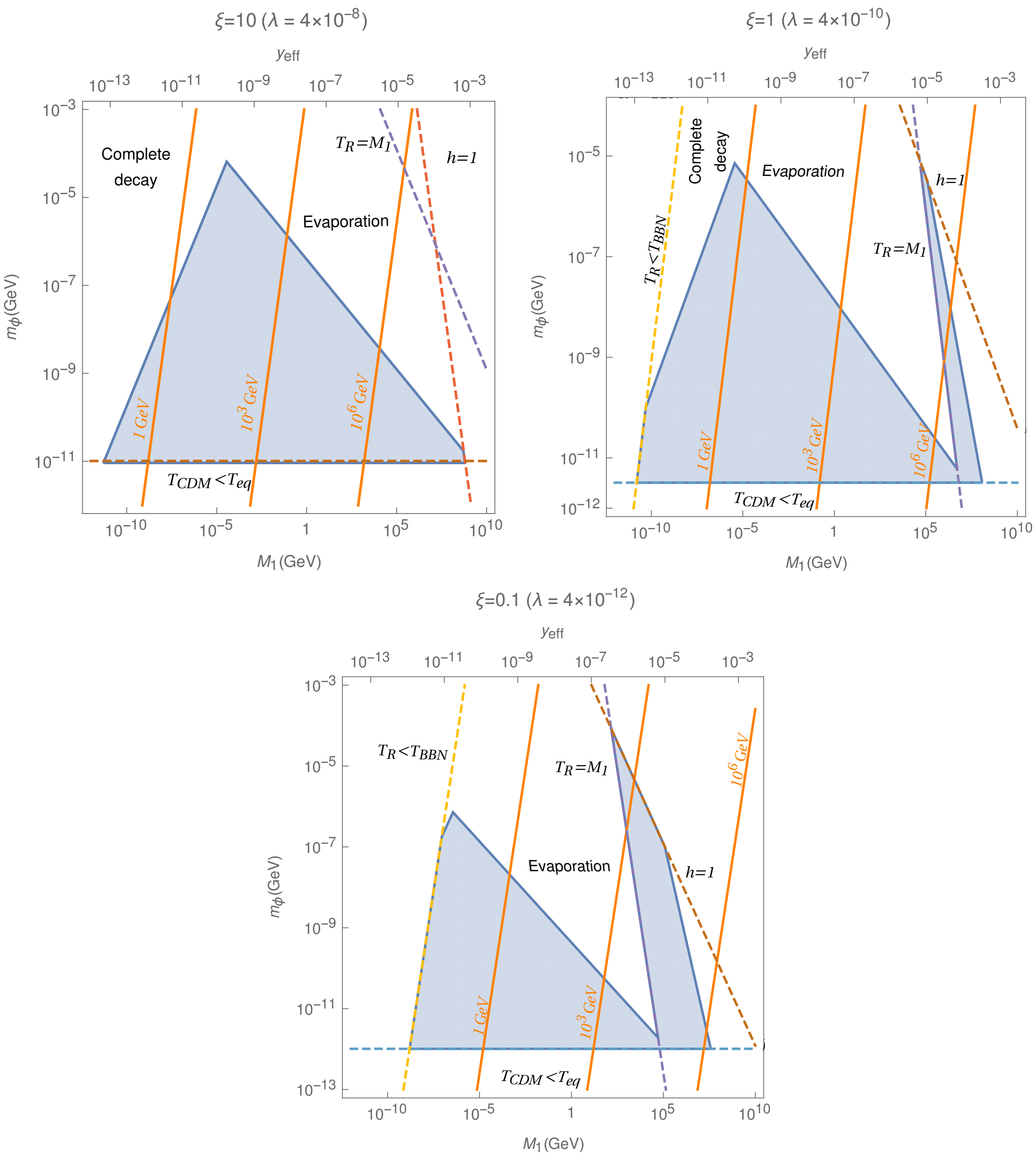


FIGURE 8.5: Resulting parameter space for $\xi = 0.1$, 1, and 10 for $g_\star = 100$ with no evaporation. Orange lines represent reheating temperatures and the blue dashed line, $M_1 = T_R$, limits the evaporation conditions. The $h = 1$, $T_R < T_{BBN}$ and $T_{CDM} < T_{eq}$ limits are also represented with the dashed lines. Condition (8.96) defines the complete decay and no reheating regions and conditions (8.97) and (8.98) limit the evaporation region.

# Chapter 9

# Leptogenesis in the Inflaton Dark Matter Model

As was briefly discussed in chapter 6, the observed baryon asymmetry in the Universe could be generated from a lepton number violation. We may recall that, as described in chapter 2, one of the most important consequences of the seesaw mechanism, introduced to account for the observed lightness of neutrino masses, was precisely a lepton number violation. At the same time, this generation of a neutrino mass generally requires new CP violating phases in Yukawa interactions and new heavy singlet neutrino which may decay out of equilibrium. Thus, all three Sakharov conditions seem to be satisfied within such a mechanism. The challenge is then to assess whether such a scenario can actually account for the observed asymmetry.

In this chapter, we will try to embed a Leptogenesis scenario within the Inflaton Dark Matter Model, with a thermal production of the third right-handed neutrino, $N_3$, lighter than the ones produced by the inflaton decay, $M_3 \ll M_1$. Only in the evaporation scenario will we embed the thermal Leptogenesis due to the required high reheating temperatures, as we will see later in this chapter. Here we will describe the basic features of such a Leptogenesis scenario within our construction, and the reader is referred to the literature for a more complete description [73, 91].

A lower bound, coming from the required CP violation, will be imposed on $M_3$ and, as a consequence, on the reheating temperature. We will see that, within the IDM model parameter's space, with a non-minimal coupling $\xi \gtrsim 2$, the necessary baryon asymmetry can be produced. Different leptogenesis scenarios may also be possible, for example with only non-thermal production of the two right-handed neutrinos coupled to the inflaton [92, 93], but this is beyond the scope of this work

## 9.1 A model of Thermal Leptogenesis

The existence of a seesaw mechanism, introduced to generate the observed light neutrino masses, has as a direct consequence the generation of a lepton asymmetry. In the lightest right-handed neutrino ($N_3$) decay to the SM particles we expect to generate this lepton asymmetry, which is later converted into a baryon asymmetry by the $B + L$ violating processes existent in the SM [83, 91]. A simple description of these non-perturbative effects will be given further in this section.

Following the Sakharov conditions, we can write the baryon asymmetry as

$$Y_{\Delta B} \simeq \left( \frac{n_{N_3}}{s_{T \gg M_3}} \right) \times C_{sphal} \times \eta \times \epsilon = \left( \frac{135\zeta(3)}{4\pi^4 g_\star} \right) \times C_{sphal} \times \eta \times \epsilon \,. \tag{9.1}$$

The first term is the equilibrium number density for a thermal production of $N_3$. The second factor, $C_{sphal}$ represents a dilution of the asymmetry due to some processes that redistribute the lepton asymmetry among other particle species. In this we may include Yukawa, gauge and $B + L$ violating non-perturbative effects. The $\eta$ factor represents an efficiency parameter. Thermal equilibrium dynamics includes some interactions, such as inverse decays, that may "washout" the lepton asymmetry produced in the decays of $N_3$. Such processes result in $0 < \eta < 1$ , with a limiting case of $\eta = 0$ for perfect equilibrium and no asymmetry production. Finally, the $\epsilon$ factor represents the CP asymmetry in the $N_3$ decays. For every $1/\epsilon$ $N_3$ decays, there is one more lepton than anti-leptons.

Next, we will further develop this first estimate of the baryon asymmetry by detailing a little more about these suppression factors.

### CP Violation ($\epsilon$)

The CP asymmetry produced in $N_3$ decays is defined as

$$\epsilon \equiv \frac{\Gamma\left(N_3 \to HL\right) - \Gamma\left(N_3 \to \bar{H}\bar{L}\right)}{\Gamma\left(N_3 \to HL\right) + \Gamma\left(N_3 \to \bar{H}\bar{L}\right)} \tag{9.2}$$

where $L$ and $H$ represent the lepton and Higgs doublets and $N_3 = \bar{N}_3$, since the heavy neutrino is a Majorana particle.

This asymmetry arises from the interference of tree-level and one-loop amplitudes [73] corresponding to the following Feynman diagrams:

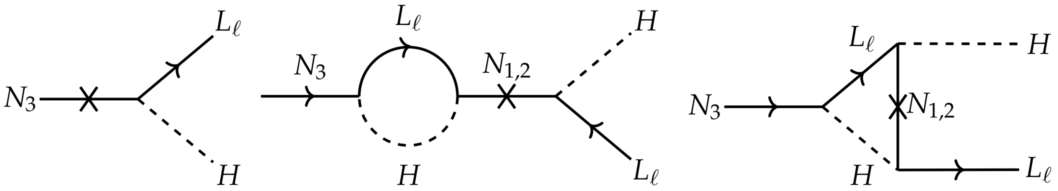


FIGURE 9.1: Diagrams contributing to the CP asymmetry $\epsilon$.

We can separate both tree and loop matrix elements into a coupling constant and an amplitude $\mathcal{A}_i$

$$\mathcal{M} = \mathcal{M}_0 + \mathcal{M}_1 = c_0\mathcal{A}_0 + c_1\mathcal{A}_1 \,. \tag{9.3}$$

In the simplest case, for the tree-level decay represented in the Feynman diagrams above

$$c_0 = y_{3\ell}, \quad \mathcal{A}_0\left(N \to HL_\ell\right) = \overline{v}_{L_\ell} P_R u_N \,. \tag{9.4}$$

where $P_R$ is right chiral projector. The CP conjugated process matrix element can be written as

$$\overline{\mathcal{M}} = c_0^* \bar{\mathcal{A}}_0 + c_1^* \bar{\mathcal{A}}_1 \,, \tag{9.5}$$

where in the CP conjugate amplitude, $\bar{\mathcal{A}}$, the $v_{L_\ell}$ spinors are replaced by $u_{L_\ell}$ spinors. Using the relations $\overline{u}_{L_\ell}(p)u_{L_\ell}(p) = \not{p} = \overline{v}_{L_\ell}(p)v_{L_\ell}(p)$, the amplitudes are the same $\left|\bar{\mathcal{A}}_i\right|^2 = \left|\mathcal{A}_i\right|^2$. The CP asymmetry can then be written as

$$\begin{aligned}\epsilon &= \frac{\int \left|c_0\mathcal{A}_0 + c_1\mathcal{A}_1\right|^2 \tilde{\delta} d\Pi_{L,H} - \int \left|c_0^*\bar{\mathcal{A}}_0 + c_1^*\bar{\mathcal{A}}_1\right|^2 \tilde{\delta} d\Pi_{L,H}}{2\int \left|c_0\mathcal{A}_0\right|^2 \tilde{\delta} d\Pi_{L,H}} \\ &= \frac{\mathcal{I}m\left(c_o c_1^*\right)}{\left|c_0\right|^2} \frac{2\int \mathcal{I}m(\mathcal{A}_0\mathcal{A}_1^*)\tilde{\delta} d\Pi_{L,H}}{\int \left|\mathcal{A}_0\right|^2 \tilde{\delta} d\Pi_{L,H}}\end{aligned} \tag{9.6}$$

where $\tilde{\delta} = (2\pi)^4 \delta^4\left(P_i - P_f\right)$, $d\Pi_{L\ell,H} = \frac{d^3 p_{L\ell}}{2E_L(2\pi)^3}\frac{d^3 p_H}{2E_H(2\pi)^3}$ and $P_i$, $P_f$ are the incoming and outgoing four momenta, respectively.

The first order loop amplitude $\mathcal{A}_1$ has an imaginary part when there are branch cuts corresponding to intermediate on-shell particles, recall Cutkosky rules [94], which may be created when, in the loops represented in the Feynman diagrams, the Higgs and the Leptons doublets elements are on-shell, thus

$$2\int \mathcal{I}m(\mathcal{A}_0\mathcal{A}_1^*) = \mathcal{A}_0\left(N \to HL\right)\int \mathcal{A}_0^*\left(N \to \bar{L}'\bar{H}'\right)\tilde{\delta}' d\Pi_{L',H'}\mathcal{A}_0\left(\bar{L}'\bar{H}' \to HL\right) \tag{9.7}$$

where the $X'$ notation was used to distinguish the intermediate, and assumed massless, onshell states.

We can now study the limit in which $M_3 \ll M_1$. In this scenario the effects of $N_{1,2}$ may be represented by an effective theory with a dimension-5 operator, corresponding to a point interaction instead of a $N_{1,2}$ propagator.

In our $\epsilon$ calculation, as a Feynman rule for this operator, we can use $\propto 2\,\mathcal{M}_\nu/v^2$ [73], where $\mathcal{M}_\nu$ is the light neutrino mass matrix, first defined in chapter 2. This comes quite naturally when we look into the seesaw dynamics. Even though there is also a contribution to $\mathcal{M}_\nu$ coming from $N_3$ which we did not integrate out, its contribution to the light neutrino mass matrix does not contribute to the imaginary part, present in $\epsilon$.

In this approximation we have

$$c_0 = y_{3\ell}, \qquad c_1 = \frac{3}{v^2/2}\sum_{\ell'} y^*_{3\ell'}\,[\mathcal{M}^*_\nu]_{\ell'\ell} \tag{9.8}$$

where the factor 3 comes from the counting of $SU(2)_L$ indices.

Using $\mathcal{A}_0\left(\bar{L}'\bar{H}' \to HL\right) = \bar{v}_L P_L u_L$ we get

$$\epsilon = \frac{3M_3}{16\pi}\frac{2}{v^2\,[\mathbf{y}\cdot\mathbf{y}^\dagger_\nu]_{33}}\mathcal{I}m\left[\sum_{\ell,\ell'} y_{3\ell}y_{3\ell'}\,[\mathcal{M}_\nu]_{\ell'\ell}\right]. \tag{9.9}$$

Having in mind that we wish to obtain a bound on the CP parameter, we will further simplify this expression [91].

Defining the unit three-vector

$$\hat{y}_\ell = \frac{y_{3\ell}}{\sqrt{[\mathbf{y}\cdot\mathbf{y}^\dagger_\nu]_{33}}}, \tag{9.10}$$

and using that $U^T_{PMNS}\mathcal{M}_\nu U_{PMNS} = M^d_\nu$, where the $U_{PMNS}$ is the neutrino mixing matrix introduced in chapter 2, we have

$$\mathcal{I}m\left[\hat{y}^T\mathcal{M}_\nu\hat{y}\right] = \mathcal{I}m\left[\hat{y}^T U^* U^T\mathcal{M}_\nu U U^\dagger\hat{y}\right] = \mathcal{I}m\left[\hat{y}'^T M^d_\nu\hat{y}'\right] = \mathcal{I}m\left[\sum_\ell \hat{y}'^2_\ell m_\ell\right] \leq m_{max} \tag{9.11}$$

due to the unitarity of $U_{PMNS}$, $\hat{y}'$ is also an unit vector and $m_{max}$ is the heaviest light neutrino mass.

As a consequence, we attribute an upper bound to $\epsilon$, called the Davidson-Ibarra bound [92],

$$|\epsilon| \leq \frac{3M_3 m_{max}}{8\pi v^2}. \tag{9.12}$$

From here it is possible to obtain a lower bound on $M_3$ and consequently on the required reheating temperature. However, we can first try to refine this analysis by incorporating the other two right-handed neutrinos as dynamical degrees of freedom and obtain a better expression to apply in our IDM model.

For a not-too degenerate spectrum [73, 92], for instance if $M_i - M_j \gg \Gamma_D$, one can write

$$\epsilon_i = \frac{1}{8\pi}\frac{1}{[\mathbf{y}\cdot\mathbf{y}_\nu^\dagger]_{ii}}\sum_j \mathcal{I}m\left\{\left[y_\nu y_\nu^\dagger\right]_{ij}^2\right\} g\left(x_i\right) \tag{9.13}$$

where $x_i \equiv M_j^2/M_i^2$ and

$$g(x) = \sqrt{x}\left[\frac{1}{1-x} + 1 - (1+x)\ln\left(\frac{1+x}{x}\right)\right] \overset{x\ll 1}{\to} -\frac{3}{2\sqrt{x}} + \dots . \tag{9.14}$$

If we assume again that the masses of the right-handed neutrinos are hierarchical, with $M_3 \ll M_1$ the lepton asymmetry is mostly generated by $M_3$ resulting in

$$\epsilon \simeq \frac{3}{16\pi}\frac{1}{[\mathbf{y}\cdot\mathbf{y}_\nu^\dagger]_{33}}\sum_j \mathcal{I}m\left\{\left[y_\nu y_\nu^\dagger\right]_{3j}^2\right\}\left(\frac{M_3}{M_j}\right) . \tag{9.15}$$

Using the seesaw result

$$\mathcal{M}_\nu = -m_D^T M_R^{-1} m_D = -\mathbf{y}_\nu^T M^{-1}\mathbf{y}_\nu \frac{v^2}{2} \tag{9.16}$$

we may write

$$\epsilon \simeq \frac{3}{8\pi}\frac{M_3}{v^2}\frac{1}{[\mathbf{y}\cdot\mathbf{y}_\nu^\dagger]_{33}}\mathcal{I}m\left\{\left[y_\nu \mathcal{M}_\nu^\dagger y_\nu^T\right]_{33}\right\} , \tag{9.17}$$

that will have as upper bound equation (9.12). The observed value of the baryon asymmetry combined with the other suppression factors results in $\epsilon \gtrsim 10^{-6}$.

### Out-of-equilibrium Dynamics ($\eta$)

The non-equilibrium condition necessary for Leptogenesis is ensured by the expansion of the Universe. With the decrease of the Hubble parameter, after reheating and while in a radiation dominated Universe, interactions rates will change from faster to slower than $H$ [73].

As we have seen above, after inflation the Universe is reheated into a thermal bath at $T_R$. The radiation bath may be composed of the SM particles, if evaporation of the inflaton has already occurred, or the $N_{1,2}$ right-handed neutrinos, if $M_1 < T_R$.

If the reheating temperature is higher than the mass of the third and lightest right-handed neutrino, $M_3 < T_R$ and if the production time scale for such particles is smaller that the age of the Universe, $\Gamma_{prod} > H$, a thermal number density of $N_3$ particles may be produced. Since there is no direct decay from the inflaton into the third right handed neutrino, its production channels are through inverse decays and in 2-2 scatterings involving the electroweak gauge bosons and the top quark. We can estimate such a rate as [73]

$$\Gamma_{prod} \sim \sum_{\ell} \frac{y_t^2 \, |y_{3\ell}|^2}{4\pi} T \,. \tag{9.18}$$

If we assume that $\Gamma_{prod} > H$, since $y_t \sim 1$ the $N_3$ decay $\Gamma_D$, defined in the previous sections,

$$\Gamma_D = \frac{\left[y_\nu y_\nu^\dagger\right]_{33} M_3}{8\pi} \,, \tag{9.19}$$

is also in equilibrium, $\Gamma_D > H$.

In the above discussion we had to assume $\Gamma_{prod} > H$, so let us see what consequences it brings to the IDM parameters. After defining

$$y_{3eff}^2 = \sum_{\ell} |y_{3\ell}|^2 \tag{9.20}$$

we can write

$$\frac{\Gamma_D}{H} \simeq 0.2 \, g_\star^{-1/2} \, y_{3eff}^2 \frac{M_P}{T} > 1 \,. \tag{9.21}$$

Assuming that for a thermal production of the third right-handed neutrino we need $T \sim 10\, M_3$ we then obtain a relation between this effective coupling and the neutrino mass

$$y_{3eff}^2 \gtrsim 1.7 \times 10^{-16} \frac{M_3}{\text{GeV}} \tag{9.22}$$

If we recover the light neutrino mass solutions from chapter 8, equations (8.67) and (8.70), and use the experimental values for the masses, we see that in the first case

$$y_{3eff}^2 \simeq 1.6 \times 10^{-15} \frac{M_3}{\text{GeV}} \,, \tag{9.23}$$

thus fitting the restrictions. In the second solution, if Eq. (9.22) holds we verify that $y_{eff}^2 / M_1$ and $y_{3eff}^2 / M_3$ are of the same order confirming the utility of the parameter $k \sim 1 - 10$. We thus see that the thermal production assumption is satisfied within the IDM model and no extra restrictions have to be imposed.

Interactions that are faster than $H$ impose chemical and kinetic equilibrium conditions on the involved particles and in this scenario the total lepton asymmetry $Y_L \simeq 0$. Although a lepton asymmetry may arise in $N_3$ decays, any asymmetry is washed out by processes like the inverse decay or scatterings between the leptons and the Higgs or the leptons and the $N_3$.

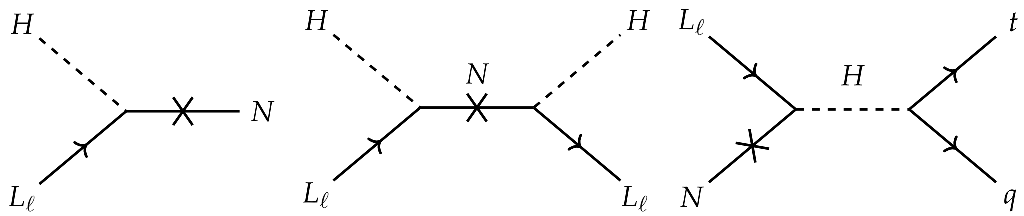


FIGURE 9.2: Washout processes: Inverse decay, 2↔2 processes $\Delta L = 2$ and $\Delta L = 1$.

An asymmetry will only arise once, for instance, the partial inverse decay width becomes out of equilibrium

$$\Gamma_{ID}(HL \to N_3) \simeq \Gamma_D e^{-M_3/T_*} < H \,. \tag{9.24}$$

At $T_*$ the inverse decay rate becomes smaller than $H$, blocking the production of $N_3$, and the remaining $N_3$ density becomes Boltzmann suppressed, making these right-handed neutrinos decay out-of-equilibrium.

The efficiency factor can be estimated as

$$\eta \simeq \frac{n_{N_3}(T_*)}{n_{N3}(T \gg M)} \simeq e^{-M_3/T_*} \simeq \frac{H(T = M_3)}{\Gamma_D} \,. \tag{9.25}$$

### Lepton and $B + L$ violation ($C_{sphal}$)

The $N_3$ decay violates lepton number, since no consistent attribution of a lepton number can be assigned to the right-handed neutrinos with the presence of both Majorana and Yukawa mass terms. The heavy neutrino mass eigenstate, being a Majorana particle, meaning it is its own anti-particle, can decay into both $LH$ and $\bar{L}\bar{H}$. With an asymmetry in the decay rates, a net lepton asymmetry will be generated. The conversion to a baryon asymmetry is obtained through $(B + L)$-violating non-perturbative processes existent in the SM.

The renormalizable SM Lagrangian conserves baryon number and the tree lepton flavour numbers $L_\ell$. However, due to the chiral anomaly, there are non-perturbative processes that violate the total lepton number summed with the baryon number, $B + L$. These configurations, called sphalerons, occurred in the early Universe at temperatures above the electroweak phase transition producing very fast $B + L$ violations. Let us now take a look at these chiral anomalies.

#### Chiral Anomalies and $B + L$ violation rates

Let us start from the Lagrangian for a massless Dirac fermion $\psi$ with a $U(1)$ gauge interactions

$$\mathcal{L} = \bar{\psi}\gamma^{\mu}\left(\partial_{\mu} - iA_{\mu}\right)\psi - \frac{1}{4e^2}F_{\mu\nu}F^{\mu\nu}\,. \tag{9.26}$$

In this Lagrangian there is an invariance under the $U(1)$ symmetry with,

$$\psi(x) \to e^{i\theta(x)}\psi(x), \qquad A_{\mu}(x) \to A_{\mu}(x) + \partial_{\mu}\theta(x)\,, \tag{9.27}$$

and under a global "chiral" symmetry

$$\psi(x) \to e^{i\gamma_5\kappa}\psi(x). \tag{9.28}$$

However in the latter case, the associated current

$$j_5^{\mu} = \bar{\psi}\gamma_5\gamma^{\mu}\psi \tag{9.29}$$

is only conserved at tree-level and not at loop level. This can be attributed to the loop regularization, that by introducing a scale, will break chiral symmetry, similarly to a fermion mass [94]. At one loop order the total divergence involving the gauge fields gives

$$\partial_{\mu}j_5^{\mu} = \frac{\epsilon_{\rho\sigma\mu\nu}}{16\pi^2}F^{\rho\sigma}F^{\mu\nu}\,. \tag{9.30}$$

The space-time integral of (9.30) in the case of an Abelian theory is zero, however in the non-Abelian case, where $\left[A_{\mu}^{a}, A_{\nu}^{b}\right] \neq 0$, we obtain a non zero result.

In regards to leptogenesis, the anomalies appearing in $SU(2)_L$, with chiral and non-Abelian gauge interactions, are of great importance. The participating fermions are the three generations of quark and lepton left-handed $SU(2)_L$ doublets $\left\{\psi_L^i\right\} = \{q_L^{a,\alpha}, \ell_L^{\alpha}\}$ where $a$ and $\alpha$ represent, respectively, the color and the generation index. We can write the Lagrangian representing the $SU(2)_L$ interactions as

$$\mathcal{L} = \bar{\psi}_L^i\left(\partial_{\mu} - i\frac{g}{2}\sigma^A W_{\mu}^A\right)\psi_L^i, \tag{9.31}$$

where $A$ is an $SU(2)_L$ generator index.

Having twelve fields participating in such interactions, 3 lepton and 9 quark fields, we have one global $U(1)$ symmetry for each field. The chiral currents associated with these transformations , as before, are conserved at tree-level, but anomalies appear in loop corrections

$$\partial_{\mu}j_{\mu}^{i} = \frac{1}{64\pi^2}F_{\mu\nu}^{A}\tilde{F}^{\mu\nu A}\,. \tag{9.32}$$

Defining the charge associated with this current as $Q^i(t) = \int j_0^i d^3x$, and using $\Delta Q = Q^i(+\infty) - Q^i(-\infty)$, we see that it is possible to have a field configuration such that

$$\Delta Q^i = \frac{1}{64\pi^2} \int d^4x F^A_{\mu\nu} \tilde{F}^{\mu\nu A} \,, \tag{9.33}$$

which is a non-zero integer. This has a consequence, without perturbative processes, of fermion production [73].

At zero temperature such gauge field configurations are called instantons and have highly suppressed rates, resulting in negligible $B + L$ violations [73, 95]. In the Leptogenesis picture, where temperatures are well above the electroweak phase transition, the dominant $(B + L)$-violating processes are called sphalerons and have an approximate rate [96]

$$\Gamma_{B+L\,violation} \simeq 250\alpha_W^5 T \,. \tag{9.34}$$

Between the temperatures of the electroweak phase transition and $10^{12}$ GeV this rate is faster than the Hubble expansion, $H$. Thus, the lepton asymmetry produced in the $N_3$ decay, or the $B - L$ asymmetry, will be converted into a final baryon asymmetry following

$$Y_{\Delta B} \simeq \frac{12}{37} Y_{\Delta(B-L)} \,, \tag{9.35}$$

where $Y_{\Delta(B-L)}$ is the $B - L$ asymmetry divided by the entropy density.

## 9.2 Thermal Leptogenesis and the Inflaton Dark Matter model

Putting all together, with equations (9.1) and (9.35), we have

$$Y_{\Delta B} \simeq 10^{-3} \epsilon \eta \,. \tag{9.36}$$

After some work with the Boltzmann equations we expect $0.01 \lesssim \eta \lesssim 0.1$, thus to account for the observed $Y_{\Delta B} \sim 10^{-10}$ we need $|\epsilon| \gtrsim 10^{-5} - 10^{-6}$ .

We have obtained a lower bound on the required CP violation to reproduce a successful leptogenesis and in (9.12) we saw an important relation between the right-handed neutrino mass $M_3$ and the CP factor, the Davidson-Ibarra bound. Such a result could be explored in the IDM model in order to obtain a constraint on the lightest right-handed neutrino mass.

After a more rigorous analysis equation (9.17), which is model dependent, can be obtained. Having our Yukawa and mass matrices defined for the IDM model in chapter 8, it is possible to further develop such a result for each case obtained in section 8.5.

When studying the neutrino mass matrices, with a goal of extracting their mass squared, we have neglected both Majorana and Dirac CP phases existent in the neutrino mixing matrices. Now, since we are interested in CP violation, such phases are crucial and we will reintroduce them in our parametrization.

In the first case where

$$m_2 = -\frac{v^2}{M_3}\left(\frac{y_{3e}^2}{2} + y_{3\mu}^2\right), \qquad m_3 = 0, \tag{9.37}$$

the Yukawa matrix can be written as

$$\mathbf{y}_\nu = \begin{pmatrix} \pm y_{3\mu}\gamma^{1/2} & \pm\frac{y_{3e}}{2}\gamma^{1/2} & y_{1\tau} \\ \pm y_{3\mu}\gamma^{1/2} & \pm\frac{y_{3e}}{2}\gamma^{1/2} & y_{1\tau} \\ y_{3e} & y_{3\mu} & -y_{3\mu} \end{pmatrix}, \tag{9.38}$$

and the light neutrino mass matrix

$$\mathcal{M}_\nu = \frac{m_2}{3}\begin{pmatrix} 2+e^{-2i\phi_1} & -1+e^{-2i\phi_1} & 1+e^{-2i\phi_1} \\ -1+e^{-2i\phi_1} & \frac{1}{2}+e^{-2i\phi_1} & -\frac{1}{2}+e^{-2i\phi_1} \\ 1-e^{-2i\phi_1} & -\frac{1}{2}+e^{-2i\phi_1} & \frac{1}{2}+e^{-2i\phi_1} \end{pmatrix}, \tag{9.39}$$

where $\gamma = M_1/M_3$ and $\phi_1$ is the Majorana CP parameter associated with $m_2$ in (2.24). Developing equation (9.17) we obtain

$$\left[y_\nu \mathcal{M}_\nu^\dagger y_\nu^T\right]_{33} = \frac{m_2}{3}\left\{2(y_{3\mu}-y_{3\mu})^2 + \left(y_{3e}+2y_{3\mu}\right)^2 e^{2i\phi_1}\right\}, \tag{9.40}$$

$$\left[\mathbf{y}\cdot\mathbf{y}_\nu^\dagger\right]_{33} = |y_{3e}|^2 + 2\,|y_{3\mu}|^2 . \tag{9.41}$$

If we write $y_{i\ell} = |y_{i\ell}|\, e^{i\psi_{1\ell}}$ and further develop equation (9.40)

$$\epsilon \simeq \frac{3}{8\pi}\frac{M_3}{v^2}\frac{1}{[\mathbf{y}\cdot\mathbf{y}_\nu^\dagger]_{33}}\mathcal{I}m\left\{\left[y_\nu\mathcal{M}_\nu^\dagger y_\nu^T\right]_{33}\right\} \tag{9.42}$$

we obtain

$$\begin{aligned}\epsilon \simeq\ & \frac{3}{8\pi}\frac{M_3 m_2}{v^2}\frac{1}{|y_{3e}|^2+2\,|y_{3\mu}|^2}\,\cdot \\ \times&\left\{\frac{|y_{3e}|^2}{3}\left[2\sin(2\psi_{3e})+\sin(2\psi_{3e}+2\phi_1)\right] + \frac{4\,|y_{3e}|\,|y_{3\mu}|}{3}\left[\sin\left(\psi_{3e}+\psi_{3\mu}+2\phi_1\right)-\sin\left(\psi_{3e}+\psi_{3\mu}\right)\right]\right. \\ &\left. +\frac{2\,|y_{3\mu}|^2}{3}\left[\sin\left(2\psi_{3\mu}\right)+2\sin\left(2\psi_{3\mu}+2\phi_1\right)\right]\right\}.\end{aligned} \tag{9.43}$$

As an upper limit, the ratio $\frac{\mathcal{I}m\{[y_\nu \mathcal{M}_\nu^\dagger y_\nu^T]_{33}\}}{m_2[\mathbf{y}\cdot\mathbf{y}_\nu^\dagger]_{33}} \leq 1$ resulting in an upper bound

$$|\epsilon| \lesssim \frac{3M_3 m_2}{8\pi v^2}\,. \tag{9.44}$$

In the second case

$$m_3 = -v^2\left(\frac{2y_{1\mu}^2}{M_1} + \frac{y_{3\mu}^2}{M_3}\right), \qquad m_2 = 0, \tag{9.45}$$

by performing a similar analysis with

$$\mathbf{y}_\nu = \begin{pmatrix} 0 & y_{1\mu} & y_{1\mu} \\ 0 & y_{1\mu} & y_{1\mu} \\ 0 & y_{3\mu} & y_{3\mu} \end{pmatrix}, \tag{9.46}$$

and

$$\mathcal{M}_\nu = \frac{m_3 e^{-2i\phi_2}}{2}\begin{pmatrix} 0 & 0 & 0 \\ 0 & 1 & 1 \\ 0 & 1 & 1 \end{pmatrix}, \tag{9.47}$$

we obtain

$$\epsilon \simeq \frac{3}{8\pi}\frac{m_3 M_3}{v^2}\frac{2\left|y_{3\mu}\right|^2 \sin\left(2\psi_{3\mu} + 2\phi_2\right)}{2\left|y_{3\mu}\right|^2} = \frac{3}{8\pi}\frac{m_3 M_3}{v^2}\sin\left(2\psi_{3\mu} + 2\phi_2\right)\,. \tag{9.48}$$

In both scenarios the model independent bound on $\epsilon$ was recovered with $m_{max} = m_{2,3}$.

Finally, we can obtain the lower bound on $M_3$ and apply it to the IDM model. From equation (9.12) we have

$$M_3 \gtrsim \frac{8\pi}{3}\frac{v^2}{m_{max}}|\epsilon| \simeq 10^9\text{ GeV}. \tag{9.49}$$

Since the only mean of $N_3$ production is through thermal interactions the condition $T_R > M_3$ is required. Imposing $T_R \gtrsim 10\, M_3$, we arrive at a lower bound on the reheating temperature

$$T_R \gtrsim 10^{10}\text{ GeV}. \tag{9.50}$$

Unlike the $M_3$ value, we can apply the bound on the reheating temperature on the IDM model with evaporation parameter space and observe its restrictions as shown in figure 9.3.

As we can see, thermal leptogenesis is only realizable for $\xi \gtrsim 2$ and in the region where $T_R < M_1$, due to the very high required reheating temperature . Moreover, thermal Leptogenesis can only occur in the upper limit of the parameters $h$, $m_\phi$ and $y_{eff}$, excluding the parameter space of the no-evaporation regime, as seen in chapter 8. The allowed values stay around $h \sim 1$ or $m_\phi \sim 10^3$ GeV and $y_{eff} \sim 0.1$.

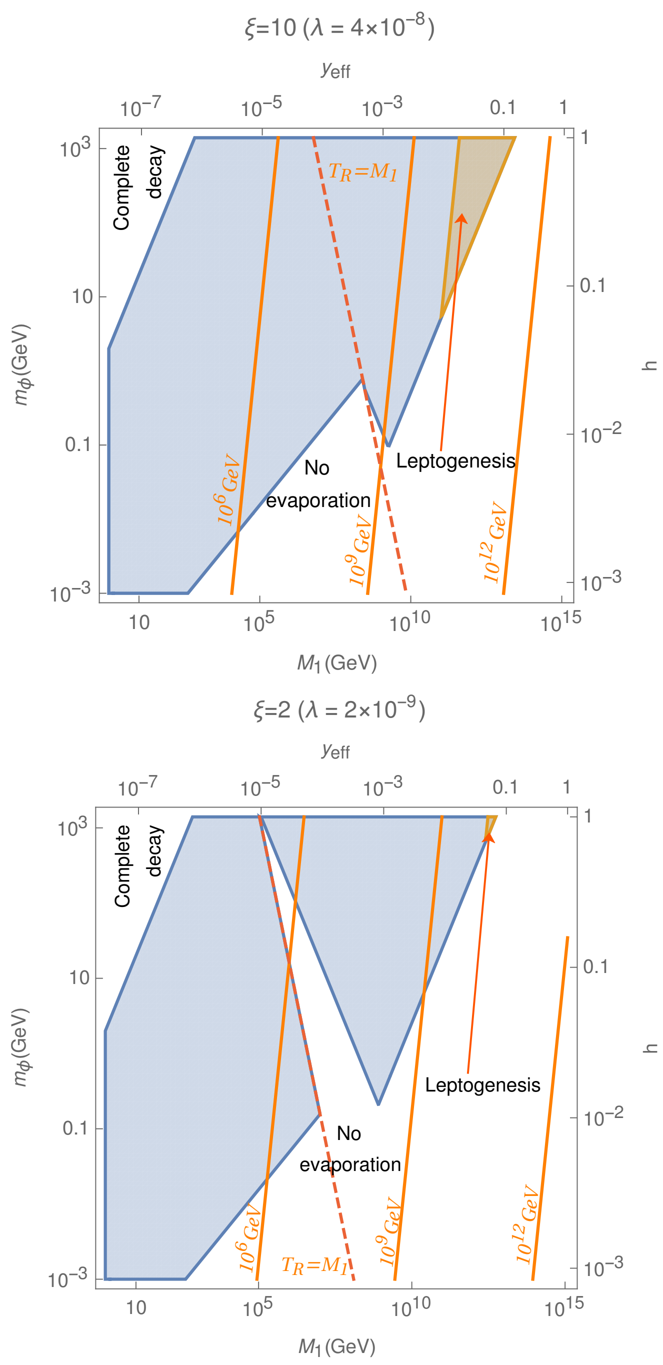


FIGURE 9.3: Resulting parameter space for $\xi = 2, 10$. Thermal leptogenesis region starts to appear for $\xi = 2$ due to the high required reheating temperatures.

Other means of generating a lepton asymmetry could be realizable, for instance, with only non-thermal production of the right-handed neutrinos during inflation, but this is outside the scope of this work.

# Chapter 10

# Conclusions

In this work, we have developed an unification model where we describe, using the same field, an inflationary evolution and the dark matter content of the Universe, due to an incomplete decay of the inflaton. At the same time, this incomplete decay introduces right-handed neutrinos that allow the generation of light neutrino masses and also the generation of the observed baryon asymmetry in the Universe through a thermal Leptogenesis evolution.

We started with a review of the introductory topics for this thesis. First, we gave a description of the basic features of neutrino physics including the seesaw mechanism, a description of neutrino mass and mixing matrices and neutrino oscillations. Moving to cosmology, we introduced the Standard Cosmological paradigm and then the inflationary evolution. In the latter, after describing the basic dynamics, we have detailed how the experimental observables can be related to the metric and matter fluctuations and to the slow-roll parameters. We then discussed Dark Matter basic notions and reproduced the standard WIMP's abundance calculation. Finally, we discussed the three Sakharov Conditions [2] to then introduce some models of Baryogenesis.

After setting the ground, we then moved to the model's description. We began by reviewing the incomplete decay features of the Inflaton Dark Matter model [1]. We described a system composed of the inflaton, following the inflationary slow-roll description, and two fermions, later to be identified with two right-handed neutrinos. The imposition of a discrete symmetry resulted in a coupling between the two fermions and the inflaton with the same modulus but opposite sign, and the same bare mass for the two fermions. The symmetry also forbids all inflaton decay channels except into the two fermions, even in decays through off-shell fermion modes. Thus, if the fermion tree-level mass $M_1 > m_\phi/2$, where $m_\phi$ is the inflaton mass, the inflaton may be stable at late times leaving room for it to account for dark matter. From the coupling with the inflaton the two fermions acquire an effective mass, dependent on the scalar field values, $M_\pm = |M_1 \pm h\phi|$, which unlocks the inflaton decay while the field is oscillating with large amplitudes. We then verified that an effective reheating is possible within the described dynamics, while using a quadratic term in the inflaton potential.

As a next step, since no real description of the transition to the Standard Model (SM) particles was given and inflation with a quadratic potential does not agree with experimental results, we provided a more realistic construction of the IDM dynamics. To solve the first problem we have introduced right-handed neutrinos as the model's fermions and allowed the interaction with the SM degrees of freedom through an Yukawa coupling with the Higgs and the lepton doublets. To answer the second issue a non-minimal coupling to gravity and an extra quartic potential term were introduced.

The non-minimal coupling between gravity and the inflaton field and the complete potential resulted in a relation between the non-minimal coupling, $\xi$, and quartic potential couping constant, $\lambda$. This relation was fixed by Planck's data [54] on scalar perturbations. The experimental values of the scalar to tensor ration and the scalar spectral index imposed a lower bound on the $\xi$ value and consequently on the 4-point self interaction of the inflaton.

Since inflation occurs for high $\phi$ values the quartic potential dominates and describes the reheating period. Similarly to the quadratic case we verified that is possible to generate a successful reheating. Such requirement resulted in an upper bound on the right-handed neutrino mass. Then, we have described how the transition to both standard cosmology and particle physics may have occurred.

We described the right-handed neutrinos decay into the SM degrees of freedom and we concluded that there are two different regimes for the right-handed neutrino mass, with important implications to the evolution of the remnant inflaton particles. The incomplete decay of the inflaton produces a thermal bath of right-handed neutrinos and possibly of the SM particles, if their decay is already allowed. These particles present in the radiation bath will in turn scatter off the inflaton bosons in the condensate state leading to its evaporation.

In the regime where the reheating temperature $T_R > M_1$ the right-handed neutrinos will still be in the thermal bath, thus participating in the evaporation process together with the other SM particles. However if $T_R < M_1$ , the right-handed neutrinos would already have decayed leaving only its decay products for the evaporation process. Naturally, this resulted in two different evaporation conditions for each regime. Having evaporated, the inflaton becomes a part of the thermal bath and will follow the common WIMP evolution, allowing us to relate our parameters to the dark matter measured abundance.

A different path may occur, since the inflaton may not evaporate. In this scenario the inflaton may evolve as a Bose condensate. After the inflaton decays become kinematically blocked, the inflaton becomes stable and the condensate enters a Dark Radiation regime while the field oscillates in the quartic potential. When the quadratic potential term becomes dominant the condensate will mimic a stable non-relativistic fluid, thus behaving as Cold Dark Matter. Using the fact that the ratio of $n_\phi/s$ becomes constant, with $n_\phi$ being the inflaton number density and $s$ the entropy density of the Universe, we can again relate our parameters to the measured dark matter abundance.

We have then studied the low energy implications of the introduction of the right-handed neutrinos. The Majorana mass term, coming from the masses of $N_1$, $N_2$ and $N_3$, and the Dirac mass term, from the Yukawa interactions with the Higgs boson and the left-handed neutrinos, through the seesaw mechanism generate masses for the light neutrino states. The IDM imposed symmetry resulted in a massless and two other massive light neutrinos. Using a tribimaximal mixing matrix we obtained two independent solutions for the neutrino masses and with the experimental values coming from neutrino oscillations [45] we have obtained a relation between our parameters.

Putting everything together we have obtained the results in figures 8.4 and 8.5 for both the evaporation and no-evaporation hypothesis. In the former we saw a broad parameter space including high mass, $M_1 \gtrsim 10^{10}$ GeV, $m_\phi \gtrsim 10^3$ GeV, or high couplings and low energy solutions, $M_1 \lesssim 1$ GeV, $m_\phi \lesssim 10^{-3}$ GeV. The $M_1 = T_R$ equality plays a very important role since it limits the allowed evaporation processes. In the no-evaporation case, the possible solutions rest in the low energy limit, $M_1 \sim 10^{-5}$ GeV, $m_\phi \sim 1$ eV, with the reheating temperatures very close to the required temperatures for the synthesis of light elements.

Finally, we embedded a thermal Leptogenesis description within our model. We described the thermal production of a third right handed-neutrino, $N_3$, lighter than the other two, recalling that the inflaton can only decay to the other two right handed neutrinos. The lepton asymmetry is produced in the $N_3$ out-of-equilibrium decay to the SM lepton and Higgs doublets that later is converted to a baryon asymmetry through non-perturbative sphaleron processes existent in the SM. Studying the CP violation in these lepton number violating processes we recovered the Davidson-Ibarra bound [92]. Applying it to our model and using the values of the measured baryon asymmetry we have obtained a bound on $M_3$. Since for a thermal production of the third right-handed neutrino $T_R \gtrsim 10\ M_3$, we derived a condition for the IDM parameters. As described in figure 9.3, only solutions with $\xi \gtrsim 2$ and at very large masses for both the inflaton and the $N_1$, $N_2$ neutrinos are possible.

In summary, our results reveal that we have conceived a consistent model that may connect some of the current and most important problems in particle physics and cosmology, namely the inflationary dynamics, the mass nature of light neutrinos, the unknown structure of dark matter and the observed baryon asymmetry in the Universe.

As paths for further development of our model we may for instance, look for possible LHC interaction signatures for direct or indirect detection of our model particles. However, their detection seems to be difficult, since its particles stay either in a very high energy regime, with $M_1$ well above the TeV scale, making impossible in a near future to detect them, or at very low couplings, $y_{eff} \sim 10^{-7}$, turning the interactions very hard to detect. Another possibility to expand our model is through a supersymmetric extension, addressing the radiative corrections problem. A different path also left to explore is through a non-thermal production of the right-handed neutrinos responsible for the lepton asymmetry generation.

# Bibliography


[1] M. Bastero-Gil, R. Cerezo and J. G. Rosa, *Inflaton dark matter from incomplete decay*, Phys. Rev. **D93**, 103531 (2016), arXiv:1501.05539 [hep-ph] .

[2] A. D. Sakharov, *Violation of CP Invariance, C asymmetry, and baryon asymmetry of the universe*, Pisma Zh. Eksp. Teor. Fiz. **5**, 32 (1967), [Usp. Fiz. Nauk161,no.5,61(1991)].

[3] A. E. Bernardini and O. Bertolami, *Perturbative approach for mass varying neutrinos coupled to the dark sector in the generalized Chaplygin gas scenario*, Phys. Rev. **D77**, 083506 (2008), arXiv:0712.1534 [astro-ph] .

[4] A. E. Bernardini and O. Bertolami, *Stationary condition in a perturbative approach for mass varying neutrinos*, Phys. Lett. **B662**, 97 (2008), arXiv:0802.4449 [hep-ph] .

[5] A. T. Manso and J. G. Rosa, *$\nu$-Inflaton Dark Matter*, (2018), arXiv:1811.02302 [hep-ph] .

[6] H. Fritzsch, M. Gell-Mann and H. Leutwyler, *Advantages of the color octet gluon picture*, Physics Letters B **47**, 365 (1973).

[7] D. J. Gross and F. Wilczek, *Ultraviolet Behavior of Non-Abelian Gauge Theories*, Phys. Rev. Lett. **30**, 1343 (1973).

[8] S. Weinberg, *Non-Abelian Gauge Theories of the Strong Interactions*, Phys. Rev. Lett. **31**, 494 (1973).

[9] S. L. Glashow, *Partial-symmetries of weak interactions*, Nuclear Physics **22**, 579 (1961).

[10] S. Weinberg, *A Model of Leptons*, Phys. Rev. Lett. **19**, 1264 (1967).

[11] A. Salam, *Weak and Electromagnetic Interactions*, *8th Nobel Symposium Lerum, Sweden, May 19-25, 1968*, Conf. Proc. **C680519**, 367 (1968).

[12] P. Higgs, *Broken symmetries, massless particles and gauge fields*, Physics Letters **12**, 132 (1964).

[13] F. Englert and R. Brout, *Broken Symmetry and the Mass of Gauge Vector Mesons*, Phys. Rev. Lett. **13**, 321 (1964).

[14] J. Goldstone, A. Salam and S. Weinberg, *Broken Symmetries*, Phys. Rev. **127**, 965 (1962).

[15] R. N. Mohapatra and A. Y. Smirnov, *Neutrino Mass and New Physics*, *Elementary particle physics. Proceedings, Corfu Summer Institute, CORFU2005, Corfu, Greece, September 4-26, 2005*, Ann. Rev. Nucl. Part. Sci. **56**, 569 (2006), arXiv:hep-ph/0603118 [hep-ph] .

[16] A. de Gouvêa, *Neutrino Mass Models*, Ann. Rev. Nucl. Part. Sci. **66**, 197 (2016).

[17] S. Weinberg, *Baryon and Lepton Nonconserving Processes*, Phys. Rev. Lett. **43**, 1566 (1979).

[18] R. Barbieri, J. R. Ellis and M. K. Gaillard, *Neutrino Masses and Oscillations in SU(5)*, Phys. Lett. **90B**, 249 (1980).

[19] E. K. Akhmedov, Z. G. Berezhiani and G. Senjanovic, *Planck scale physics and neutrino masses*, Phys. Rev. Lett. **69**, 3013 (1992), arXiv:hep-ph/9205230 [hep-ph] .

[20] P. Minkowski, *$\mu \to e\gamma$ at a Rate of One Out of $10^9$ Muon Decays?*, Phys. Lett. **67B**, 421 (1977).

[21] M. Gell-Mann, P. Ramond and R. Slansky, *Complex Spinors and Unified Theories*, *Supergravity Workshop Stony Brook, New York, September 27-28, 1979*, Conf. Proc. **C790927**, 315 (1979), arXiv:1306.4669 [hep-th] .

[22] T. Yanagida, *HORIZONTAL SYMMETRY AND MASSES OF NEUTRINOS*, *Proceedings: Workshop on the Unified Theories and the Baryon Number in the Universe: Tsukuba, Japan, February 13-14, 1979*, Conf. Proc. **C7902131**, 95 (1979).

[23] S. L. Glashow, *The Future of Elementary Particle Physics*, *Cargese Summer Institute: Quarks and Leptons Cargese, France, July 9-29, 1979*, NATO Sci. Ser. B **61**, 687 (1980).

[24] R. N. Mohapatra and G. Senjanovic, *Neutrino Mass and Spontaneous Parity Violation*, Phys. Rev. Lett. **44**, 912 (1980), [,231(1979)].

[25] B. Pontecorvo, *Mesonium and anti-mesonium*, Sov. Phys. JETP **6**, 429 (1957), [Zh. Eksp. Teor. Fiz.33,549(1957)].

[26] B. Pontecorvo, *Inverse beta processes and nonconservation of lepton charge*, Sov. Phys. JETP **7**, 172 (1958), [Zh. Eksp. Teor. Fiz.34,247(1957)].

[27] Z. Maki, M. Nakagawa and S. Sakata, *Remarks on the unified model of elementary particles*, Prog. Theor. Phys. **28**, 870 (1962), [,34(1962)].

[28] B. T. Cleveland, T. Daily, R. Davis, Jr., J. R. Distel, *et al.*, *Measurement of the solar electron neutrino flux with the Homestake chlorine detector*, Astrophys. J. **496**, 505 (1998).

[29] Q. R. Ahmad, *et al.* (SNO), *Direct evidence for neutrino flavor transformation from neutral current interactions in the Sudbury Neutrino Observatory*, Phys. Rev. Lett. **89**, 011301 (2002), arXiv:nucl-ex/0204008 [nucl-ex] .

[30] W. Hampel, *et al.* (GALLEX), *Final results of the Cr-51 neutrino source experiments in GALLEX*, Phys. Lett. **B420**, 114 (1998).

[31] M. Altmann, *et al.* (GNO), *GNO solar neutrino observations: Results for GNO I*, Phys. Lett. **B490**, 16 (2000), arXiv:hep-ex/0006034 [hep-ex] .

[32] J. P. Cravens, *et al.* (Super-Kamiokande), *Solar neutrino measurements in Super-Kamiokande-II*, Phys. Rev. **D78**, 032002 (2008), arXiv:0803.4312 [hep-ex] .

[33] Y. Fukuda, *et al.* (Super-Kamiokande), *Evidence for oscillation of atmospheric neutrinos*, Phys. Rev. Lett. **81**, 1562 (1998), arXiv:hep-ex/9807003 [hep-ex] .

[34] M. H. Ahn, *et al.* (K2K), *Measurement of Neutrino Oscillation by the K2K Experiment*, Phys. Rev. **D74**, 072003 (2006), arXiv:hep-ex/0606032 [hep-ex] .

[35] Y. Itow, *et al.* (T2K), in *Neutrino oscillations and their origin. Proceedings, 3rd International Workshop, NOON 2001, Kashiwa, Tokyo, Japan, December 508, 2001* (2001) pp. 239–248, arXiv:hep-ex/0106019 [hep-ex] .

[36] D. S. Ayres, *et al.* (NOvA), *NOvA: Proposal to Build a 30 Kiloton Off-Axis Detector to Study $\nu_\mu \to \nu_e$ Oscillations in the NuMI Beamline*, (2004), arXiv:hep-ex/0503053 [hep-ex] .

[37] D. G. Michael, *et al.* (MINOS), *Observation of muon neutrino disappearance with the MINOS detectors and the NuMI neutrino beam*, Phys. Rev. Lett. **97**, 191801 (2006), arXiv:hep-ex/0607088 [hep-ex] .

[38] H. Pessard (OPERA), *Status of the OPERA neutrino experiment*, *Proceedings, Europhysics Conference on High energy physics (EPS-HEP 2009): Cracow, Poland, July 16-22, 2009*, PoS **EPS-HEP2009**, 280 (2009), arXiv:0910.5701 [hep-ex] .

[39] M. Apollonio, *et al.* (CHOOZ), *Initial results from the CHOOZ long baseline reactor neutrino oscillation experiment*, Phys. Lett. **B420**, 397 (1998), arXiv:hep-ex/9711002 [hep-ex] .

[40] S. Abe, *et al.* (KamLAND), *Precision Measurement of Neutrino Oscillation Parameters with KamLAND*, Phys. Rev. Lett. **100**, 221803 (2008), arXiv:0801.4589 [hep-ex] .

[41] P. Bhattacharjee and G. Sigl, *Origin and propagation of extremely high-energy cosmic rays*, Phys. Rept. **327**, 109 (2000), arXiv:astro-ph/9811011 [astro-ph] .

[42] E. Andres, *et al.*, *The AMANDA neutrino telescope: Principle of operation and first results*, Astropart. Phys. **13**, 1 (2000), arXiv:astro-ph/9906203 [astro-ph] .

[43] J. W. Cronin, *Recent results from the Pierre Auger Observatory*, (2009), arXiv:0911.4714 [astro-ph.HE] .

[44] F. Halzen and D. Hooper, *Gamma-ray astronomy with IceCube*, JCAP **0308**, 006 (2003), arXiv:astro-ph/0305234 [astro-ph] .

[45] S. Gariazzo, M. Archidiacono, P. F. de Salas, O. Mena, *et al.*, *Neutrino masses and their ordering: Global Data, Priors and Models*, JCAP **1803**, 011 (2018), arXiv:1801.04946 [hep-ph] .

[46] L. Wolfenstein, *Neutrino Oscillations in Matter*, Phys. Rev. **D17**, 2369 (1978), [,294(1977)].

[47] S. P. Mikheyev and A. Yu. Smirnov, *Resonance Amplification of Oscillations in Matter and Spectroscopy of Solar Neutrinos*, Sov. J. Nucl. Phys. **42**, 913 (1985), [,305(1986)].

[48] J. G. Rosa, "Introduction to cosmology: Lecture," .

[49] D. Baumann, in *Physics of the large and the small, TASI 09, proceedings of the Theoretical Advanced Study Institute in Elementary Particle Physics, Boulder, Colorado, USA, 1-26 June 2009* (2011) pp. 523–686, arXiv:0907.5424 [hep-th] .

[50] E. W. Kolb and M. S. Turner, *The Early Universe*, Front. Phys. **69**, 1 (1990).

[51] A. H. Guth, *The Inflationary Universe: A Possible Solution to the Horizon and Flatness Problems*, Phys. Rev. **D23**, 347 (1981), [Adv. Ser. Astrophys. Cosmol.3,139(1987)].

[52] A. D. Linde, *A New Inflationary Universe Scenario: A Possible Solution of the Horizon, Flatness, Homogeneity, Isotropy and Primordial Monopole Problems*, *QUANTUM COSMOLOGY*, Phys. Lett. **108B**, 389 (1982), [Adv. Ser. Astrophys. Cosmol.3,149(1987)].

[53] A. Albrecht and P. J. Steinhardt, *Cosmology for Grand Unified Theories with Radiatively Induced Symmetry Breaking*, Phys. Rev. Lett. **48**, 1220 (1982), [Adv. Ser. Astrophys. Cosmol.3,158(1987)].

[54] P. A. R. Ade, *et al.* (Planck), *Planck 2015 results. XIII. Cosmological parameters*, Astron. Astrophys. **594**, A13 (2016), arXiv:1502.01589 [astro-ph.CO] .

[55] A. Borriello and P. Salucci, *The Dark matter distribution in disk galaxies*, Mon. Not. Roy. Astron. Soc. **323**, 285 (2001), arXiv:astro-ph/0001082 [astro-ph] .

[56] H. Hoekstra, H. Yee and M. Gladders, *Current status of weak gravitational lensing*, New Astron. Rev. **46**, 767 (2002), arXiv:astro-ph/0205205 [astro-ph] .

[57] R. B. Metcalf, L. A. Moustakas, A. J. Bunker and I. R. Parry, *Spectroscopic gravitational lensing and limits on the dark matter substructure in Q2237+0305*, Astrophys. J. **607**, 43 (2004), arXiv:astro-ph/0309738 [astro-ph] .

[58] L. A. Moustakas and R. B. Metcalf, *Detecting dark matter substructure spectroscopically in strong gravitational lenses*, Mon. Not. Roy. Astron. Soc. **339**, 607 (2003), arXiv:astro-ph/0206176 [astro-ph] .

[59] J. A. Tyson, G. P. Kochanski and I. P. Dell'Antonio, *Detailed mass map of CL0024+1654 from strong lensing*, Astrophys. J. **498**, L107 (1998), arXiv:astro-ph/9801193 [astro-ph] .

[60] H. Dahle, *A compilation of weak gravitational lensing studies of clusters of galaxies*, (2007), arXiv:astro-ph/0701598 [astro-ph] .

[61] B. Paczynski, *Gravitational microlensing by the galactic halo*, Astrophys. J. **304**, 1 (1986).

[62] K. G. Begeman, A. H. Broeils and R. H. Sanders, *Extended rotation curves of spiral galaxies: Dark haloes and modified dynamics*, Mon. Not. Roy. Astron. Soc. **249**, 523 (1991).

[63] F. Zwicky, *Die Rotverschiebung von extragalaktischen Nebeln*, Helv. Phys. Acta **6**, 110 (1933), [Gen. Rel. Grav.41,207(2009)].

[64] D. Clowe, M. Bradac, A. H. Gonzalez, M. Markevitch, *et al.*, *A direct empirical proof of the existence of dark matter*, Astrophys. J. **648**, L109 (2006), arXiv:astro-ph/0608407 [astro-ph] .

[65] R. D. Peccei and H. R. Quinn, CP *Conservation in the Presence of Pseudoparticles*, Phys. Rev. Lett. **38**, 1440 (1977).

[66] R. D. Peccei and H. R. Quinn, *Constraints imposed by* CP *conservation in the presence of pseudoparticles*, Phys. Rev. D **16**, 1791 (1977).

[67] S. Weinberg, *A New Light Boson?*, Phys. Rev. Lett. **40**, 223 (1978).

[68] F. Wilczek, *Problem of Strong P and T Invariance in the Presence of Instantons*, Phys. Rev. Lett. **40**, 279 (1978).

[69] J. Preskill, M. B. Wise and F. Wilczek, *Cosmology of the invisible axion*, Physics Letters B **120**, 127 (1983).

[70] S. P. Martin, *A Supersymmetry primer*, , 1 (1997), [Adv. Ser. Direct. High Energy Phys.18,1(1998)], arXiv:hep-ph/9709356 [hep-ph] .

[71] H. Pagels and J. R. Primack, *Supersymmetry, Cosmology, and New Physics at Teraelectronvolt Energies*, Phys. Rev. Lett. **48**, 223 (1982).

[72] G. Bertone, D. Hooper and J. Silk, *Particle dark matter: Evidence, candidates and constraints*, Phys. Rept. **405**, 279 (2005), arXiv:hep-ph/0404175 [hep-ph] .

[73] S. Davidson, E. Nardi and Y. Nir, *Leptogenesis*, Phys. Rept. **466**, 105 (2008), arXiv:0802.2962 [hep-ph] .

[74] G. Steigman, *Primordial nucleosynthesis: successes and challenges*, Int. J. Mod. Phys. **E15**, 1 (2006), arXiv:astro-ph/0511534 [astro-ph] .

[75] W. M. Yao, *et al.* (Particle Data Group), *Review of Particle Physics*, J. Phys. **G33**, 1 (2006).

[76] R. H. Cyburt, B. D. Fields, K. A. Olive and E. Skillman, *New BBN limits on physics beyond the standard model from* $^4He$, Astropart. Phys. **23**, 313 (2005), arXiv:astro-ph/0408033 [astro-ph] .

[77] C. Patrignani, *et al.* (Particle Data Group), *Review of Particle Physics*, Chin. Phys. **C40**, 100001 (2016).

[78] G. Hinshaw, *et al.* (WMAP), *Nine-Year Wilkinson Microwave Anisotropy Probe (WMAP) Observations: Cosmological Parameter Results*, Astrophys. J. Suppl. **208**, 19 (2013), arXiv:1212.5226 [astro-ph.CO] .

[79] C. L. Bennett, *et al.* (WMAP), *Nine-Year Wilkinson Microwave Anisotropy Probe (WMAP) Observations: Final Maps and Results*, Astrophys. J. Suppl. **208**, 20 (2013), arXiv:1212.5225 [astro-ph.CO] .

[80] J. M. Cline, in *Les Houches Summer School - Session 86: Particle Physics and Cosmology: The Fabric of Spacetime Les Houches, France, July 31-August 25, 2006* (2006) arXiv:hep-ph/0609145 [hep-ph] .

[81] G. 't Hooft, *Symmetry Breaking Through Bell-Jackiw Anomalies*, Phys. Rev. Lett. **37**, 8 (1976), [,226(1976)].

[82] V. A. Kuzmin, V. A. Rubakov and M. E. Shaposhnikov, *On the Anomalous Electroweak Baryon Number Nonconservation in the Early Universe*, Phys. Lett. **155B**, 36 (1985).

[83] V. A. Rubakov and M. E. Shaposhnikov, *Electroweak baryon number nonconservation in the early universe and in high-energy collisions*, Usp. Fiz. Nauk **166**, 493 (1996), [Phys. Usp.39,461(1996)], arXiv:hep-ph/9603208 [hep-ph] .

[84] M. Trodden, *Electroweak baryogenesis*, Rev. Mod. Phys. **71**, 1463 (1999), arXiv:hep-ph/9803479 [hep-ph] .

[85] M. Kobayashi and T. Maskawa, *CP Violation in the Renormalizable Theory of Weak Interaction*, Prog. Theor. Phys. **49**, 652 (1973).

[86] C. Jarlskog, *Commutator of the Quark Mass Matrices in the Standard Electroweak Model and a Measure of Maximal CP Violation*, Phys. Rev. Lett. **55**, 1039 (1985).

[87] M. Fukugita and T. Yanagida, *Baryogenesis Without Grand Unification*, Phys. Lett. **B174**, 45 (1986).

[88] I. Affleck and M. Dine, *A New Mechanism for Baryogenesis*, Nucl. Phys. **B249**, 361 (1985).

[89] O. Bertolami, D. Colladay, V. A. Kostelecky and R. Potting, *CPT violation and baryogenesis*, Phys. Lett. **B395**, 178 (1997), arXiv:hep-ph/9612437 [hep-ph] .

[90] M. Postma and M. Volponi, *Equivalence of the Einstein and Jordan frames*, Phys. Rev. **D90**, 103516 (2014), arXiv:1407.6874 [astro-ph.CO] .

[91] Y. Nir, *Leptogenesis: A Pedagogical Introduction*, (2018).

[92] S. Davidson and A. Ibarra, *A Lower bound on the right-handed neutrino mass from leptogenesis*, Phys. Lett. **B535**, 25 (2002), arXiv:hep-ph/0202239 [hep-ph] .

[93] T. Asaka, H. B. Nielsen and Y. Takanishi, *Nonthermal leptogenesis from the heavier Majorana neutrinos*, Nucl. Phys. **B647**, 252 (2002), arXiv:hep-ph/0207023 [hep-ph] .

[94] M. E. Peskin and D. V. Schroeder, *An Introduction to quantum field theory* (Addison-Wesley, Reading, USA, 1995).

[95] S. R. Coleman, *The Uses of Instantons*, *Instantons in gauge theories*, Subnucl. Ser. **15**, 805 (1979), [,382(1978)].

[96] Y. Burnier, M. Laine and M. Shaposhnikov, *Baryon and lepton number violation rates across the electroweak crossover*, JCAP **0602**, 007 (2006), arXiv:hep-ph/0511246 [hep-ph] .